



National Library  
of Canada

Canadian Theses Service

Ottawa, Canada  
K1A 0N4

Bibliothèque nationale  
du Canada

Service des thèses canadiennes

## NOTICE

The quality of this microform is heavily dependent upon the quality of the original thesis submitted for microfilming. Every effort has been made to ensure the highest quality of reproduction possible.

If pages are missing, contact the university which granted the degree.

Some pages may have indistinct print especially if the original pages were typed with a poor typewriter ribbon or if the university sent us an inferior photocopy.

Previously copyrighted materials (journal articles, published tests, etc.) are not filmed.

Reproduction in full or in part of this microform is governed by the Canadian Copyright Act, R.S.C. 1970, c. C-30.

## AVIS

La qualité de cette microforme dépend grandement de la qualité de la thèse soumise au microfilmage. Nous avons tout fait pour assurer une qualité supérieure de reproduction.

S'il manque des pages, veuillez communiquer avec l'université qui a conféré le grade.

La qualité d'impression de certaines pages peut laisser à désirer, surtout si les pages originales ont été dactylographiées à l'aide d'un ruban usé ou si l'université nous a fait parvenir une photocopie de qualité inférieure.

Les documents qui font déjà l'objet d'un droit d'auteur (articles de revue, tests publiés, etc.) ne sont pas microfilmés.

La reproduction, même partielle, de cette microforme est soumise à la Loi canadienne sur le droit d'auteur, SRC 1970, c. C-30.

THE UNIVERSITY OF ALBERTA

A STUDY OF OPEN CHANNEL FLOW IN COMMERCIAL PIPES.

BY

DONALD K. MAY

A THESIS

SUBMITTED TO THE FACULTY OF GRADUATE STUDIES AND RESEARCH  
IN PARTIAL FULFILMENT OF THE REQUIREMENTS FOR THE DEGREE  
OF MASTER OF SCIENCE

DEPARTMENT OF CIVIL ENGINEERING

EDMONTON, ALBERTA.

FALL, 1988

Permission has been granted  
to the National Library of  
Canada to microfilm this  
thesis and to lend or sell  
copies of the film.

The author (copyright owner)  
has reserved other  
publication rights, and  
neither the thesis nor  
extensive extracts from it  
may be printed or otherwise  
reproduced without his/her  
written permission.

L'autorisation a été accordée  
à la Bibliothèque nationale  
du Canada de microfilmer  
cette thèse et de prêter ou  
de vendre des exemplaires du  
film.

L'auteur (titulaire du droit  
d'auteur) se réserve les  
autres droits de publication;  
ni la thèse ni de longs  
extraits de celle-ci ne  
doivent être imprimés ou  
autrement reproduits sans son  
autorisation écrite.

ISBN 0-315-45842-9

THE UNIVERSITY OF ALBERTA

RELEASE FORM

NAME OF AUTHOR: DONALD KENNETH MAY

TITLE OF THESIS: A STUDY OF OPEN CHANNEL FLOW IN  
COMMERCIAL PIPES

DEGREE FOR WHICH THESIS WAS PRESENTED MASTER OF SCIENCE

YEAR THIS DEGREE GRANTED FALL 1988

Permission is hereby granted to THE UNIVERSITY OF  
ALBERTA LIBRARY to reproduce single copies of this  
thesis and to lend or sell such copies for private,  
scholarly or scientific research purposes only.

The author reserves other publication rights, and  
neither the thesis nor extensive extracts from it may  
be printed or otherwise reproduced without the author's  
written permission.

(SIGNED)

Donald K. May

PERMANENT ADDRESS:

3465 Overlander Drive  
Kamloops, B.C.  
V2B 6X4

DATED ... September 29 ... 1988

THE UNIVERSITY OF ALBERTA

FACULTY OF GRADUATE STUDIES AND RESEARCH

The undersigned certify that they have read, and  
recommend to the Faculty of Graduate Studies and Research for  
acceptance, a thesis entitled A STUDY OF OPEN CHANNEL FLOW IN  
COMMERCIAL PIPES submitted by Donald K. May in partial  
fulfilment of the requirements for the degree of MASTER OF  
SCIENCE in CIVIL ENGINEERING.

*M. Jayaraman*  
Supervisor

*A. White*

*K.C. Cheng*

Date 29 Sept '88

## Abstract

This thesis presents the results of clean water, open channel hydraulic tests done in the T. Blench Graduate Hydraulics Laboratory on commercially available concrete and plastic pipes. The purpose of the tests was to compare the hydraulic characteristics of the two pipe materials under similar conditions of steady uniform flow.

Flow development in two of the pipes was analyzed by measuring velocity profiles along the central axis of flow. It was concluded by examining velocity profile overlap, that the flow was fully developed within 40 pipe diameters of the inlet.

Uniform flow experiments fell into the transition zone between hydraulically smooth and rough turbulent flow. Manning's  $n$  was found to vary with slope and depth to diameter ratio. However, the variations in Manning's  $n$  were small enough to allow useful average values to be calculated. Ratios of the hydraulic elements and the variation in Manning's  $n$  expressed as a ratio of the average  $n$  value were plotted for each pipe. The latter was found to be a useful way to illustrate the variability in Manning's  $n$ .

Some classical theories concerning boundary layer growth in a two dimensional flow field were compared to the results of these tests. The boundary layer defined as, the point in the flow where the velocity attains ninety-nine percent of the free stream velocity, is not applicable to boundary layer growth in a circular section. The Blasius seventh power equation was found to agree with observed boundary layer growth as a first approximation. However developing flow in part full pipes should be analyzed as a three dimensional problem due to the presence of secondary currents.

A discussion of the experimental uncertainties is presented. Even in controlled laboratory conditions experimental error in the order of twenty-five percent is common for measured friction coefficients. This suggests that more than two significant figures cannot be justified when reporting these coefficients.

### Acknowledgements

The writer would like to thank Dr. N. Rajaratnam and Professor A. W. Peterson for their guidance and assistance and the staff of the T. Blench Graduate Hydraulics Laboratory, particularly S. Lovell, L. Flint-Petersen, and J. Gagne for contributing many ideas and help with work moving pipes and setting up the experiments. Special thanks go to G. Flato, L. Flint Peterson and R. Powley for contributing to the boundary layer analysis. For their ideas, encouragement and support the writer would like to thank Dr. R. Gerard, Professor P. Bouthillier, P. G. Van Der Vinne and R. and B. Chyz. Sincerest thanks to C. Lawler of Consolidated Concrete Limited who supplied the pipes and much of the financial support for conducting the tests.

Most of all the writer would like to thank his wife, Patricia and children, Laura and Shannon for their enduring patience and understanding.

## Table of Contents

Chapter	Page
1 Introduction.....	1
2 Literature Review.....	7
2.1 Boundary Layer Theory.....	7
2.1.1 Boundary Layer Formulae.....	7
2.2 Uniform Flow Equations.....	12
2.2.1 Empirical Approach.....	13
2.2.2 Theoretical Approach.....	17
2.2.3 Previous Studies.....	20
2.2.4 Effects of Aging on Sewers.....	23
2.2.5 Summary.....	26
3 Apparatus and Procedure.....	29
3.1 Experimental Set-up.....	29
3.1.1 Boundary Layer Measurements.....	32
3.1.2 Uniform Flow Measurements.....	33
3.1.3 Measurements of pipes.....	34
3.2 Procedure.....	35
3.2.1 Pipe Assembly.....	35
3.2.2 Uniform Flow Measurements.....	36
3.2.3 Boundary Layer Measurements.....	37
3.2.4 Roughness Measurements.....	40
3.2.5 Repeatability of Results.....	43
4 Formulae Used.....	44

4.1 Boundary Layer Analysis.....	44
4.2 Friction Coefficients.....	44
4.3 Hydraulic Elements.....	51
5 Results .....	54
5.1 Boundary Layer Development.....	54
5.1.1 Mild Slopes.....	54
5.1.2 Steep Slopes.....	54
5.2 Friction Factors.....	56
5.3 Hydraulic Elements.....	58
5.4 Repeatability of Results.....	59
5.5 Roughness Analysis.....	59
5.5.1 Description of Surface Roughness.....	60
5.5.2 Observed versus Measured Roughness.....	62
6 Analysis and Discussion.....	64
6.1 Boundary Layer Development.....	64
6.2 Uniform Flow.....	66
6.2.1 Experimental Uncertainty.....	66
6.2.2 Resistance to Flow.....	70
7 Conclusions.....	71
8 Recommendations.....	73
9 References.....	121
Appendix A Manufacturers and ASTM specifications for the pipes tested.....	126
Appendix B Specifications for pumps, flowmeters and other hardware.....	127
Appendix C Pipe diameter measurements.....	130

Appendix D	Typical datasheet.....	132
Appendix E	Root mean squared roughness of the pipes tested.....	133
Appendix F	Fortran programs.....	135
Appendix G	Error analysis.....	147
Appendix H	Results in tabular form.....	152

## List of Tables

Table 1 Values of Manning n from two types of concrete pipe, From Bloodgood and Bell (1961).....	74
Table 2 Equivalent roughness for concrete pipes. From Straub and Morris (1950).....	74
Table 3 Information about pipe dimensions and total installed length of each pipe.....	75
Table 4 Measured and calculated boundary layer parameters.....	76
Table 5 Average values of Manning's n from this study.....	82
Table 6 Root mean squared roughness and standard deviation for the pipes tested.....	84
Table 7 Physical roughness compared to calculated values of equivalent roughness ( $k_s$ ).....	85

## List of Figures

Fig. 1	Laboratory set-up showing the flume, installed pipe, and details of the pressure tappings and pipe cradles.....	86
Fig. 2	Device used to measure inside surface roughness of the pipes.....	87
Fig. 3	Typical output from depth capacitance probes.....	88
Fig. 4	Typical readout from the Validyne pressure transducer used to measure velocity profiles.....	89
Fig. 5	Typical roughness records from the roughness measuring device.....	90
Fig. 6	Measured and theoretical boundary layer growth in the 200 mm concrete pipe.....	91
Fig. 7	Measured and theoretical boundary layer growth in the 200 mm concrete pipe with measurements extended further down pipe.....	92
Fig. 8	Boundary layer growth in the 200 and 380 mm concrete pipes.....	93
Fig. 9	Velocity profiles in the 200 mm concrete pipe.....	94
Fig. 10	Velocity profiles in the 200 mm concrete pipe.....	95
Fig. 11	Velocity profiles in the 200 and 380 mm concrete pipes.....	96

Fig. 12 Plot of depth ratio versus the ratio of distance from the pipe inlet to pipe diameter.....	97
Fig. 13 Water surface profiles in the 250 mm concrete pipe: mild slopes.....	98
Fig. 14 Water surface profiles in the 250 mm concrete pipe: steep slopes.....	99
Fig. 15 Water surface profiles in the 250 mm plastic pipe: mild slopes.....	100
Fig. 16 Water surface profiles in the 250 mm plastic pipe: steep slopes.....	101
Fig. 17 Shear stress downstream from the inlet of the 200 and 380 mm concrete pipes.....	102
Fig. 18 Manning n versus depth ratio for the 200 mm concrete and plastic pipes.....	103
Fig. 19 Manning n versus depth ratio for the 250 mm concrete and plastic pipes.....	104
Fig. 20 Manning n versus depth ratio for the 380 mm concrete and 450 mm plastic pipes.....	105
Fig. 21 Dispersion of Manning n with depth ratio for the 200 mm concrete and plastic pipes.....	106
Fig. 22 Dispersion of Manning n with depth ratio for the 250 mm concrete and plastic pipes.....	107
Fig. 23 Dispersion of Manning n with depth ratio for the 380 mm concrete and 450 mm plastic pipes.....	108
Fig. 24 Moody diagram for the 200 mm concrete and plastic pipes.....	109

Fig. 25	Moody diagram for the 250 mm concrete and plastic pipes.....,.....	110
Fig. 26	Moody diagram for the 380 mm concrete and 450 mm plastic pipes.....,.....	111
Fig. 27	Plots of the hydraulic elements for the 200 mm concrete and plastic pipes.....,.....	112
Fig. 28	Plots of the hydraulic elements for the 250 mm concrete and plastic pipes.....,.....	113
Fig. 29	Plots of the hydraulic elements for the 380 mm concrete and 450 mm plastic pipes.....,.....	114
Fig. 30	Repeatability of results demonstrated by Manning n versus depth ratio.....,.....	115

## List of Plates

- Plate 1 Experimental set-up showing the flume with  
the 380 mm concrete pipe installed.....116
- Plate 2 Typical joints in the 250 mm concrete pipe  
with and without flowing water.....117
- Plate 3 Roughness measuring device.....118
- Plate 4 Manometers at mild and steep slopes.....119
- Plate 5 Manometers showing standing waves in pipe....120

### List of Symbols

- $A_0$  = constant in the universal velocity distribution law  
in Schlichting (1979)
- $A^*$  = area occupied by the flow in a channel
- $B$  = constant in the universal velocity distribution law
- $C$  = Chezy's resistance coefficient
- $D$  = inside diameter of pipe
- $F$  = Froude number
- $H$  = head loss
- $J$  = velocity function used by Pomeroy (1967)
- $K$  = Pomeroy's resistance coefficient
- $K_L$  = entrance loss coefficient
- $L$  = length of pipe used in Darcy's equation for full pipe flow
- $P$  = wetted perimeter
- $Q$  = rate of flow
- $R$  = hydraulic radius
- $R_e$  = Reynold's number
- $S$  = bed slope
- $S_f$  = slope of the hydraulic grade line
- $T$  = top width of an open channel
- $U_0$  = free stream velocity
- $V$  = average velocity of flow
- $V_*$  = friction velocity
- $\alpha$  = exponent of R used by Pavlovskii (in Chow, 1959)

- $c_s$  = shape correction factor used by Powell (1946)
- $c$  = Powell's roughness coefficient
- $f$  = Darcy's friction coefficient
- $g$  = acceleration due to gravity
- $h_L$  = head loss in Darcy's equation
- $k_s$  = equivalent sand grain roughness
- $l$  = representative length
- $m$  = coefficient of hydraulic elements used by Pomeroy
- $n$  = Manning's coefficient of resistance
- $r$  = pipe radius
- $u$  = velocity at a point in the flow
- $u_s$  = shear velocity
- $w$  = exponent of hydraulic elements used by Pomeroy
- $x$  = distance down the channel measured from the inlet
- $y$  = distance above invert measured normal to the pipe boundary
- $y_0$  = normal depth of flow
- $\delta$  = boundary layer thickness
- $\delta_1$  = displacement thickness
- $\delta_2$  = momentum thickness
- $\delta_0$  = definition of boundary layer thickness
- $\pi$  = 3.1416
- $\Theta$  = radial angle occupied by the flow

$\nu$  = kinematic viscosity

$\rho$  = mass density of water

$T_0$  = boundary shear stress

## 1 Introduction

This research was undertaken to examine uniform gravity flow in commercially available precast concrete and extruded plastic pipes typically used for sanitary and storm sewer applications. The study was designed as a controlled comparison between the two pipe materials to produce reliable uniform flow data required to generate resistance coefficients.

The requisite condition for steady uniform flow as stated by Henderson (1966) is that the hydraulic properties of the flow are constant in the direction of the flow. To attain this condition in a laboratory or field installation the flow must not suffer any external perturbations beyond the steady reactions to the gravitational field. There can be no change in the channel slope, cross-sectional properties, or discharge over the length of the channel or in time. Assuming the above conditions have been satisfied, then the channel length needed to reach the steady uniform state, the flow development length, must be determined.

Water entering a channel from a reservoir or a section with different properties adjusts to the changing conditions. It will decelerate or accelerate depending on the change in the channel geometry. As the fluid moves from

an upstream reservoir it accelerates down the channel.

Immediately upon entering a channel the boundary of the channel begins to exert a shearing resistance on the flow such that the water molecules in contact with the boundary are held motionless (Streeter and Wylie, 1981). The shearing resistance to the flow is proportional to the flow velocity as shown by equation (1).

$$\tau_0 = \frac{\rho f V^2}{8} \quad (1)$$

where:  $\tau_0$  = boundary shear stress (Pa)

$\rho$  = water density ( $\text{kg/m}^3$ )

$V$  = mean flow velocity ( $\text{m/s}$ )

$f$  = Darcy's friction coefficient

The influence of the channel boundaries are not immediately experienced by the elements of the flow remote from the walls, but as the water progresses downstream the wall effects propagate into the flow. The layer of fluid which is experiencing shearing resistance is called the boundary layer. The boundary layer continues to expand until it occupies the entire flow. At this point the shearing resistance forces and the driving gravitational forces are in equilibrium and the flow is uniform and fully developed.

The velocity profiles varied down the channel in the developing flow region, but remain constant when the flow is fully developed.

The growth of the boundary layer at the entrance to a pipe is something that is often ignored by hydraulic engineers. The effect of the boundary layer on the flow is usually accounted for in an empirically determined entrance loss coefficient. This coefficient also includes energy losses due to the geometry of the inlet and due to separation. The head loss is determined from an equation of the form:

$$H = K_L \frac{V^2}{2g} \quad (2)$$

where:  $H$  = head loss at the pipe entrance

$V$  = mean velocity of flow

$g$  = acceleration due to gravity

$K_L$  = entrance loss coefficient

For a well rounded entrance, the coefficient  $K_L$  is equal to about 0.10.

Standard uniform flow equations, like Darcy-Weisbach, Manning, and Chezy assume that the velocity distribution is fully developed. In most cases the effect of the boundary layer development zone is assumed to apply to such a short

length, compared to the overall length of the pipe, that the uniform flow equations can be used for the entire pipe with a correction applied over zero length at the entrance.

Under some circumstances, this simplified approach may not be justified. One important example is in laboratory studies where the length of pipe may be limited to 50 or less and the flow development zone may comprise a large proportion of the total pipe length.

A great deal of time and effort was expended during this study to determine the flow development length. Measurements were compared to classical theories of boundary layer development over flat plates of zero incidence and for axisymmetric flow in pipes flowing full. These theories were not developed to accurately describe a three dimensional flow field.

Initial inspection may lead a researcher to assume that open channel flow in a circular section is similar to axisymmetric flow in full pipes. However, unequal shear stresses develop along the walls in a part full pipe section which cause a double spiral flow pattern normal to the central axis of the pipe. These secondary currents, commented on by Replogle and Chow (1966), depress the

filament of maximum velocity to a point well below the water surface and tend to mask the development of the boundary layer parallel to the central axis of the pipe.

Without undertaking a complete three dimensional study of the flow, it is left to the researcher to examine velocity profiles taken along the central axis of the pipe to determine if the flow is fully developed. This was the approach used in this study. Due to time constraints, velocity profiles were obtained for only two of the six pipes tested. Comparisons were made between the velocity profiles and water surface profiles which allowed the flow development lengths for the other pipes to be estimated as well.

The second part of the study focused on the analysis of the uniform flow region. Flow parameters including average depth, channel geometry, and discharge were measured. There are experimental uncertainties inherent in the measurement of these parameters. Even in a laboratory installation where the profile grade and alignment are carefully controlled, standing waves develop in the flow which cause error in average depth measurements. There are also the effects of the pipe joints which are a source of continuing perturbation to the flow. In effect, a new boundary layer must develop each time the flow encounters a joint. These small scale flow characteristics are beyond the scope of

most of the practical uniform flow equations used by hydraulic engineers, but must be dealt with before any analytical expression can be developed. A thorough treatment of these flow characteristics was not attempted as part of this study. The approach used was to obtain sufficient measurements to average or dampen the effects of the small scale flow irregularities.

In conjunction with the uniform flow experiments, physical measurements were also made on all the pipes tested. It was hoped that by measuring the size of the roughness features on the pipe boundaries that conclusions could be drawn about the reliability of the equivalent roughness measurement used in some formulas (Colebrook-White). In addition, if calculated values of equivalent roughness were significantly larger than the mean roughness measured, this could provide an indication about the effect of the pipe joints and alignment irregularities on the overall resistance of the pipe.

Prior to describing the study in detail, a brief review of the theory and relevant previous literature is presented. Due to the bulk of previous work on boundary layer analysis and uniform flow in open channels, it was necessary to limit this review primarily to studies dealing with circular channel sections.

## 2 Literature Review

### 2.1 Boundary Layer Theory

Nikuradse (reported in Schlichting, 1979) determined that the fully developed velocity distribution had been attained within 25 to 40 pipe diameters of the entrance for turbulent pipe flow. However, Straub, Bowers, and Pilch (1960) found that in rough concrete pipe, even though the hydraulic grade line showed no further curvature, the velocity profile was still not fully developed after 20 to 30 pipe diameters from the entrance. Most researchers rely on boundary layer expressions developed for axisymmetric flow to estimate boundary layer growth and flow development length. The relevant theory is shown below.

#### 2.1.1 Boundary Layer Formulae

As mentioned, most of the classical work in boundary layer theory considered only idealized two dimensional situations such as axisymmetric flows (pipes flowing full) or flows with semi-infinite boundaries. Unfortunately, boundary layer development in pipes flowing part-full is more complicated, and has not been investigated to any great degree. However, there is value in comparing the results of these tests to standard theory.

The displacement thickness is defined by Schlichting (1979) as "the distance by which the external streamlines are shifted owing to the formation of the boundary layer".

The displacement thickness is defined by the following equation:

$$\delta_1 = \int_{y=0}^{\infty} \left(1 - \frac{u}{U_\infty}\right) dy \quad (3)$$

where:  $\delta_1$  = displacement thickness

$u$  = velocity at some point

$U_\infty$  = free stream velocity

$y$  = distance normal to the boundary

The momentum loss in the boundary layer is given by the expression:

$$\rho \int_{y=0}^{\infty} u(U_\infty - u) dy \quad (4)$$

$\rho$  = fluid density

This allows the definition of an additional thickness called the momentum thickness by the following relationship:

$$\delta_2 = \int_{y=0}^{\infty} \frac{u}{U_\infty} \left(1 - \frac{u}{U_\infty}\right) dy \quad (5)$$

where:  $\delta_2$  = momentum thickness

It is reported by Schlichting that the momentum thickness and the displacement thickness compare to the boundary layer thickness as follows:

$$\delta_1 = \frac{1}{2} \delta \quad (6)$$

$$\delta_2 = \frac{1}{6} \delta \quad (7)$$

where:  $\delta$  = boundary layer thickness

The boundary layer thickness is usually defined somewhat arbitrarily as the distance from the boundary to the point in the flow where the velocity is ninety-nine percent of the free stream velocity. The location of the displacement thickness is obtained directly from the velocity profiles and can be plotted versus distance from the entrance to determine the location where the flow becomes fully developed. The results of such a plot are usually compared to the Blasius seventh power law for growth of the dimensionless boundary layer on a flat plate of zero incidence:

$$\frac{\delta}{x} = 0.37 \left( \frac{U_\infty x}{v} \right)^{-0.2} \quad (8)$$

where:  $x$  = the distance from the entrance

$v$  = kinematic viscosity

The boundary shear stress depends on the velocity gradient normal to the flow boundary. At the point of origin, the boundary layer is infinitely thin. Therefore, the velocity gradient and the shear stress at this point are infinitely large. As the flow proceeds down the channel the boundary layer grows in thickness and the velocity gradients between any two points in the boundary layer, normal to the boundary, become less. At the location where the boundary layer becomes fully developed the velocity gradient reaches equilibrium and the shear stress is constant in the direction of the flow. The relationship for the shear stress at the pipe boundary is developed below.

The universal law for velocity distribution in the vicinity of hydrodynamically rough surfaces is stated as follows:

$$\frac{u}{u_*} = A_0 \log \frac{y}{k_s} + B \quad (9)$$

where:  $u$  = the velocity at a point in the flow

$$u_* = \text{shear velocity equal to } \sqrt{\frac{\tau_0}{\rho}}$$

$A_0$  and  $B$  are constants determined experimentally

$y$  = distance normal to the boundary

$k_s$  = equivalent sand grain roughness

$$u = A_0 u \cdot \log y - u \cdot (A_0 \log k_s + B) \quad (10)$$

If the boundary layer velocity measurements are plotted versus depth on semi-logarithmic paper the resulting curve should be linear. The slope of the straight line is related to the shear stress as follows:

For one log cycle:

$$y_2 = 10y_1$$

so:

$$u_2 - u_1 = A_0 u \cdot \log \frac{y_2}{y_1} = A u. \quad (11)$$

or:

$$u_* = \frac{u_2 - u_1}{A_0}$$

Careful experiments by Nikuradse on rough pipes flowing full with the assumption that the universal constant described by Karman was 0.4 yielded the constants needed for application of this theory. Nikuradse determined that constant  $A_0$  can be taken as 5.75 and that  $B$  is 8.5. It follows that:

$$u_* = \frac{u_2 - u_1}{5.75} \quad (12)$$

substituting:

$$u_* = \sqrt{\frac{\tau_0}{\rho}} \quad (13)$$

results in the expression for boundary shear stress:

$$\tau_0 = \rho \left( \frac{u_2 - u_1}{5.75} \right)^2 \quad (14)$$

The results of these tests were compared to theoretical boundary layer thickness calculated with equation (8). The shear stress was determined from the measured velocity distributions by plotting the points on semi-logarithmic paper. The velocity distributions should plot on a straight line and the slope of this line is related to the shear stress by equation (14). These theoretical equations are often used to describe boundary layer development. For comparison purposes, measurements taken in these tests were used in the above formulas to gain insight into the flow development length.

## 2.2 Uniform Flow Equations

The study of frictional resistance to flow in open channels follows two approaches. First, the empirical approach is represented by well known formula like Manning's and Chezy equations. These expressions have been applied to

a wide variety of channel shapes and to a broad spectrum of flow conditions and are favored by many engineers for their simplicity.

The second approach is theoretical and is based primarily on the work of Von Karman, Prandtl, and Nikuradse done in the early part of the twentieth century. The logarithmic expressions commonly used for flow resistance and velocity profile formulations are based on this work.

### 2.2.1 Empirical Approach

One of the earliest attempt to formulate the resistance to flow in open channels was by Antionne Chezy (in Chow, 1959). His well known resistance formula:

$$C = \frac{V^2}{(RS)} \quad (15)$$

or:

$$V = C\sqrt{RS}$$

where: C = Chezy's coefficient of resistance

V = mean velocity of flow

R = hydraulic radius = A/P

A = cross sectional area occupied by the flow

P = wetted perimeter of the channel

Various researchers have attempted to describe Chezy's coefficient. Ganguillet and Kutter (in Chow, 1959) devised a complicated formula for C which depended on channel slope, hydraulic radius, and Kutter's n. Bazin (in Chow) and Powell (1950) also developed formulas but these have not been widely used.

Manning (1891) reported the equation which would later bear his name and is currently written in the SI form:

$$V = \frac{R^{2/3} S^{1/2}}{n} \quad (16)$$

Where: n = Manning's n

R = hydraulic radius (m)

S = slope of the hydraulic grade line

= slope of the pipe invert for uniform flow

V = average velocity of flow (m/s)

Manning's coefficient of resistance has gained considerable recognition. Manning's n is not solely dependent on the relative roughness of the channel wall. For a given roughness, n has also been reported to be dependent on slope, pipe diameter, and depth of flow (hydraulic radius). Johnson (1944) states that Manning's n decreases as the normal depth to pipe diameter ratio (y/D) increases. However Camp (1944) states that there is not enough information in Johnson's paper to prove this. The work of

Wilcox (1924) does show that Manning's  $n$  decreases as  $y/D$  increases indisputably. As stated by Powell (1946) in his conclusions:

"It is too much to expect that formulas like Kutter's or Manning's formulas can be expected to handle all cases that arise if  $n$  is considered to depend on roughness only."

Schmidt (1959) found that Manning's  $n$  varied with the depth of flow. Straub and Morris (1950) found an increase in the value of Manning's  $n$  with an increase in the pipe diameter when the pipes were flowing full. The pipes they tested at the St. Anthony Falls Laboratory were commercially available/precast concrete pipes. The American Society of Civil Engineering (ASCE) Task Committee (1963) studied open channel flow to determine the range of suitability for each of the accepted resistance equations and stated the following with respect to Manning's equation:

"The Manning equation is suitable only for fully developed, hydraulically rough flow".

Bloodgood and Bell (1961) found that slope, pipe size, and discharge were all significant in determining Manning's  $n$  values. They reported a decrease in Manning's  $n$  with an increase in the channel slope. The factor showing the strongest correlation with the variation in Manning's  $n$  was

the depth to diameter ratio. Chow (1959) has shown that the Chezy formula and Manning's formula are related by the following expression:

$$C = \frac{R^{1/6}}{n} \quad (17)$$

Chow noted that the value of the exponent in Manning's equation was derived from Bazin's data. The actual value of the exponent of the hydraulic radius varies between 0.6499 and 0.8395 for various shapes of surface roughness. For this reason the above equation is sometimes written in the more general form:

$$C = \frac{1}{n} R^a \quad (18)$$

in which  $y$  is a variable. Pavlovskii (in Chow, 1959) used the formula:

$$a = 2.5\sqrt{n} - 0.13 - 0.75\sqrt{R}(\sqrt{n} - 0.10) \quad (19)$$

for metric units where:

$a$  = the variable exponent for the hydraulic radius ( $R$ ) shown above and

$n$  = Manning's  $n$

The equation is valid when the hydraulic radius ( $R$ ) is between 0.1 and 3.0. For practical purposes it can be written as follows:

$$\alpha = 1.5\sqrt{n}$$

for  $R < 1.0$  m

$$\alpha = 1.3\sqrt{n}$$

for  $R > 1.0$  m

In summary it seems practical to use Manning's formula only for fully developed, fully rough flow conditions.

### 2.2.2 Theoretical Approach

Weisbach (reported in Rouse, 1957) first proposed the dimensionless friction coefficient ( $f$ ) which was dependent on the flow dynamics (Reynolds number) and on the equivalent roughness as originally presented by Nikuradse. As stated in the ASCE Task Force (1963):

"Darcy proposed formulas for the friction coefficient but it remained for Blasius using the boundary layer theory developed by Prandtl to prove that Darcy's  $f$  is dependent on Reynolds number only for smooth pipe flow."

By 1933 Nikuradse and Prandtl had formulated laws for hydrodynamically rough and smooth flow in pipes flowing full. Keulegan (1938) used hydraulic radius as the characteristic length to replace the pipe diameter used by Nikuradse to generalize the full pipe flow equations to include open channel flow in pipes. He presented the following well known formulae:

## (1) Smooth Flow:

$$V = V_* \left( 3.25 + 5.75 \log \frac{RV_f}{\nu} \right) \quad (20)$$

where:  $V_*$  = friction velocity

$f$  = Darcy's  $f$

$R$  = hydraulic radius

$$V_* = \sqrt{gRS} \quad (21)$$

$$= \frac{(V\sqrt{g})}{C}$$

$$C = \sqrt{\frac{(8g)}{f}} \quad (22)$$

so:

$$C = 4\sqrt{2g} \log \frac{(R_*\sqrt{8g})}{2.51C} \quad (23)$$

or:

$$\frac{1}{\sqrt{f}} = 2 \log \frac{(R_*\sqrt{f})}{2.51} \quad (24)$$

where:  $R_*$  = Reynold's number =  $\frac{RV}{\nu}$

The other variables are as previously defined.

## (2) Rough Flow:

$$\frac{1}{\sqrt{f}} = \frac{C}{\sqrt{8g}} = 2 \log \frac{(12R)}{k_s} \quad (25)$$

where:  $k_s$  = equivalent sand grain roughness

Colebrook (1938) published the Colebrook-White equation describing flow transition between the hydrodynamically smooth and rough equations of Nikuradse. This transition equation lacks the characteristic "dip" shown in Nikuradse's data and is useful for describing the flow in commercial pipes which is characterized by random surface roughness elements.

$$\frac{C}{\sqrt{8g}} = -2 \log \left( \frac{k_s}{(12R)} + \frac{2.5}{(R_s \sqrt{f})} \right) \quad (26)$$

The transition region is usually defined by:

$$4 < \frac{V \cdot k_s}{v} < 100$$

A variety of friction coefficients have been presented in the literature. However, the most popular for investigations of open channel flow in pipes are the equivalent sand grain roughness, Darcy's  $f$ , Chezy  $C$  and Manning's  $n$ .

### 2.2.3 Previous Studies

Keulegan's work triggered a great deal of interest in flow resistance in open channels and a number of very good studies focussing on pipes have been published.

Wilcox (1924) tested 8 inch vitrified clay pipes and found that the effects of surface roughness on Chezy C tend to decrease with increased slope. His results also show a decrease in resistance (an increase in Chezy C) with increasing depth to diameter ratios. Wilcox used the salt-velocity method of velocity measurement. Johnson (1944) studied four domestic sewers to determine Kutter's n.<sup>1</sup> Sewer "D" tested by Johnson had a circular cross section and his conclusions regarding this sewer were as follows:

- (1) Higher values of Kutter's n should be used for low flows in sewers than for larger flows of greater depth.
- (2) Kutter's n values are higher than those reported by others for clean water flow in sewer pipes, probably due to the thin layer of slime and grease deposited on the sewer walls.

Johnson reported Kutter's n values between 0.0146 and 0.0201, the latter being for a circular brick-lined sewer. Wilcox, on the other hand found much lower n values of

---

<sup>1</sup> Kutter's n was first devised as a method to determine Chezy C. Chow (1959) makes no distinction between Kutter's n and Manning's n.

0.0095 for the vitrified clay pipe and 0.0102 for concrete pipe. Coulter (1944) explains that variation in Manning's n is caused by fixing the exponents of the hydraulic radius and slope. Therefore, when n is determined for various depths of flow in a given channel, it causes n not only to reflect channel roughness, but also changes in the hydraulic radius. Ramser (1944) shows results from a 30 inch concrete tile line and also found a consistent decrease in the value of Kutter's n with an increase in flow and the magnitude of n were close to Johnson's values.

Powell (1946) found the following relationship based on the equation set forth by Keulegan for a smooth semi-circular channel:

$$C - c_s = 32.65 \log \frac{R_e}{C} + 21.69 \quad (27)$$

where C = Chezy's C

$R_e$  = Reynold's number

$c_s$  = shape correction factor

Bloodgood and Bell (1961) found that variation in Manning's n were all related to the depth to diameter ratio. The values they reported are listed in table 1.

Ackers (1961) recommends the following form of the Colebrook-White equation in imperial units for circular conduits flowing part full:

$$V = -\sqrt{32gRS} \log \left( \frac{k_s}{14.8R} + \frac{1.255v}{R\sqrt{32gRS}} \right) \quad (28)$$

Ackers (1958) shows that within the range:

$$7 < \frac{4R}{k_s} < 130$$

that Manning's equation is within two percent of the logarithmic expression for fully rough flow. Ackers also compares Manning's  $n$  to the equivalent sand grain roughness for fully rough flow (imperial units) as follows:

$$n = \frac{1}{32} k_s^{0.67} \quad (29)$$

Results from the tests of Straub and Morris (1950) show equivalent roughness values ( $k_s$ ) for various precast concrete pipes as shown in table 2.

Ackers (1961) evaluated the data in the paper by Straub and Morris (1950). He found that the apparent roughness was greater under part-full flow conditions than full bore tests and gives the following possible explanations:

- (1) Transformation of the general section by using hydraulic radius may be an oversimplification.
- (2) There may be a real change in the effective roughness as the wetted perimeter changes.
- (3) There are additional energy losses under free surface

flow because of surface waves which are dependent on the Froude number.

(4) There are secondary currents produced which use energy and help to retard the flow.

(5) The measured depth may not accurately represent the mean water level due to (3) and (4) above.

Powell and Posey (1959) did extensive tests on open channel flow in a triangular flume and, contrary to popular opinion at the time, found Manning's equation to be as reliable as the logarithmic expressions for both smooth and rough triangular channels. Powell (1946) obtained solutions for open channel flow similar to those obtained for full pipe flow by Nikuradse, and defined his own roughness coefficient. However, as pointed out by Thisse (1951), there was no method mentioned by Powell to obtain the roughness height. As a result Powell's work has not gained wide recognition.

#### 2.2.4 Effects of Aging on In-situ Sewers

Wilcox (1924) recommended that tests should be done on actual sewer installations to determine the effect on resistance from fouling and silting. Johnson (1944) carried out tests on in-situ sewers and found Manning's n values

significantly higher than Wilcox's laboratory results.

Johnson states that the higher resistance was probably caused by a build-up of slime and grease in the sewer.

Schmidt (1959) studied sewers under actual field conditions and found Manning's  $n$  varied with changes in the depth of flow. However, deposits or other factors which alter the invert surface of the sewer probably cause a greater variation in Manning's  $n$  than changes in the depth of flow.

Ackers (1959) realized the need for more field information and undertook a study of hydraulic head losses at sewer manhole junctions and recommended that more work be done to measure friction coefficients in old sewers.

Ackers, Crickmore, and Holmes (1964) presented a survey of field tests done in England and combined with previously published data provided a good basis for design of new sewers considering the effects of aging on surface roughness in the sewers. The primary causes of increased roughness with aging are:

- (1) slime build-up in the sewer
- (2) deposits of sediment in the pipe invert
- (3) joint offsets and alignment
- (4) degradation of the interior pipe surface

Ackers found a range of  $k_s$  values from 0.00003 feet in a clean 15 inch concrete pipe to 0.4 feet in a slimed 27 inch diameter concrete pipe with sediment deposits on the invert. Both of these sewers had been in operation for only two years. Fifty percent of Ackers' equivalent roughness results lie in the range of 0.001 to 0.01 feet. The median value is 0.006 feet. For precast concrete a typical equivalent roughness value was 0.005 feet with sliming up to 5 mm thick. The effect of sliming was stated concisely by Ackers et al (1964):

"With normal workmanship a sewer when new will probably have an equivalent roughness of about 0.005 feet. With a slime layer not exceeding 5 mm the  $k_s$  values may deteriorate to 0.005 feet, while with a thickness of up to 25 mm a  $k_s$  value of 0.05 would be appropriate".

Pomeroy (1967) reported the following factors effecting the flow velocity in sewers:

(1) Fouling of Sewers

Low flow velocities are both cause and result of fouling of the sewer. He defines:

$$J = S^{0.41} Q^{0.24} \quad (30)$$

as a useful velocity promoting function. The velocity function ( $J$ ) should exceed 0.03 or 0.35 for at least an hour

each day to prevent accumulations of solids in the sewers. Even if this criterion is met, the sewer may not maintain good hydraulic performance indefinitely without cleaning.

### (2) Critical Depth Effects

Pomeroy proposes the equation:

$$V = KS^{0.41} Q^{0.24} \quad (31)$$

where: K = Pomeroy's resistance coefficient  
to represent the velocity in a pipe up to a depth to diameter ratio of 0.85.

### (3) Relative Flow Depths (y/D)

Pomeroy compared Manning's n and Hazen-Williams C with his own K with respect to relative depth effects (Froude number between 0.9 and 1.4). He found Manning's n was considerably lower for low flows and that equation (33) was effected the least by changes in relative dept

#### 2.2.5 Summary

Following the work published by Keulegan (1938) research in open channel resistance formulae focused on the logarithmic equations describing turbulent flow in pipes. Researchers compared the analytical logarithmic expressions with the traditional empirical equations.

The confusion about friction factors in open channels prompted the American Society of Civil Engineering to form a Task Committee (1963) to study the problem. The committee recommended the following formula for steady fully developed flow in open channels:

$$S = \frac{f V^2}{4R^2 g} \quad (32)$$

where  $S$  = slope of the hydraulic grade line and the channel bottom. These must be equal by definition

$f$  = if the flow is steady and uniform.

friction coefficient as described by

$R$  = Darcy-Weisbach equation. The friction coefficient

$V$  = depends on Reynolds number.

hydraulic radius (m)

average velocity of flow ( $m^3/s$ )

The following relationships hold between the friction factor ( $f$ ) and other coefficients:

$$C = \sqrt{\frac{8g}{f}} \quad (33)$$

$$n = R^{1/6} \sqrt{\frac{f}{8g}} \quad (34)$$

The ASCE committee recommended the use of the friction coefficient  $f$  over the other coefficients. Manning's equation should be applied only in cases of fully rough

turbulent flow. Unfortunately, it is not always easy to determine if the channel is behaving as hydraulically smooth, partly rough, or fully rough and it is not certain that partly rough gravity flow will behave the same as transition pipe flow.

### 3 Apparatus and Procedure

#### 3.1 Experimental Set-up

Three concrete and three plastic pipes were tested. The nominal inside diameters of the concrete pipes were 200, 250 and 380 mm (8, 10 and 15 inches). The nominal inside diameters of the plastic pipes were 200, 250 and 457 mm (8, 10 and 18 inches). A complete listing of the pipe dimensions, ASTM Specifications and manufacturers is given in appendix A. Each concrete pipe section was supplied with one manometer tapping. Observation ports were drilled 180 degrees from the pressure tappings in the spigot end of each pipe section. The plastic pipes which are manufactured in longer sections (4.13 m compared to 1.28 m for the 200 mm pipes) were supplied with a pressure tapping and a observation port at each end. After installation it was necessary to cut extra observation ports in all the pipes to facilitate boundary layer measurements and to obtain more information in the fully developed flow region.

Pipes to be tested were installed in a 37 m long tilting flume (see figure 1 and plate 1). The 0.9 m wide by 0.8 m deep fiberglass lined flume was supported on a steel joist framework. Twelve 32 mm threaded stainless steel legs supported the steel framework and were turned with a system of gears and chains driven by an electric motor. The gears

were sized such that the flume swivelled on a pin connection at the upstream end while maintaining a linear bed profile. Lateral support for the flume was provided by steel I-beams embedded in the concrete floor of the laboratory. The maximum flume slope was one percent. The slope of the pipe invert in the flume was measured independently using a surveyors level attached to the ceiling of the laboratory.

Pipes to be tested were placed in the flume on wooden cradles as shown in figure 1. The cradles were designed so that the pipes fit snugly into semicircular notches in the top of each cradle. Cradles were the same width as the inside of the flume, which in theory, should have provided a straight pipe alignment. In practise due to slight variations in the cradle dimensions it was necessary to do some minor adjustments to obtain accurate alignments. The concrete pipes were placed with a cradle under each joint. The plastic pipes were supported at each joint and at the mid-point of each section to prevent vertical deflections.

Two systems of magnetic flow meters, supply lines and valves were used to supply water to the flume. For low flows (0 to 10 L/s) a small pump, 75 mm supply line and a 75 mm magnetic flow meter were used. Higher flows (up to 250 L/s) were produced by a larger pump with a 300 mm supply line and a 200 mm magnetic flow meter. Together the systems could

produce up to 260 L/s. A calibrator was used to set the ranges of discharge corresponding to the voltage output from the magnetic flow meters so that the flow rate could be read directly from a voltmeter. The specifications for the pumps, magnetic flow meters and calibrators are shown in appendix B. Both supply lines discharged into a head tank as shown in figure 1. The head tank was large enough to dissipate the turbulence generated by the supply lines and supply constant head at the pipe inlet.

A vertical plywood head wall at the pipe inlet was used to restrict the flow. Concrete pipes were mounted flush with the head wall with the socket inside the bell on the first section mortared to provide a smooth rounded entrance. Plastic pipes were allowed to project slightly into the head tank to alleviate sealing difficulties around the head wall. The re-entrant inlets submerged sooner than the flush concrete inlets. In the case of the 250 mm plastic pipe the head needed to obtain almost full flow in the pipe overflowed the head tank, so an aluminum bell-mouth inlet was installed on the pipe. The 457 mm plastic pipe was not a problem because the limiting factor was the discharge available from the supply systems. Table 3 lists information such as the number of pipe sections used, test section length, and inlet conditions. The flow from the test section discharged freely to a outlet box.

Water surface fluctuations within the test pipes were monitored with capacitance depth probes (see Appendix B for specifications) which provided continuous output to a strip chart recorder. The pressure tappings in the invert of each pipe section were connected with Tygon tubing to a sloping manometer board equipped with a metric grid and scale.

### 3.1.1 Boundary Layer Measurements

Velocity profiles were done in the 200 mm concrete pipe for mild slopes of 0.2 percent or less and in the 380 mm concrete pipe at a slope of one percent. Due to time restrictions developing flow was not analyzed for intermediate ranges of slope or in the plastic pipes.

The 200 mm concrete pipe was used for boundary layer analysis for mild slopes. The upstream half of the pipe installation was used for these measurements. Extra 75 mm ports were drilled into the first five pipe sections downstream of the inlet using a diamond bit coring machine reducing the port spacing to 1.2 m. Velocity measurements were done using a 1.70 mm Prandtl pitot tube and a Validyne model DP45 pressure transducer sensitive to pressure differences between 1 and 30 mm of water (maximum velocities less than 0.8 m/s). The voltage signal from the pressure transducer was recorded on a strip chart recorder for later analysis. A vernier scale was used to position the pitot

tube and the profiles were measured in a vertical alignment along the central axis of the pipe. Measurements were taken starting at the pipe invert and moving towards the surface. A greater density of velocity readings were taken near the invert to gain as many readings as possible near the boundary. Depth readings were adjusted upward by one half of the diameter of the pitot tube.

Boundary layer measurements in the 380 mm concrete pipe were done at a slope of one percent. Again, extra 75 mm observation ports were drilled in the crown of the pipes to facilitate velocity measurements. Four Prandtl pitot tubes were used varying in diameter from 2.4 to 3.2 mm. The pitot tubes were connected with rubber tubing to sloping differential manometer boards to evaluate the velocity head difference. The measurements were recorded by visual observation of the manometers.

### 3.1.2 Uniform Flow Measurements

Apparatus used for the uniform flow region measurements were the sloping manometer board, a point gauge attached to a vernier scale mounted on a transverse member which rested across the sides of the flume, two Delavan capacitance depth probes, and the magnetic flow meters.

### 3.1.3 Measurement of Pipe Characteristics

Joint gap and alignment were measured in the 250 mm concrete pipe. The joint gap was measured using a metric scale ruler and the joint offset was determined by pressing a lump of modeling clay into the joint. The clay was carefully removed and the offset could be measured using a pair of vernier calipers. Photographs were also taken inside the pipe with and without water flowing (plate 2).

To measure the roughness elements on the inside surface of the pipe sections, a device incorporating a linear voltage displacement transducer (LVDT) was used. A fine-tipped carbon steel stylus was attached by an arm to the LVDT and this assembly was mounted on a threaded shaft. The shaft was turned by a six volt electric motor causing the LVDT and stylus assembly to be dragged across the surface of the pipe specimen. Samples of the concrete and plastic pipes tested were cored from the pipes. Output from the LVDT was magnified fifty-five times and recorded on a strip chart recorder. Calibration of the LVDT was done with an inside micrometer accurate to 0.001 inches. A schematic drawing of the apparatus is shown in figure 2 and plate 3 shows the device in use.

The micrometer was also used to measure the inside diameters of all the pipes tested. Out-of-roundness and variation of pipe diameter within and between pipe sections was measured. This information is included in Appendix C.

### 3.2 Procedure

#### 3.2.1 Pipe Assembly

Pipe sections were installed in the flume by hand or with an overhead crane. Pipes were placed with the bell ends facing upstream as recommended by Neale and Price (1964). Rubber gaskets and standard gasket lubricant were used to seal the joints. Pipes were rotated to ensure that the pressure tappings were at the invert. Horizontal alignment was done using string lines and a surveyors level to obtain an alignment which varied less than 1 cm.

The pipe profile was surveyed using a level. Once the zero slope was established a scale was mounted on the outlet box and marked for slopes of 0.001, 0.002, 0.0025, 0.0035, 0.004, 0.005, 0.006, 0.008, and 0.010. The bed slope and profile were checked with the level at various times during the study to verify that the slope scale was accurate.

### 3.2.2 Uniform Flow Measurements

All experiments were conducted in a similar manner. The desired flume slope was set using the slope scale on the outlet box. The small pump discharge was set at a predetermined level, calculated assuming a value for Manning's n. Manometer tubing from the pipe pressure tappings was flushed of all air bubbles. Discharge from the magnetic flowmeter was recorded. Output from the depth capacitance probes was monitored until the water surface reached an equilibrium depth. The manometer readings for the entire line were recorded. Figure 3 shows typical capacitance probe output photocopied from strip chart record.

By visual observation of the manometer board, the region of uniform flow was selected. Ideally this was represented by a linear surface profile in the middle third of the profile for subcritical flow (Froude number less than unity) and increased to the latter two thirds of the profile for supercritical flow (Froude number greater than unity). Developing flow was characterized by curvature in the upstream portion of the profile, and was excluded from the test section. Plates 4 and 5 show typical manometer profiles obtained during tests on the 250 mm concrete pipe.

Transition flow conditions ( Froude number close to unity) presented problems due to the unstable nature of the flow. Standing waves developed in the surface profile in the pipes, best illustrated by plate 5. In these cases the middle third of the profile was selected for measurements.

A point gauge equipped with a vernier scale was used to measure the water depth. The water surface and the pipe invert in the uniform flow region were recorded at ten locations for each discharge to dampen the effects of surface roughness. At the end of the test run the capacitance probe output was checked for consistency during the test then the discharge and manometer readings were recorded again. The discharge was then increased and process repeated. When the required discharge exceeded the capacity of the small pump it was shut down and the valves closed to prevent leakage into the head tank, then the large pump was started and allowed to stabilize.

In all eight discharge settings were used for each of the nine slopes for each of the six pipes giving a total of 432 tests. A typical data sheet for one test is included as Appendix D.

### 3.2.3 Boundary Layer Measurements

During the boundary layer measurements the discharge and bed slope were held constant. Velocity profiles for

subcritical slopes were done using a small diameter Prandtl pitot tube. The pitot tube was positioned along the central axis of the pipe, then lowered to the pipe invert using the screw mechanism attached to the vernier scale (the central axis of the pipe was marked during the original pipe installation). Prior to recording velocity measurements the plastic tubing was allowed to drain to flush all air from the lines since the transducer was found to be extremely sensitive to air contamination. The transducer required from 3 to 5 minutes to stabilize when the pitot tube was repositioned.

Velocity readings were started at the pipe invert. The first reading was taken when the tip of the pitot tube began to vibrate against the bottom of the pipe. If the pitot tube was allowed to rest firmly against the bottom the tube stem tended to deflect which would lift the tip off the bottom of the pipe resulting in erroneous readings. A slight deflection was sufficient to cause a significant change in the velocity reading close to the pipe wall. After the transducer had stabilized, 5 and 10 minutes of continuous readings were recorded on the strip chart. Any individual reading from the transducer could vary as much as fifty percent from the true average because the transducer was sensitive to the turbulence within the flow. By analysis of

the strip chart printout it was possible to draw in an average line for the record. A typical strip chart record from the transducer is shown in figure 4.

To produce a smooth velocity profile readings were concentrated near the boundary where the greatest velocity gradient occurred. A minimum of 10 readings were taken for each profile. To obtain accurate displacements, one half the pitot tube diameter was added to all measured displacements above the pipe invert. The pitot tube was moved upstream of the pressure tappings to prevent surface irregularities from influencing the flow. The uppermost measurement in the profile was taken 3 to 5 mm below the water surface to prevent air contamination of the pitot tube. Before and after velocity measurements the pipe invert and water surface were measured and the profile of the water surface was recorded from the sloping manometer board.

The first sets of velocity measurements done at mild slopes were concentrated at the upstream end of the pipe with only one set of measurements extended to the mid-point of the installed pipes. These measurements were a learning experience and indicated that the measurements should be extended further down the pipe.

The velocity measurements done at the steeper slope were done for the entire length of the installed 380 mm concrete

10

pipe to obtain a more complete picture of the development length. Since the growth of the boundary layer did not appear to agree with the theories of boundary layer growth on a flat plate of zero incidence, the only way to detect the location where the flow became fully developed was by direct inspection of the velocity profiles.

It was found that the larger diameter Prandtl pitot tubes required about 10 minutes to stabilize when moved to a new position in the flow. Due to the large number of readings per profile and the number of ports, four setups including pitot tube, rubber tubing and manometer board were necessary to reduce the time needed to complete the set of profiles for the whole line. The method used to do velocity measurements with the larger pitot tubes was the same as with the smaller diameter tubes. Velocity heads were read from the manometer boards which were found to be much less sensitive to the flow turbulence than the finer pitot tube-transducer setup.

### 3.2.4 Roughness Measurement

The samples used for the surface roughness analysis were cored from the sections of the pipe used for testing. The samples were circular discs about 75 mm in diameter. Each sample represented one pipe section. It was noted that roughness was variable in any one pipe section and even more

variable between sections. Typical examples of roughness samples can be seen in plates 3. By using as many samples as possible it was hoped to gain a meaningful average value of equivalent roughness height.

Sample surface roughness measurement was done by mounting the sample in a vice. The sample had to be levelled to prevent the profile from being tilted. This was done using a 150 mm carpenters level which proved accurate enough to produce a level trace on the strip chart. The stylus of the roughness measuring device was placed on the sample by adjusting the leg screws of the device frame. In this way the stylus was maintained within the calibrated displacement range.

The stylus was placed at the start of the traverse and this point was marked with felt-tipped pen. The motor was then switched on which caused the stylus to be dragged across the sample. The variation in the surface profile of the sample was detected by the LVDT and converted to output reading on a strip chart recorder. The traverse was completed by switching the motor off and marking the final stylus location on the sample and the corresponding position on the strip chart. The actual length of the traverse was then measured using vernier calipers. This length was marked on the strip chart so that a horizontal scale factor could be calculated. The vertical gain on the strip chart recorder

was calibrated to give a magnification factor of fifty-five. Most traverses were done in duplicate to give a better database for the calculation of root mean squared roughness. When the sample was removed from the vise the overall width of the sample was measured with vernier calipers to check for variability in the wall thickness of the pipes.

The traverse records on the strip charts were analyzed as follows: The traverse (see figure 5 for an example record) length on the strip chart was measured using the vernier calipers. A mean line was drawn through the traverse by eye. Roughness elements were measured as vertical (positive or negative) displacements from this line at 5 mm horizontal intervals which represented 2.5 mm on the sample. A root mean square roughness was then calculated for each traverse and are included in Appendix E. The mean of all the root mean squared roughness for the samples for one size and type of pipe was calculated to give the roughness in millimetres for the pipe tested.

In addition to the above analysis, roughness periodicity was also measured. It was noted when the pipes were first examined that ridges and waves were present on the finished inside surface of both the plastic and concrete pipes. A measure of the ridging was obtained for the concrete pipe using the methods described above. The wavelength of the

waves in the plastic pipes were too long to allow an accurate measurement using the LVDT, so visual measurements were taken using the calipers.

### 3.2.5 Repeatability of Results

Some hysteresis has been observed in flows in sewers carrying foul water. This was reported by Besmehn (1986). The resistance coefficient was found to vary depending on whether the flow in the pipe was increasing or decreasing. The reasons for this were not clear. It was decided to analyze the hysteresis effect for the pipes tested in this study which are carrying clean water with no buildup of slime deposits. This was accomplished by gradually increasing the flow between measurements, then duplicating the set of tests with the discharge decreased between readings. The flow was stable and steady between each measurement. The 250 mm concrete pipe was selected for this analysis. A number of runs which had been done previously were done so that the repeatability of the results as well as the hysteresis effects could be analyzed.

## 4 Formulae Used

### 4.1 Boundary Layer Analysis

The equations used to compare the theoretical growth of the boundary layer to the observed boundary layer growth were given in the literature review. Equation (3) and (5) were used to calculate the displacement and momentum thicknesses by simple numerical integration. The Fortran program used to do these calculations is included in Appendix F. Equation (8) was used to calculate the theoretical boundary layer growth and was used for the measured velocity profiles. The shear stress was determined from the measured velocity distributions by plotting the profiles on semi-logarithmic paper and applying equation (14).

### 4.2 Friction Coefficients

Prior to calculating friction coefficients from the experimental data, two checks were done on the data. First, the percentage total error in the value of Manning's  $n$  was calculated using standard methods of error analysis as described in Taylor (1982). If the error was greater than twenty-five percent then the data was not included in further analysis. The major areas of uncertainty were caused by standing waves on the water surface, (especially at or

near critical flow conditions) and by drawdown of the water surface profile at mild slopes and high depth ratios. The extent of the drawdown ( $M_2$ ) curve was calculated for subcritical flow conditions using the standard step method which is available in Fortran subroutines written by Peterson and Howells (1981).

This was necessary because no tailwater control was used. If the depth at a distance of one half the flume length upstream from the outlet was greater than ninety-five percent of the calculated normal depth (assuming the average value of Manning's  $n$  for the pipe) then the data was included. In practise this resulted in elimination of all the results obtained at a slope of 0.001 and some of the higher discharges at the other mild slopes. The error analysis is included in Appendix G and the subroutines used to check the data are included in Appendix F.

The remaining data was used to calculate the various hydraulic parameters. First, the ratio of average centreline depth to the actual average inside diameter was calculated. The depth used was the average of all the depths taken for that particular run. This was assumed to be the normal depth of flow in the pipe. The average discharge for the run was calculated and the bed slope as indicated by the slope board attached to the flume. Using these parameters the Manning coefficient of resistance ( $n$ ) was calculated using the

following SI equation shown previously as equation (16) and rewritten in a form useful for the measurements from these experiments as follows:

$$n = \frac{AR^{2/3}S^{1/2}}{Q} \quad (35)$$

where:  $n$  = Manning's  $n$

$A$  = cross sectional area of flow ( $\text{m}^2$ )

$$A = \frac{1}{8}(\theta - \sin \theta)D^2 \quad (36)$$

If  $y < D/2$  then

$$\theta = 2\cos^{-1}\left(\frac{r - y_0}{r}\right) \quad (37)$$

If  $y > D/2$  then

$$\theta = \pi + 2\sin^{-1}\left(\frac{y_0 - r}{r}\right) \quad (38)$$

where the angle is expressed in radians

where:  $R$  = hydraulic radius =  $A/P$  ( $\text{m}$ )

$P$  = wetted perimeter ( $\text{m}$ )

$$P = D \frac{\theta}{2} \quad (39)$$

$y_0$  = average centreline depth of flow ( $\text{m}$ )

$D$  = average inside pipe diameter ( $\text{m}$ )

$r$  = pipe radius =  $D/2$  (m)

$s$  = slope of the pipe invert

= slope of the water surface

For convenience of calculation a computer program was used to calculate the hydraulic properties of area of flow, wetted perimeter, and hydraulic radius. The HYEPOL (Hydraulic Engineering Problem Oriented Library) subroutines used were available on the university mainframe and are listed in a publication by Peterson and Howells (1981). A complete listing of the main Fortran programs used to call the HYEPOL subroutines is listed in Appendix F.

To understand where the experimental results fit in comparison to other studies Darcy's friction coefficient was obtained by adapting the Darcy-Weisbach equation for pressurized flow in pipes to a general form for open channels as follows:

$$h = f \frac{LV^2}{2gD} \quad (40)$$

where:  $h$  = head loss over distance  $L$  in a pipeline  
(m)

$f$  = Darcy's friction coefficient

$L$  = length of pipeline under investigation  
(m)

$V$  = average velocity of flow (m/s)

$g$  = acceleration due to gravity ( $m/s^2$ )

$D$  = average inside pipe diameter (m)

since

$$\frac{h}{L} = S,$$

where:  $S_f$  = energy gradient

= slope of the pipe invert

$$S_f = \frac{fV^2}{2gD} \quad (41)$$

For open channel flow conditions  $D$  can be replaced by four times the hydraulic radius so:

$$S_f = \frac{fV^2}{8gR}$$

and for steady uniform flow  $S_f = S$

where  $S$  = slope of the bed

This results in:

$$f = \frac{8gRS}{V^2} \quad (42)$$

which is the Darcy formula for general open channel flow.

The viscous effects on the fluid flow are best observed in a form of the Moody or Stanton diagram, with the friction

coefficient and Reynold's number converted to the appropriate open channel forms. The following Reynold's number was used to obtain these figures:

$$R_e = \frac{4VR}{v} \quad (43)$$

where  $R_e$  = Reynold's number for open channel flow  
 $v$  = kinematic viscosity ( $\text{m}^2/\text{s}$ )  
 $= 1.007 \times 10^{-6} \text{ m}^2/\text{s}$ , for these tests

For comparative purposes the Colebrook-White equation, which spans the transition region between the turbulent smooth and fully rough turbulent flow was chosen. The open channel version of the equation is stated as follows:

$$\frac{1}{\sqrt{f}} = 1.14 - 2 \log \left( \frac{k_s}{4R} + \frac{9.35}{R_e \sqrt{f}} \right) \quad (44)$$

where:  $k_s$  = selected values of roughness to be used for comparison to test results

Due the circular shape of the channel cross section, it was difficult to define a Froude number which described the flow adequately over the full range of depth ratios ( $y/D$ ). The various formulations are shown below.

$$F = V \sqrt{\frac{y}{gA}} \quad (45)$$

$$F = \frac{V}{\sqrt{gy}} \quad (46)$$

$$F = \frac{V}{\sqrt{gP}} \quad (47)$$

$$F = \frac{V}{\sqrt{gR}} \quad (48)$$

where:  $F$  = Froude number

$V$  = mean flow velocity

$y$  = normal depth

$A$  = area of flow

$P$  = wetted perimeter

$R$  = hydraulic radius

The Froude number which includes the channel top width, which is very useful for open channel flow in rectangular or natural channels is not applicable for circular sections because as the pipe reaches the pipe full condition the Froude number approaches zero as can be seen from observation of this equation below.

$$F = \sqrt{\frac{Q^2 T}{g A^3}} \quad (49)$$

Where:  $T$  = the channel top width.

The above Froude number which includes normal depth appeared to represent the actual flow conditions the best. A Froude number of unity was assumed when the flow velocity prevented a surface disturbance from moving upstream.

#### 4.3 Hydraulic Elements

The dynamic hydraulic elements of flow were compared to standard references which are based on Manning's equation as shown in Fair, Geyer and Okun (1966) as follows:

(1) For Manning's n considered constant:  $n_p/n_f = 1.0$  then:

$$\frac{V_p}{V_f} = \frac{n_f}{n_p} \left( \frac{R_p}{R_f} \right)^{\frac{2}{3}} \quad (50)$$

and

$$\frac{Q_p}{Q_f} = \frac{n_f}{n_p} \left( \frac{A_p}{A_f} \right) \left( \frac{R_p}{R_f} \right)^{\frac{2}{3}} \quad (51)$$

where: subscript p refers to part-full flow

subscript f refers to full-pipe flow

The other variables are as previously defined

For constant n the ratio of the hydraulic elements depends on the geometry of the flow alone. There is no evidence indicating that the exponents of R and S should be constant. A more general representation of the formulas would be:

$$\frac{Q_p}{Q_i} = \frac{A_p (R_p)^n (S_i)^n n}{A_i (R_i)^n (S_i)^n} \quad (52)$$

Another method of plotting the hydraulic elements was shown by Pomeroy (1967). He avoids the use of the hydraulic radius with his equation:

$$V = K S^{0.41} Q^{0.24} \quad (53)$$

where:  $K$  = Pomeroy's friction coefficient

He found this equation was a much more satisfactory representation since the  $K$  value remained more constant than any of the other so-called constants (ie. Manning's  $n$  or the Chezy  $C$ ).

In a previous article Pomeroy presented this equation in the form:

$$\frac{V_p}{V_i} = m \left( \frac{Q_p}{Q_i} \right)^m \quad (54)$$

which fits Camp's (1946) data best. With coefficients based on a depth to diameter ratio of 0.5 and  $V_p/V_i = 0.88$  yields:

$$\frac{V_p}{V_i} = 1.093 \left( \frac{A_p}{A_i} \right)^{0.316} \quad (55)$$

$$\frac{Q_p}{Q_i} = 1.093 \left( \frac{A_p}{A_i} \right)^{1.316} \quad (56)$$

These equations are applicable to flow conditions with depth to diameter ratios less than 0.86.

Applying Darcy's equation to obtain ratios of the hydraulic elements for part-full pipe flow compared to full pipe flow yields the following equations:

$$\frac{V_f}{V_s} = \sqrt{\left(\frac{f_p}{f_s}\right)\left(\frac{R_f}{R_s}\right)} \quad (57)$$

where:  $f$  = Darcy's friction coefficient

## 5 Results

### 5.1 Boundary Layer Development

#### 5.1.1 Mild Slopes

The results of the five boundary layer tests done on the 200 mm concrete pipe at mild slopes are given in table 4. These results were used to plot actual versus theoretical boundary layer growth and are shown in figures 6 to 8. Due to the poor correlation between the theoretical boundary layer growth and the results obtained, perhaps the best information about the boundary layer development is indicated by the velocity profiles shown in figures 9 to 11. Direct observation of figure 11 illustrates that the velocity profiles begin to superimpose on themselves at about 8 m from the pipe inlet. It is interesting to note that the secondary currents also appear to be fully developed at this point as indicated by the constant curvature of the velocity profiles towards the free surface.

#### 5.1.2 Steep Slopes

Using the same technique for the steep slope in the 380 mm concrete pipe the velocity profiles began to superimpose about 14 to 18 meters from the inlet as shown in figure 11. This is also the approximate location where the theoretical boundary layer growth intersects the free surface as shown

in figure 8. Converting this distance to a dimensionless ratio of the distance from the pipe inlet to the pipe diameter ( $x/D$ ) yields a value of 39.5. Figure 12 is a plot of the depth ratio ( $y/D$ ) compared to the distance ratio ( $x/D$ ). Most of the surface fluctuations in the boundary layer tests done at both mild and steep slopes are greatly reduced at a distance ratio of 40. This converts to a development length of 8 m for the 200 mm pipe and 10 m for the 250 mm concrete pipe. Again the growth of the boundary layer along the central axis of the pipe is masked by the developing secondary currents. Similar to the mild slope tests, there is a significant disparity between the theoretical boundary layer growth and the measured growth. Table 4 (run 6) gives a complete listing of the measured and calculated parameters for the steep slope test.

No velocity measurements were taken in the plastic pipes. However, the surface profiles shown in figures 13 to 16 indicate that the profiles were relatively linear 10 m from the outlet. It was assumed that the channel length required for the flow to become fully developed in the plastic pipes also occurred at a distance ratio of 40. This is a rough estimate at best without the support of detailed velocity measurements.

The boundary shear stress was plotted and is shown in figure 17. The shear stress displays a gradual reduction in the direction of flow, but the trend is very erratic.

### 5.2 Friction Factors

A tabular listing of all the results of the uniform flow experiments are included in Appendix H. The graphs of Manning's  $n$  plotted versus depth ratio (figures 18 to 20) indicate that the depth ratio and slope influence the magnitude of Manning's  $n$  in the range of flow conditions tested. The slope effects tend to be greatest at low depth ratios and disappear at the higher depth ratios. At low depth ratios mild slopes produce significantly larger values of Manning's  $n$  than the steep slopes, especially for the concrete pipes tested. Table 5 shows the average values of Manning's  $n$  calculated for depth ratios greater and less than 0.25 which was chosen arbitrarily to divide the results. The 450 mm plastic pipe was an anomaly. It demonstrated very little dependence on the depth ratio. Whereas Manning's  $n$  values tended to decrease slightly as the depth ratio increased for the other pipes,  $n$  values increased slightly with increasing  $y/D$  values for the 450 mm plastic pipe. Figures 21 to 23 show the dispersion in the values of Manning  $n$  with depth ratio.

To gain a better understanding of the dynamics of the flow conditions, Moody diagrams were plotted for all the uniform flow tests. The results are shown in figures 24 to 26. The 200 and 250 mm PVC pipes generally follow the smooth curve of Nikuradse. That is, Darcy's friction factor decreases with increasing Reynold's number. The 450 mm Spiroloc PVC pipe shows some fluctuation from the smooth curve at higher Reynold's numbers. The trend appears to be toward fully rough flow; characterized by independence from the Reynold's number. However, as the velocity increases the friction factor again begins to decrease. This is a well defined trend at channel slopes of between 0.006 and 0.01. The other slopes show scattered results due to the transition flow conditions mentioned previously, which caused standing waves to develop in the pipe. The reduction of the value of the friction coefficient could be due to the spiral pattern of the ridges on the inside of the pipe which develops a more pronounced spiral flow pattern at higher Reynold's numbers.

Friction factors for the concrete pipes were generally parallel and above the smooth curve of Nikuradse at low Reynolds numbers. At higher Reynolds number the friction factors tended to show signs of independence from Reynolds number as would be expected for hydraulically rough surfaces. A noticeable dip occurred in plots of the friction

factor for the 380 mm concrete pipe, similar to those shown on the original work by Nikuradse. This was not expected for the pipes tested due to the random nature of the roughness elements in commercially precast concrete pipes.

The two smaller diameter concrete pipes do not show the dip in the friction factor as noticeably as the large concrete pipe. However, Chow (1959) shows similar trends in results for Bazin's and Varwick's data on triangular and circular flumes respectively. In addition the values plotted in Chow's figure also lie above the Prandtl-Von Karman smooth function. Morris (1955) explains the dip in the friction factor as a transition in the flow to a higher energy loss flow. As the Reynolds number increases the flow may change from a quasi-smooth flow to wake interference flow and then to an isolated roughness flow. The waviness found in the pipes tested could possibly produce the same effects as the isolated roughness elements studied by Morris.

### 5.3 Hydraulic Elements

The plots of the hydraulic elements (figures 27 to 29) display a definite spread in the data especially with respect to the ratio of the part-full velocity to the full-pipe velocity ( $V_p/V_f$ ). The range of  $V_p/V_f$  at a depth to diameter ratio, ( $y/D$ ) of 0.5 is from 0.9 to 1.0 for the

concrete pipes and 0.9 to 1.06 for the plastic pipes. The proportional discharge ( $Q_p/Q_t$ ) tends to follow the theoretical curve much more closely than the proportional velocity. The  $Q_p/Q_t$  experimental points show a significant difference with theoretical curve for  $y/D$  values greater than 0.8. The experimental  $Q_p/Q_t$  values tend to be greater than unity which disagrees with theory.

#### 5.4 Repeatability of Results

The results of the tests done to determine test repeatability shows good correlation between the rising limb of the curves in figure 30 and the falling limb. Therefore, hysteresis effects were not present for the flow conditions tested. The only discrepancy occurred at a slope of 0.001 for a depth to diameter ratio of 0.45 which there is no clear reason for. The results of these tests also compared closely to the original tests done.

#### 5.5 Roughness Analysis

Appendix E shows the root mean squared roughness for each specimen. The largest roughness elements were found in the 200 mm concrete pipe with an average root mean squared roughness of 0.16 mm. The 380 mm concrete pipe was almost the same with a root mean squared roughness of 0.14 mm while the 250 mm concrete pipe roughness was 0.10 mm. Roughness,

as expected was much less for the plastic pipes. The root mean squared roughness was two to three times less for the plastic pipes compared to the concrete pipes. A root mean squared roughness was not calculated for the Spirolbc 450 mm plastic pipe due to rebound described later. Table 6 lists the results of the roughness measurements and standard deviations of the root mean squared roughness calculated.

The comparatively large standard deviations shows a significant variation in the root mean squared roughness between the samples. This was obvious when samples were examined visually. The interior surface finish is particularly variable in the specimens obtained from the concrete pipes. Some samples were very smooth comparable to concrete finished carefully with a steel trowel. Other samples were rough with ridges formed as the inner mold was rotated during casting.

#### 5.5.1 Description of Surface Roughness

##### (1) Concrete Pipes:

Generally the course-grained aggregate is not exposed at the surface of the pipe due to the finishing process. The finest grained sand and mortar are exposed. Therefore, one would expect a roughness size equivalent to the sand grain sizes from a standard sieve analysis of the concrete

aggregate. Mindess and Young (1981) show that standard concrete mix designs use between 25 to 85 percent of the fine aggregate in the size range 0.15 to 0.6 mm.

The obvious characteristic of the concrete pipe inner surface is the concentric ridges which are formed during fabrication of the pipes. This type of roughness is very different than the uniform sand grain roughness used by Nikuradse and others because there are very few isolated sand particles projecting into the flow. Instead the sand and aggregate particles are embedded into a matrix of cement mortar paste. The mortar is brought to the surface during the finishing process which involves rotation and vibration of the inner cylindrical form. A very low slump concrete is used which allows the inner and outer forms to be stripped while the concrete is still in a plastic state. As the inner form is rotated and removed from the pipe it leaves the concentric ridges of mortar which are the dominant roughness feature of the concrete pipes. The amplitude of the ridges varies from about 0.2 mm to more than 1.5 mm. Minor sand-grained roughness elements are superimposed on these ridges.

#### (2) Plastic Pipes:

Roughness in the plastic pipes was of a wavy nature characterized by smooth sinusoidal curves. The amplitude and

wavelength of these features varied between the three plastic pipes. The surface waves in the 200 mm plastic pipe were small with amplitudes in the order of the root mean squared roughness and wavelengths of about 2 mm. When they were present, the waves on the inner surface of the 250 mm plastic pipes were an order of magnitude larger than those measured in the 200 mm pipes. These waves had amplitudes of 0.15 mm and wavelengths of 16 mm. Waves of a similar size were also measured in the 450 mm plastic pipe. The spiral grooves were the major roughness feature of the 450 mm plastic pipe. The grooves averaged 1.13 mm deep and 25 mm wide.

Roughness measurements were attempted for the 450 mm plastic pipe, however there appeared to be distortion of the sample due to stress relief which occurred when the samples were cut from the pipe sections. There was no fine-grained roughness noticeable from the results of the roughness testing. However the inner surfaces of the plastic pipes show waviness. This waviness was measured only when it was determined that it was not caused by flexing of the specimen due to stress relief.

#### 5.5.2 Observed versus Measured Roughness

The concrete pipes demonstrated a noticeable difference between the physical roughness measured and the calculated

equivalent roughness. Table 7 shows the average measured roughness for the three concrete pipes was 0.13 mm compared to the calculated equivalent roughness of 0.22 mm. This represents a 70 percent increase in the apparent roughness which can be attributed to joint and alignment effects.

The plastic pipes did not display any noticeable difference between measured and calculated roughness. This was surprising because joint effects were obvious when observations were made during the tests. Table 7 lists the results for the plastic pipes.

## 6 Analysis and Discussion

### 6.1 Boundary Layer Development

Boundary layer development in pipes flowing part-full should not be viewed simply as a two dimensional phenomenon. Analysis of the centreline measurements done in this study indicate that the boundary layer undergoes a rapid initial growth away from the pipe surface. As the flow continues downstream the propagation of the boundary layer into the flow reduces significantly. This is apparently due to the development of secondary currents in the flow. The secondary currents dissipate energy perpendicular to the axis of the pipe and depress the thread of maximum velocity in the flow to a point well below the free surface. As a result the usual definition for defining the boundary layer thickness from a measured velocity profile is not applicable. In other words, the boundary layer should not be taken as the depth where the velocity is ninety-nine percent of the free stream velocity. This is because the developing secondary or radial component of the boundary layer growth masks the growth of the boundary layer along the central axis of the pipe. The data obtained for the 380 mm concrete pipe supports this idea because the secondary currents are developed 10 to 15 m from the inlet and at this point the

vertical ascent of the boundary layer along the central axis of flow slows abruptly. Discrepancies may be explained by the presence of joints.

One puzzling aspect is that the observed boundary layer growth does not exceed the theoretical curve, considering that the theory was derived with no regard for wall effects over a semi-infinite flat plate. If the plots for measured and theoretical boundary layer growth are extrapolated back towards the origin in figures 6 to 8, the measured boundary layer exceeds the theoretical growth within a few metres of the inlet. This is best illustrated in figure 6 which indicates that the actual boundary layer may indeed develop more rapidly than suggested by theory. This question can only be fully answered by performing detailed three dimensional measurements of the flow in a part full circular section.

Although the classical equations developed for boundary layer development on a flat plate are not well suited to description of boundary layer growth in a circular open channel, the results indicate that the theoretical boundary layer development length compares closely to the observed flow development length. It is suggested that as a first approximation the Blasius seventh power law as stated in equation (8) is applicable to developing flow in part full concrete pipes.

## 6.2 Uniform Flow

### 6.2.1 Experimental Uncertainty

The primary parameters of interest when calculating the resistance to flow in a steady uniform flow field are slope of the energy gradient, discharge, and cross-sectional flow geometry (in this case a function of mean depth and pipe diameter). A brief discussion of the experimental uncertainties involved in the measurement of these parameters is important to qualify the results.

Percentage error based on the uncertainties in the parameters listed below was calculated for all values of friction coefficients used in the analysis. Any coefficient carrying an error greater than 25 percent was discarded. The magnitude of the allowable error (ie. less than 25 percent) gives an indication of the experimental error involved in these tests. The minimum error calculated for any of the results was 10.5 percent. The maximum error was 80 percent. The behavior of water confined in a channel with a free surface does not lend itself well to accurate measurements.

#### 6.2.1.1 Slope

Uncertainties in the bed slope were within five percent of the slope of the energy gradient in all but the most mild slopes. Considerable care was taken to select regions of

flow where the slope of the water surface, as indicated by the manometer profile was linear. Inspection of figures 13 to 16 shows the variation in the apparent location of the pipe invert when point gauge depth measurements were subtracted from water surface elevations as indicated by the manometer profiles. It was assumed that in this region the slope of the water surface (energy gradient) was equal to the bed slope.

Tests done at mild slopes with high depth to diameter ratios were affected by drawdown of the water surface profile caused by the unrestricted outlet. The careful use of tailwater control would have alleviated this problem, but can be very time consuming. A trial and error approach must be used with tailwater control until the slope of the water surface profile as indicated by the manometer board equals the slope of the pipe bed. Profiles influenced by drawdown effects were eliminated from the results of these tests after the fact.

#### 6.2.1.2 Discharge

The listed accuracy of the magnetic flow meters was one percent of the full scale output. This converts to about 0.1 L/s for the small magnetic flow meter and about 2.5 L/s for the large meter. In practise, the discharge meters performed

within finer tolerances. Both the small and large meters were calibrated and found to be accurate to 0.21 and 0.20 percent of the full scale readings respectively.

#### 6.2.1.3 Depth

The experiments were conducted such that the depth of uniform flow was obtained from maximum allowable number of depth measurements. As mentioned, transition of the flow from subcritical to supercritical conditions presented a problem due to standing waves of 50 mm in extreme cases. These waves were generated at the entrance and by joints between pipe sections. All pipes exhibited inlet waves of the same and magnitude regardless of the type of inlet used. The large undular waves at the inlet tended to dampen as they progressed downstream to be replaced by waves generated by the joints. At mild slopes (zero to 0.003) and steep slopes (0.006 to 0.10) the waves were much less pronounced. Despite the averaging process, which tends to dampen the effects of the surface waves on the calculations, the waves undoubtedly produce some of the scatter found in friction factors calculated for transition conditions.

#### 6.2.1.4 Diameter

The most noticeable variations in the inside diameters of the pipe sections tested were caused by the following:

(1) Out-of-roundness (5 mm between orthogonal measurements observed in the plastic pipe).

(2) A slight decrease in the inside diameter at the bell end of all the concrete pipes tested (usually in the order of a few mm).

These variations did not produce significant error in the results compared to previously mentioned parameters.

Much more important were the noticeable effects of the pipe joints on the flow which initiated the formation of surface waves in the pipe.

#### 6.2.1.5 Repeatability of Results

As part of the study it was necessary to analyze the repeatability of the results. Due to time constraints it was not possible to do a large enough sample for any particular test to allow a standard statistical analysis to be done.

However, some of the tests were done in triplicate to determine if any significant variations between runs was apparent. Two of the tests were done with the discharge increased between tests and one was done with the discharge decreased between tests. In all instances the measured average depth of flow was well within the experimental error involved in trying to duplicate the flow conditions exactly.

### 6.2.2 Resistance to Flow

Figures 24 to 26 show clearly that the friction factors (Darcy's  $f$ ) calculated from the measurements taken in these tests fall within the transition zone between smooth and fully rough turbulent flow. Review of the available literature has cast doubt on the applicability of Manning's equation to accurately describe uniform flow in the transition zone. Manning's equation was developed primarily to describe fully rough turbulent flow conditions. It does not intrinsically consider the viscous effects in the flow. This is an important question since open channels are often designed with slopes less than one percent. The ASCE Task Committee on open channel flow (1984) recommends the use of Darcy's equation which is much more sensitive to the viscous effects in the transition flow region. Darcy's  $f$  is not constant and must be calculated iteratively for each open channel flow problem. It is recommended that this approach be taken especially when designing sewers using plastic pipes. The 200 and 250 mm plastic pipes behaved as hydraulically smooth surfaces in the range flow conditions tested.

## 7 Conclusions

Based on the results of these tests the following conclusions can be made:

(1) Boundary layer development in the partly full pipes tested appears to conform the Blasius seventh power law developed for boundary layer growth over a plate of zero incidence with semi-infinite boundaries.

(2) The standard definition of the boundary layer thickness as the point in the flow where the velocity equals ninety-nine percent of the free stream velocity is not applicable to boundary layer growth in pipes flowing part full. This is due to the development of secondary currents which prevent the apparent growth of the boundary layer radially from the pipe boundary by depressing the thread of maximum velocity to a point well below the water surface.

(3) The method of superposition of velocity profiles was demonstrated as a valuable tool in analyzing the developing flow in these tests and indicated that the flow was fully developed within 40 diameters of the inlet in the concrete pipes.

(4) The uniform flow experiments fell within the transition zone between smooth and rough turbulent flow. The

concrete pipes tested appeared to approach independence from viscous effects for the steepest slopes. The plastic pipes followed the smooth boundary equation of Nikuradse.

(5) Manning's  $n$  is theoretically not well suited for use in describing the resistance to flow in part-full concrete or plastic pipes within the transition region between smooth turbulent and fully rough turbulent flow conditions. However, these tests indicate that for depth to diameter ratios greater than 0.25 Manning's  $n$  is relatively constant for practical purposes. Applying the Darcy equation for open channel flow is a more sound approach for dealing with transition flow conditions because it is more sensitive to flow dynamics.

(6) There was no apparent hysteresis effects when the discharge was decreased or increased between tests as was reported for pipes installed under field conditions. This result indicates that the reason for the hysteresis is the growth of slime in the pipes installed in the field.

## 8 Recommendations

(1) Based on results of error analysis and assumptions involved in formulating the various resistance coefficients, it is recommended that these coefficients should not be reported to more than two significant figures.

(2) The careful use of tailwater control should be used if conditions of mild channel slopes and high depth to diameter ratios are tested. A tedious trial and error approach must be used to eliminate the drawdown of the water surface profile at the outlet to ensure that the slope of the water surface and the slope of the channel bed are identical.

(3) The use of Prandtl pitot tubes is recommended to obtain velocity profiles in tests of this nature. The resulting profiles can be analyzed to determine the boundary layer development length.

(4) Further boundary layer investigations should be performed on plastic pipes to determine if the flow fully develops by the distance ratios indicated in these tests.

(5) Three-dimensional velocity testing should be done, with velocity profiles extending radially inward from the boundary, to attempt to gain more insight into the interaction between the developing secondary currents and the boundary layer growth.

Table 1 : Values of Manning's n for two types of pipe.

Adapted from Bloodgood and Bell (1961).

Manning's n	Type of pipe
0.00995 - 0.01079	cement asbestos
0.00957 - 0.01105	vitrified clay

Table 2 : Equivalent roughness for concrete pipes.

Adapted from Straw and Morris (1950)

pipe diameter (inches)	equivalent roughness (mm)
18	0.0002
24	0.0004
36	0.0005

**Table 3: Pipe installation information.****(1) Concrete Pipes**

Pipe diameter (m)	Section length (m)	Number of sections installed	Total installed length (m)	Pressure taps
200	1.28	29	35.29	29
250	1.28	29	35.58	29
380	2.47	15	35.89	15

**(2) Plastic Pipes**

Pipe diameter (m)	Section length (m)	Number of sections installed	Total installed length (m)	Pressure taps
200	4.13	9+	37.36	18
250	4.13	9+	38.14	18
450	4.17	9+	37.32	18

Note: pieces of the plastic pipes were cut for the inlets which explains the plus sign beside the number of plastic pipes used.

**Table 4: Measured and calculated boundary layer parameters**

(1) **Run #1:** done in the 200 mm concrete pipe. The bed slope was 0.002 and the discharge was 21 l/s.

x (m)	y (mm)	$\delta_w$ (mm)	$\delta_1$ (mm)	$\delta$ (mm)	$\tau_o$ (Pa)
0.21	166	20	1.96	7.23	4.07
0.57	172	30	2.22	16.28	1.87
0.95	165	35	2.91	24.5	2.09
1.44	165	50	3.30	34.17	2.72
1.79	161	85	5.95	40.67	5.45
2.17	158	50	3.32	47.34	1.34
2.66	162	60	3.88	55.83	2.27
3.03	166	60	3.88	61.96	2.52
3.41	170	65	4.33	68.09	1.75
3.86	167	70	5.57	75.19	2.22
4.24	166	80	5.07	81.06	2.23
4.61	166	90	4.34	86.67	2.47
5.85	160	125	4.72	104.9	3.23

(2) Run #2: done in the 200 mm concrete pipe. The discharge was 14.7 L/s and the bed slope was 0.002.

$x$ (m)	$y$ (mm)	$\delta_w$	$\delta_i$	$\delta$	$\tau_0$
		(mm)	(mm)	(mm)	(Pa)
0.95	125	27	2.4	24.2	2.10
2.17	119	39	2.7	46.9	1.75
3.41	134	59	5.14	67.4	1.77
4.61	125	61	4.36	85.8	1.63
5.85	120	68	4.95	103.8	1.64
7.09	112	86	5.67	121.0	1.87
8.30	122	105	8.94	137.3	2.85

(3) Run #3: done in the 200 mm concrete pipe. The discharge was 16.4 L/s and the bed slope was 0.001.

$x$ (m)	$y$ (mm)	$\delta_m$ (mm)	$\delta_1$ (mm)	$\delta$ (mm)	$\tau_o$ (Pa)
0.95	148	25	6.5	3.1	2.07
2.17	142	38	2.3	6.1	1.24
3.41	152	50	3.9	8.7	1.78
4.61	145	60	4.3	11.1	1.57
5.85	141	70	5.2	13.4	1.20
7.09	140	93	5.6	15.6	1.72
8.30	142	110	8.0	17.7	1.63

(4) Run #4: done in the 200 mm concrete pipe. The discharge was 16.6 L/s and the bed slope was zero.

x (m)	y (mm)	$\delta_0$ (mm)	$\delta_1$ (mm)	$\delta$ (mm)	$\tau_0$ (Pa)
0.95	172	15	2.14	26	0.77
2.17	167	29	2.6	50	0.98
3.41	176	43	4.3	72	1.17
4.61	169	55	5.8	91	1.22
5.85	164	75	10.3	110	0.79
7.09	158	90	7.3	128	0.75
8.30	163	110	7.0	146	0.72
9.53	161	125	7.0	163	0.94

(5) Run 15: done in the 200 mm concrete pipe. The discharge was 14.6 L/s and the bed slope was 0.001.

$x$ (m)	$y$ (mm)	$\delta_s$ (mm)	$\delta_b$ (mm)	$\delta$ (mm)	$\tau_0$ (Pa)
0.95	138	23	4.2	25	1.70
2.17	133	35	4.3	49	1.89
3.41	145	43	7.0	70	1.71
4.61	138	55	6.4	89	1.22
5.85	132	65	5.9	108	1.31
7.09	126	72	5.2	126	1.44
8.30	132	89	8.5	143	1.07
9.53	132	100	7.9	160	0.78
10.77	132	101	9.1	176	1.08
11.99	131	102	7.8	192	0.89
13.21	134	103	9.3	207	1.14

(6) Run #6: done in the 380 mm concrete pipe. The discharge was 101 L/s and the bed slope was 0.010.

$x$ (m)	$y$ (mm)	$\delta_{yy}$ (mm)	$\delta_1$ (mm)	$\delta$ (mm)	$\tau_0$ (Pa)
2.15	204	32	3.36	38.7	6.5
4.53	200	31	4.48	69.3	15.1
6.91	201	36	6.01	97.3	14.4
9.32	191	50	7.71	122.2	23.5
10.13	185	54	8.11	130.8	15.2
11.69	189	67	9.36	145.8	13.6
14.13	184	68	8.87	168.2	11.3
16.45	186	73	8.82	190.1	10.2
18.84	181	93	10.7	210.2	9.5
21.26	179	91	10.0	231.1	9.2
23.61	180	97	10.2	250.5	11.2
26.02	178	97	12.9	270.2	16.1
28.43	187	104	14.0	291.7	14.8
30.77	182	106	12.4	310.2	12.8
33.18	179	108	12.5	329.3	12.0

Table 5: Average values of Manning's n.

(1) Depth ratios less than 0.25:

(a) Concrete pipe:

Diameter	200 mm	250 mm	380 mm
Mean n value	0.0107	0.0106	0.0094
sample size	15	16	18

(b) Plastic pipe:

Diameter	200 mm	250 mm	450 mm
Mean n value	0.0092	0.0090	0.0085
sample size	16	18	19

(2) Depth ratios greater than 0.25:

(a) Concrete Pipe:

Diameter	200 mm	250 mm	380 mm
Mean n value	0.0098	0.0100	0.0099
sample size	44	45	42

(b) Plastic pipe:

Diameter	200 mm	250 mm	450 mm
Mean n value	0.0087	0.0089	0.0091
sample size	47	44	44

Overall Averages:

depth ratios	Concrete Pipe	Plastic Pipe
y/D>0.25	0.0099	0.0089
y/D<0.25	0.0102	0.0089

Table 6: Root Mean Squared Roughness and Standard Deviation for the Pipes Tested.

Pipe	Root Mean Squared Roughness (mm)	Standard Deviation (mm)
200 mm concrete	0.16	0.04
250 mm concrete	0.09	0.04
380 mm concrete	0.14	0.06
200 mm plastic	0.05	0.01
250 mm plastic	0.06	0.03
450 mm plastic	n/a	n/a

Table 7: Actual measured physical roughness compared to calculated values of equivalent roughness for the tests conducted:

Pipe	Diameter (mm)	Measured Roughness (mm)	Equivalent Roughness (mm)
Concrete	200	0.16	0.22
	250	0.09	0.23
	380	0.14	0.21
	average:	0.13	0.22
Plastic	200	0.049	0.037
	250	0.057	0.050
	450	n/a	0.034
	average:	n/a	0.040

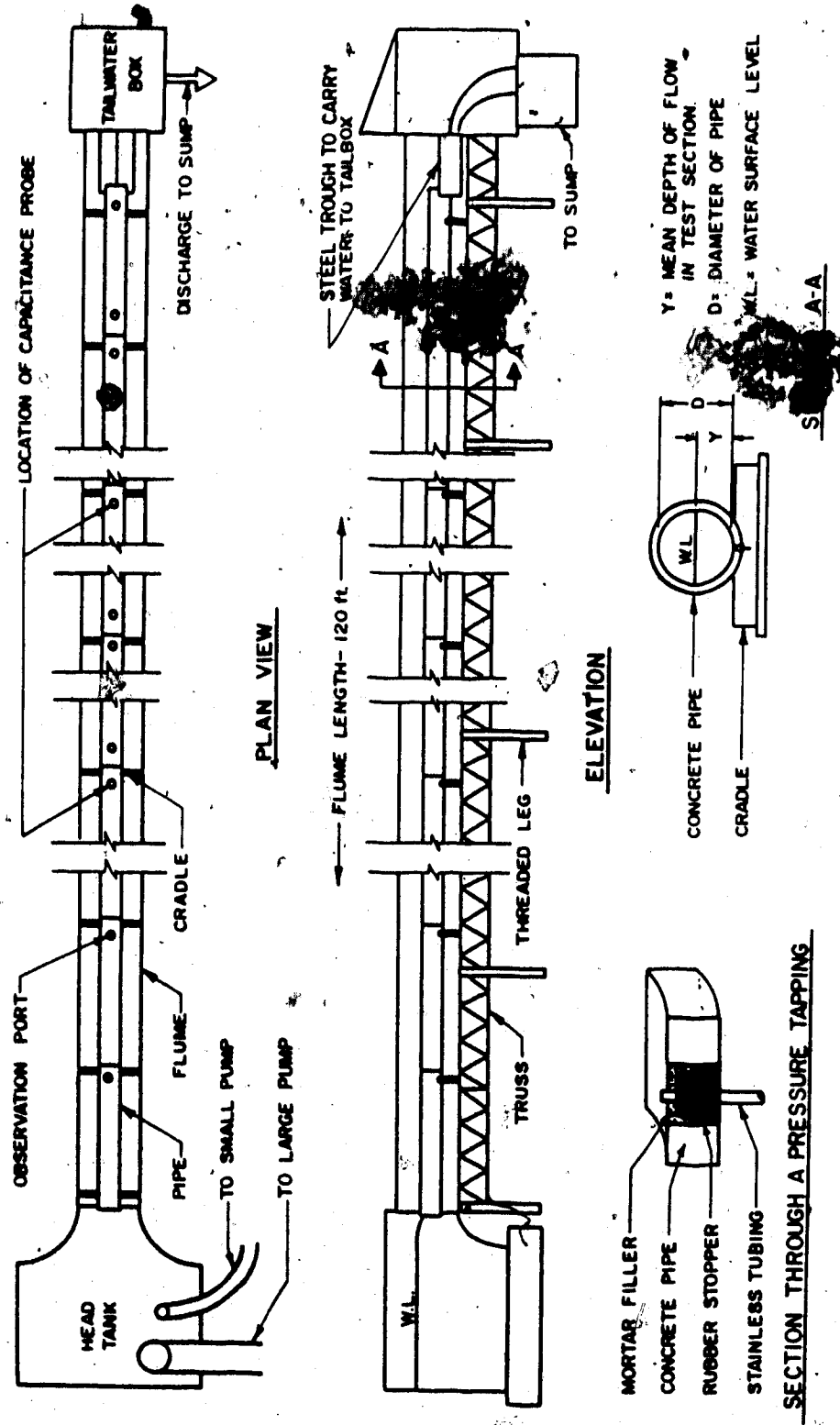


Figure 1: Laboratory set-up showing the flume, installed pipe, and details of the pressure tappings and pipe cradles.

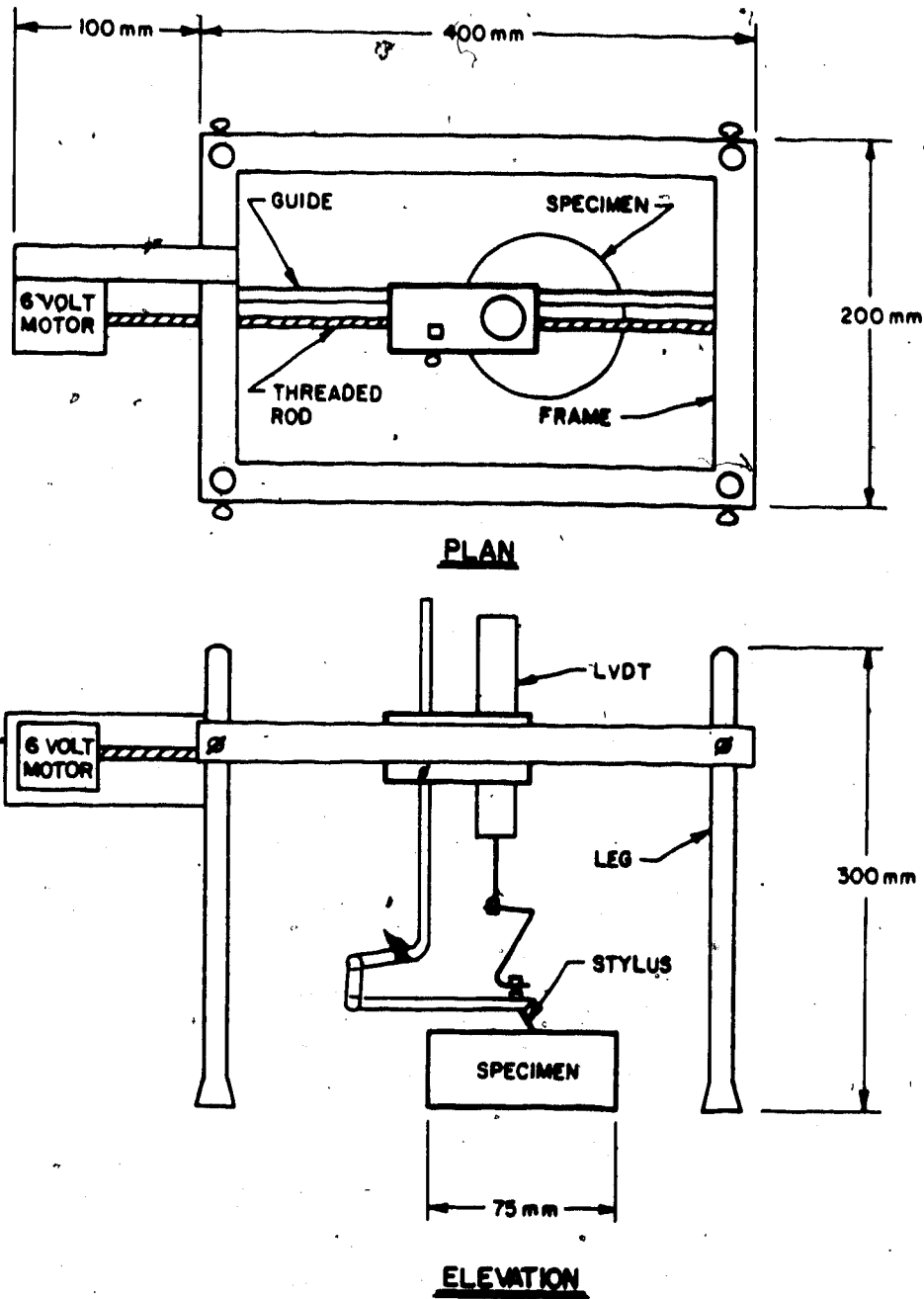


Figure 2: Sketch of the roughness measuring device used to determine the size of physical roughness elements on the interior surface of the pipes tested.

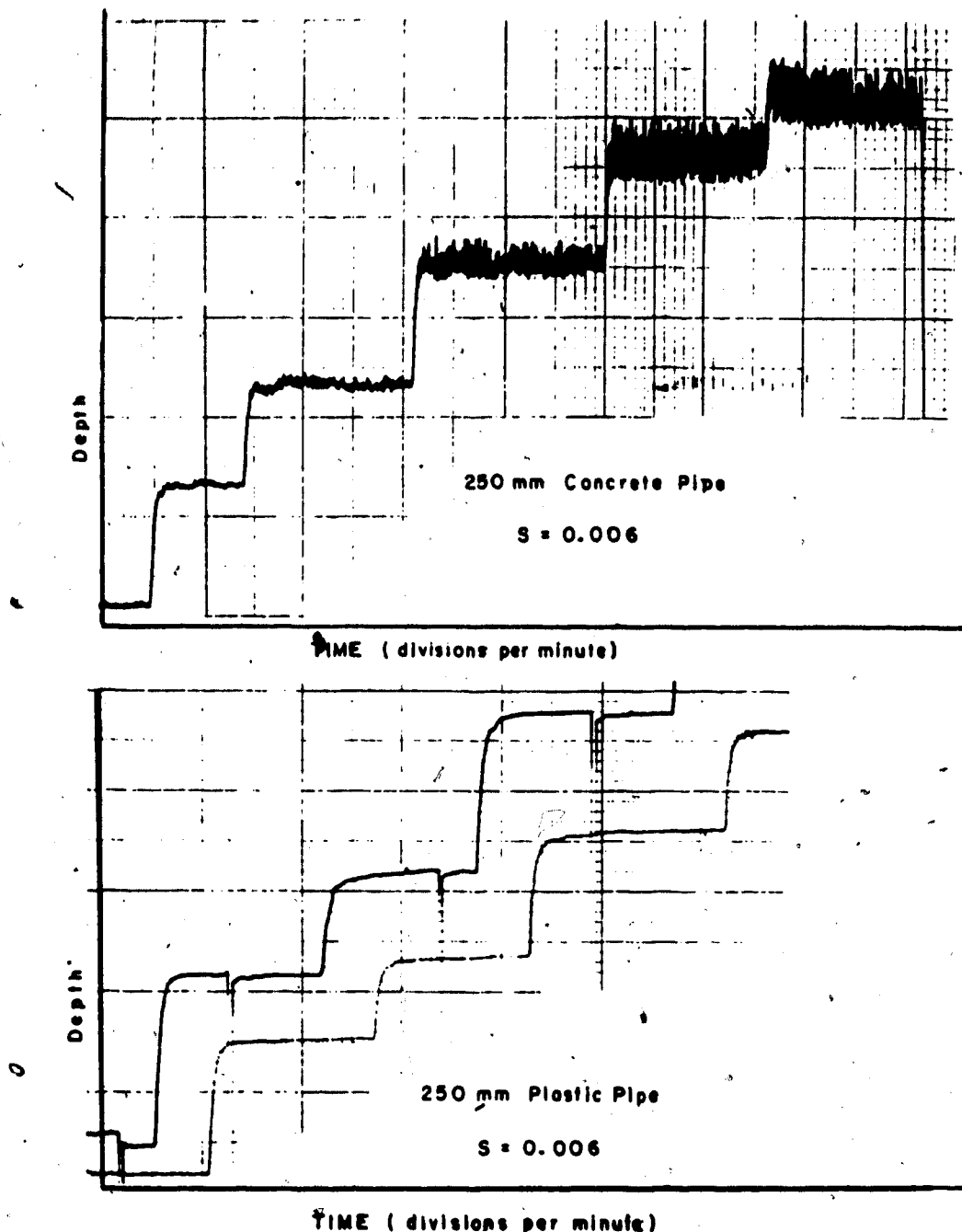


Figure 3: Typical water surface fluctuations during uniform flow testing of the 250 mm plastic and concrete pipes recorded by depth capacitance probes at a bed slope of 0.006. Surface fluctuations are almost negligible for the plastic pipe.

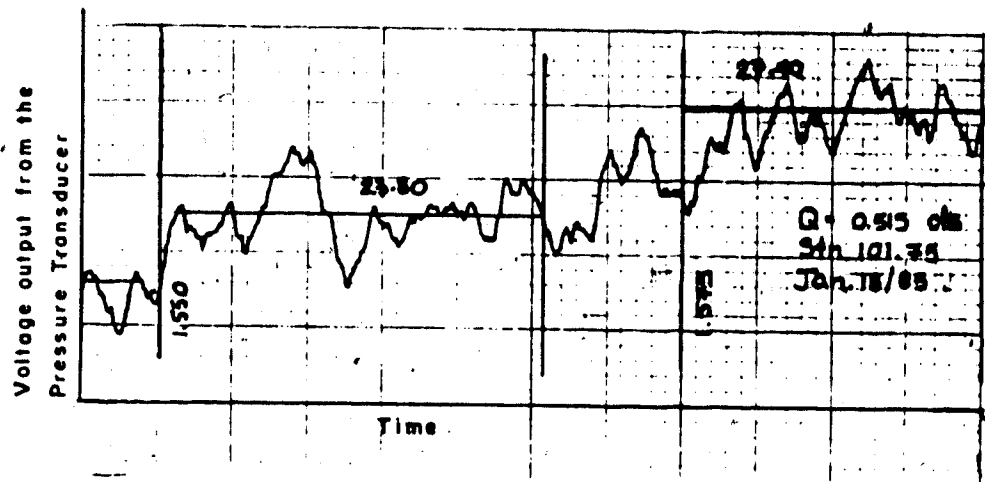


Figure 4: Typical readout from the Validyne pressure transducer used to measure velocity profiles in the developing flow region in the 200 mm concrete pipe at mild slopes. Note the fluctuations due to turbulence. The horizontal line is the best fit average velocity reading at that point.

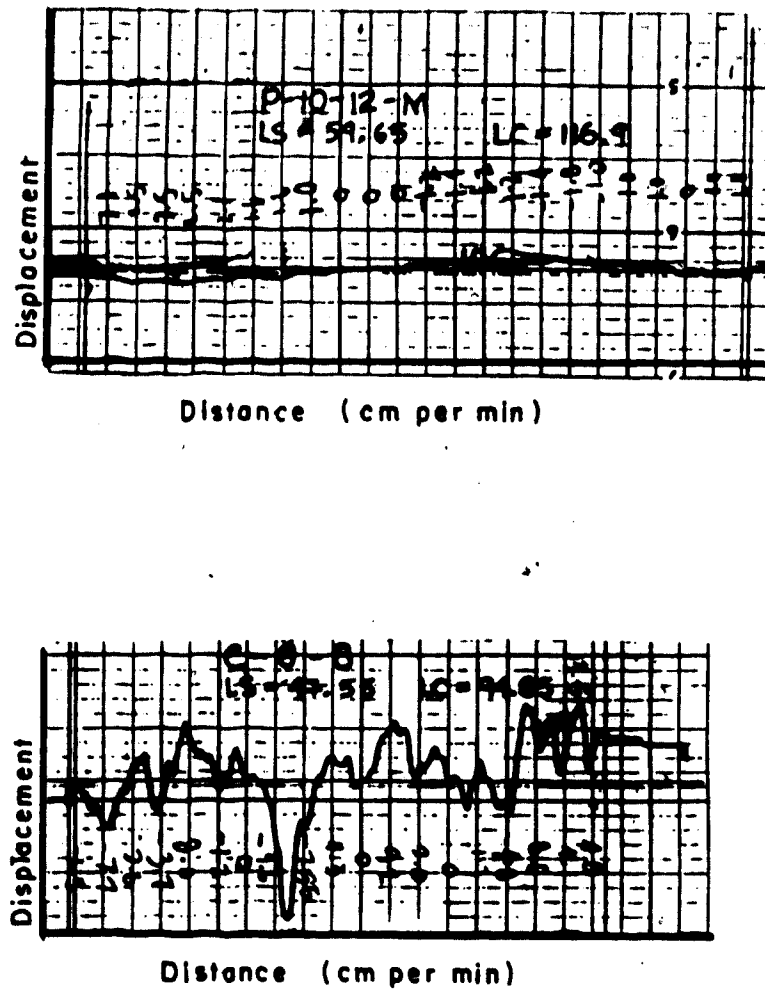


Figure 5: Typical roughness records from the roughness measuring device. The top record is for the 250 mm plastic pipe (P-10-12). The bottom record is for the 200 mm concrete pipe (C-8-8).

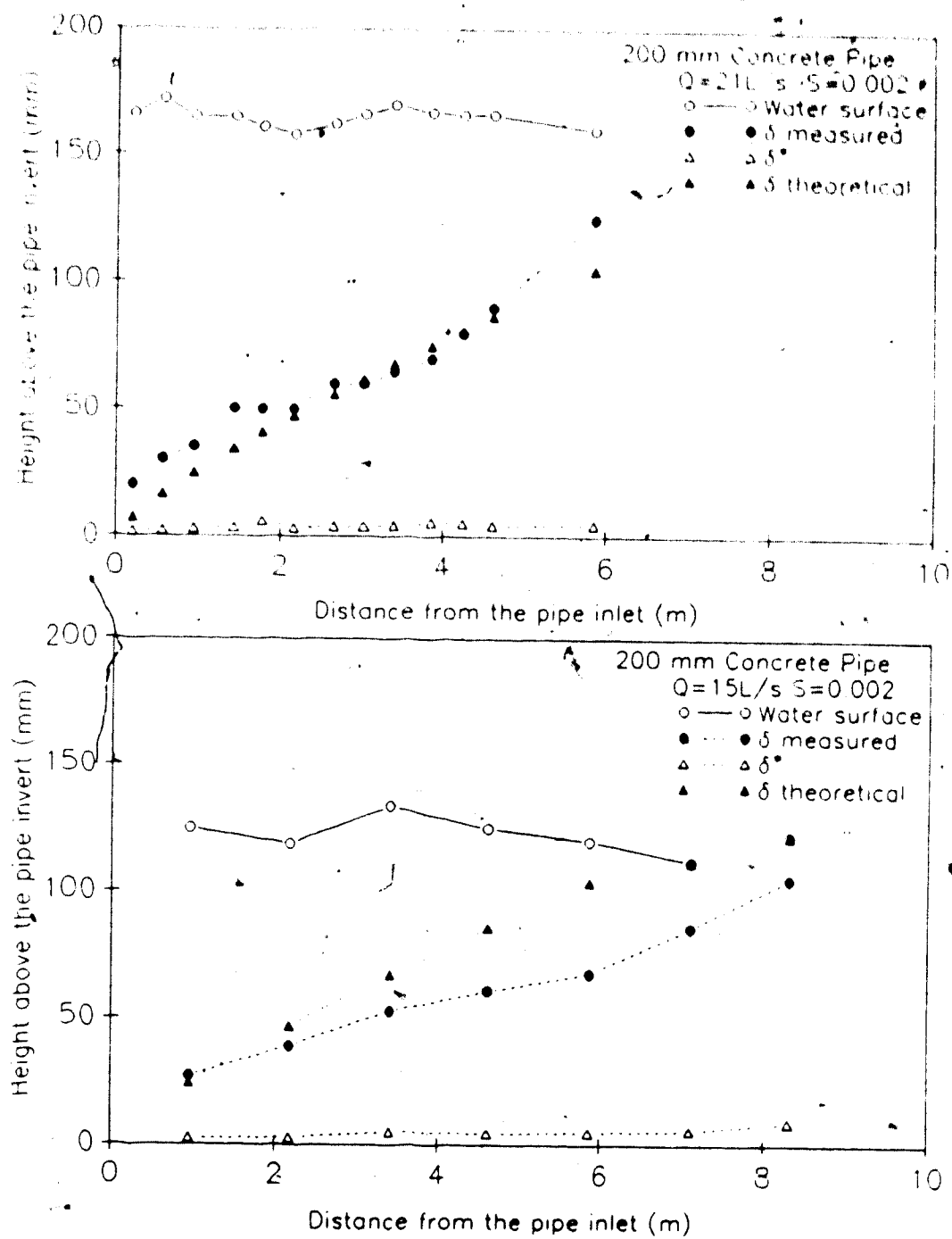
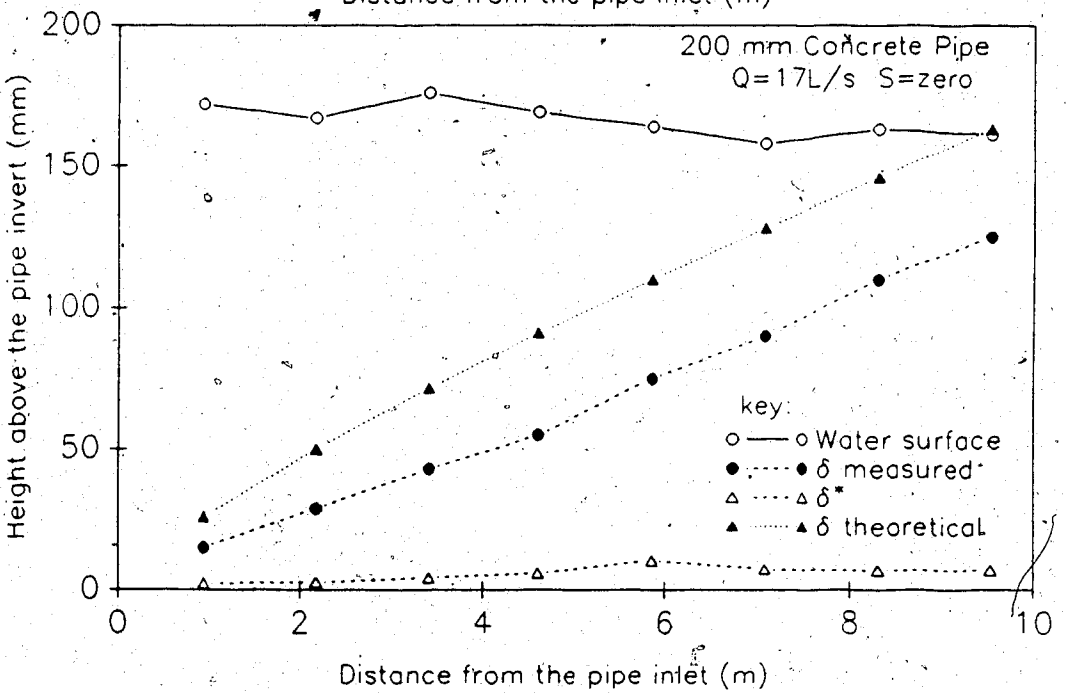
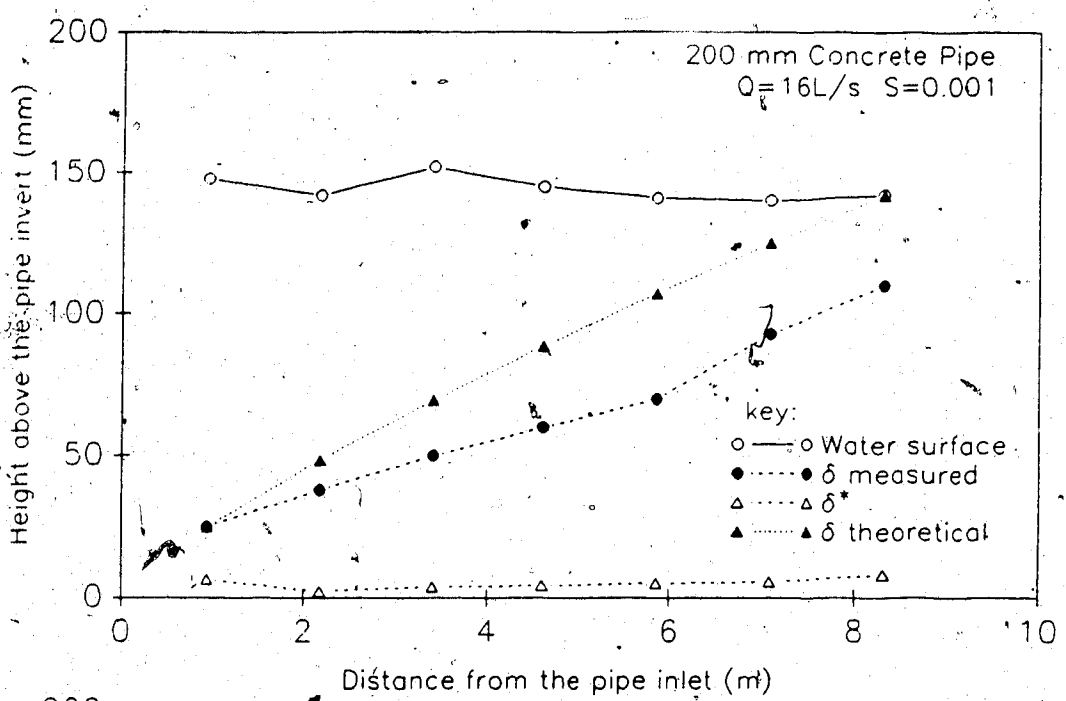
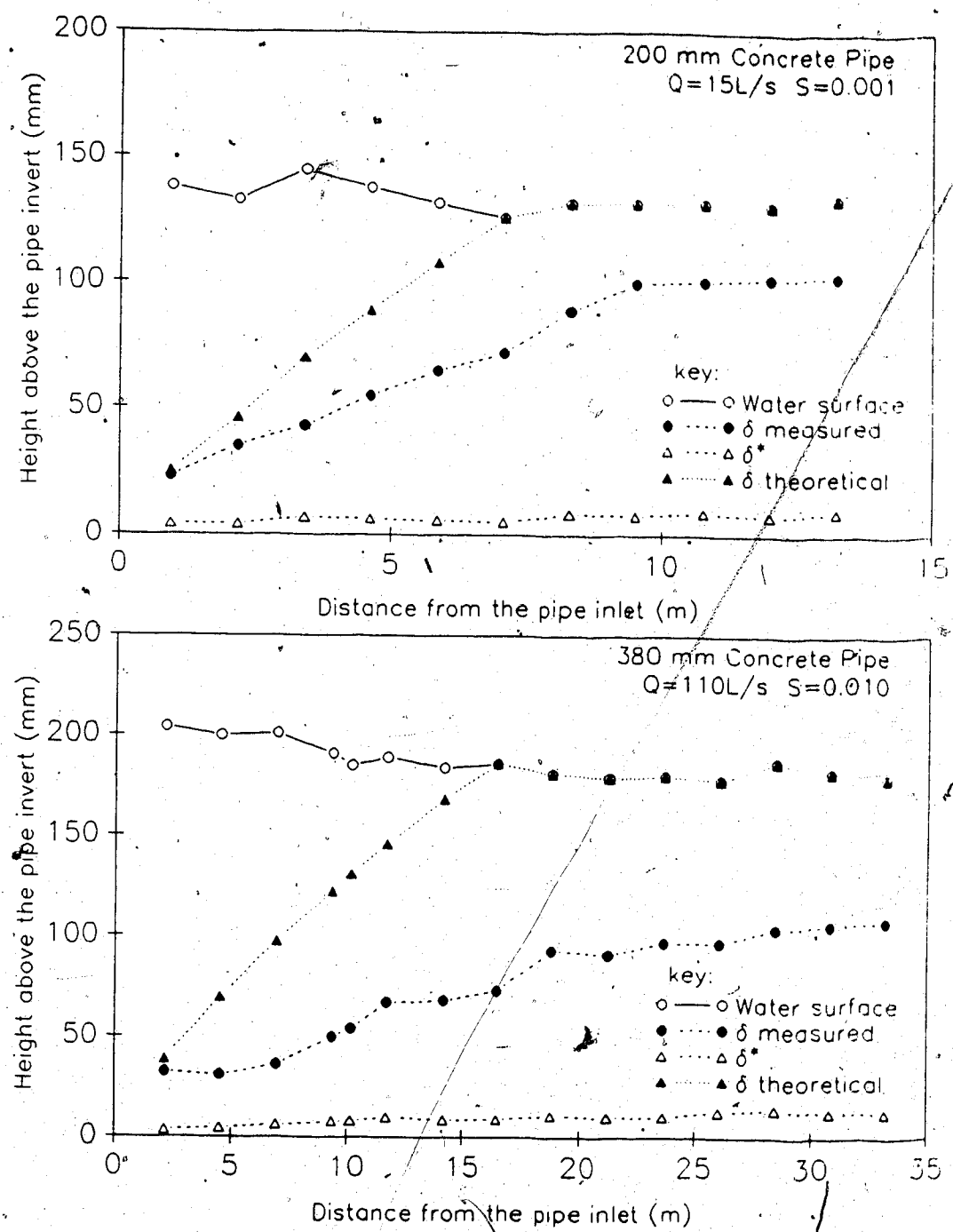


Figure 6: Measured and theoretical boundary layer growth in the 200 mm concrete pipe.



**Figure 7: Measured and theoretical boundary layer and displacement thickness in the 200 mm concrete pipe with measurements extended further down the channel.**



**Figure 8: Boundary layer growth in the 200 mm and 380 mm concrete pipes with measurements extending for the entire test length in the case of the 380 mm pipe.**

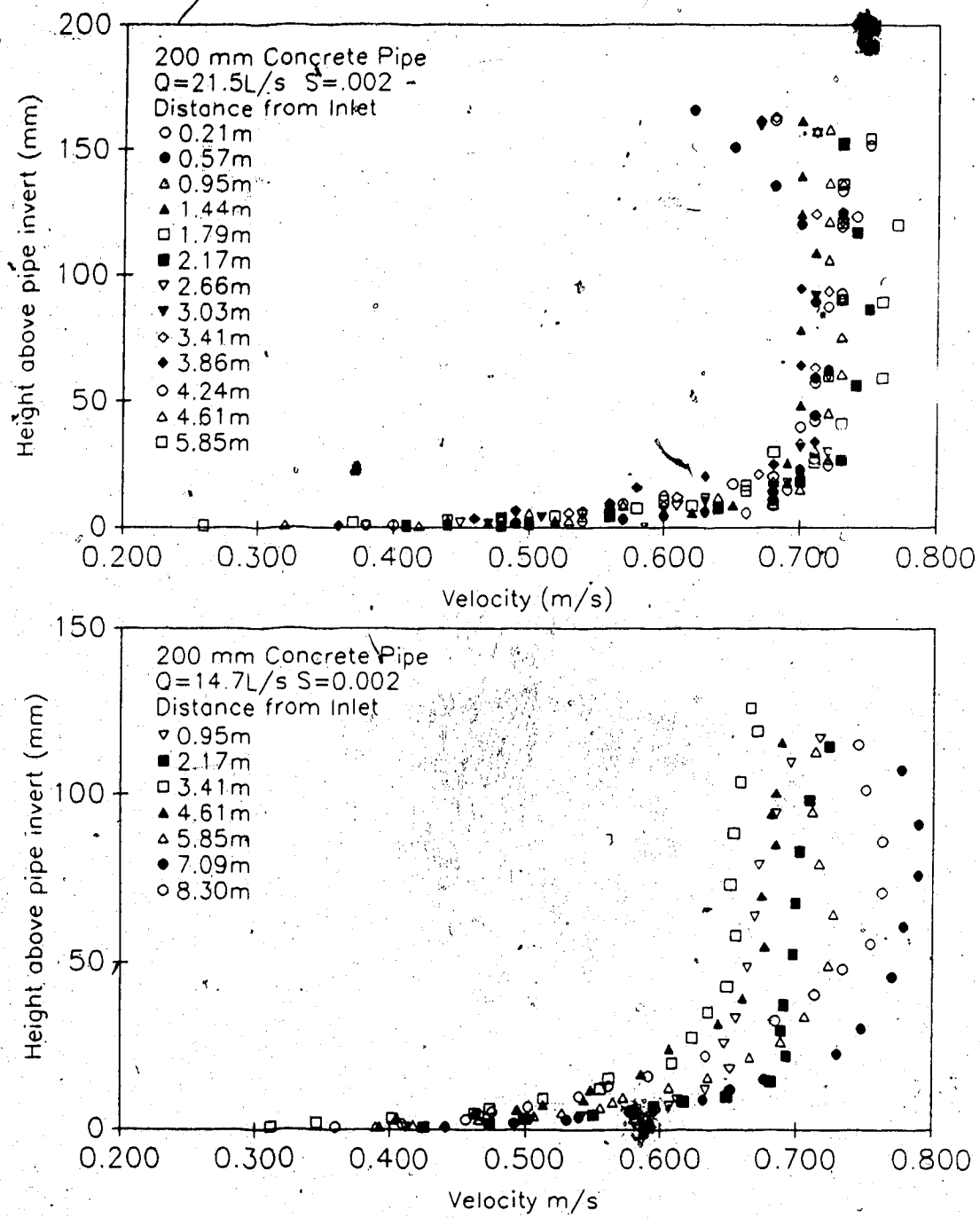


Figure 9: Velocity profiles measured in the 200 mm concrete pipe at mild slopes.

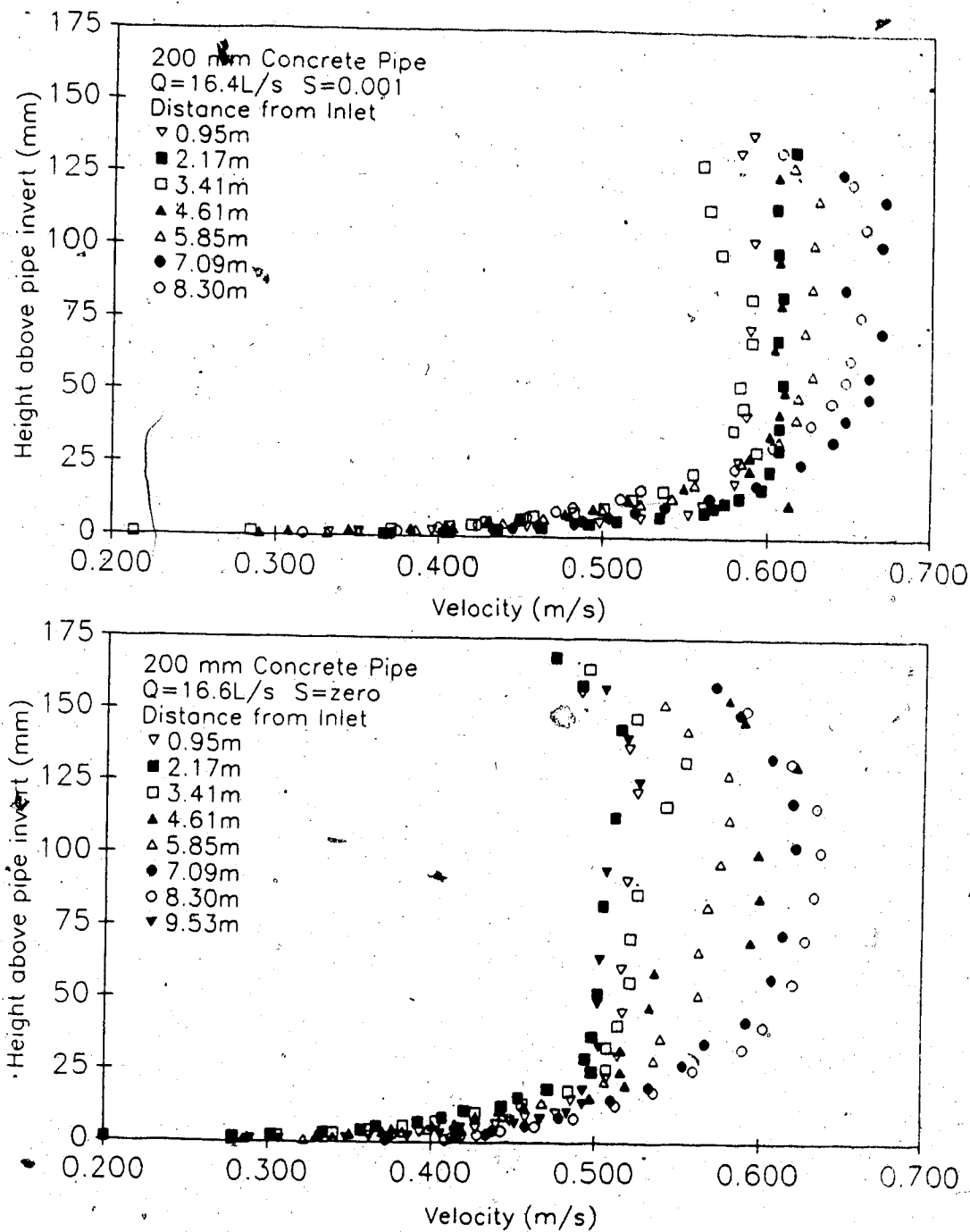
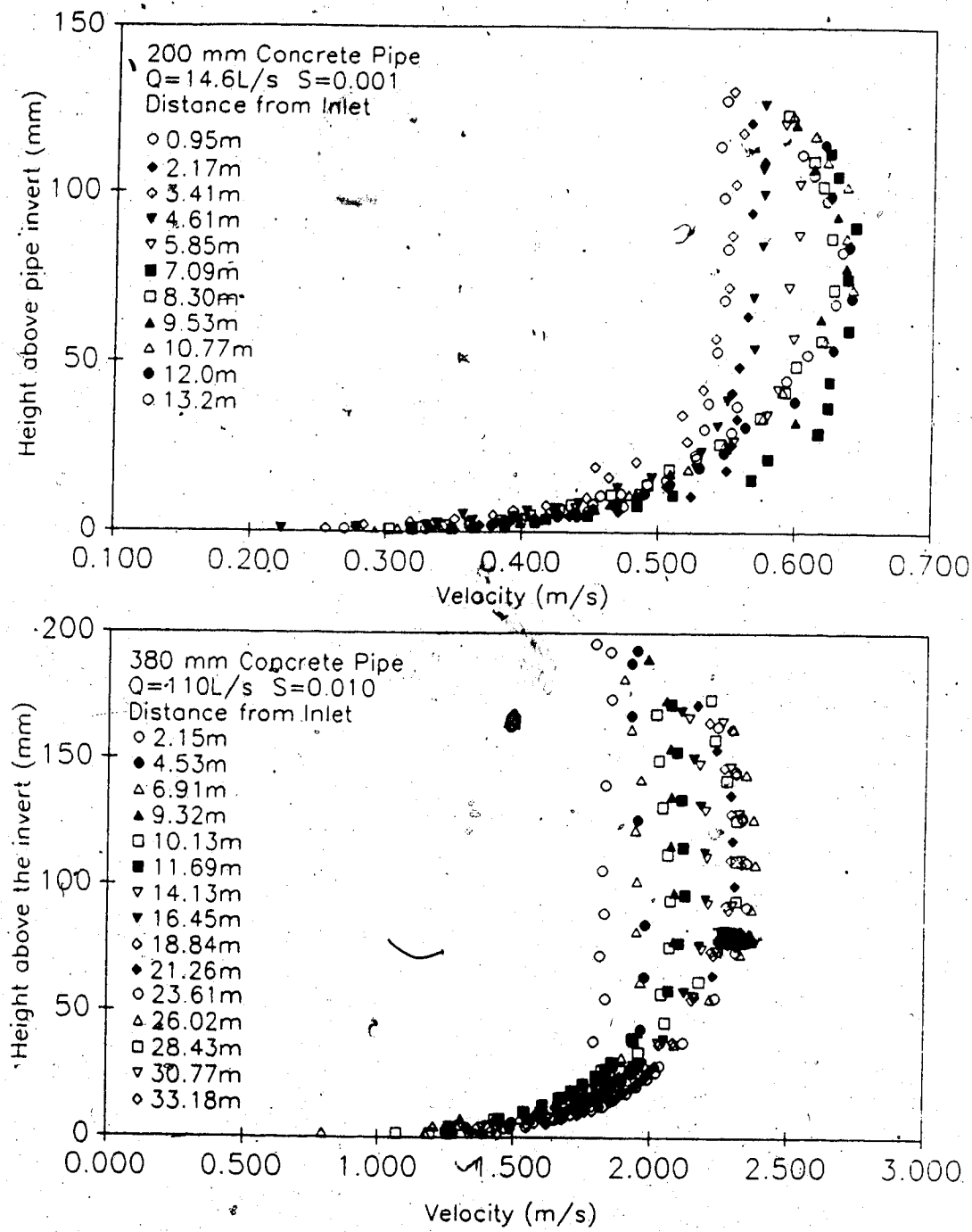


Figure 10: Velocity profiles in the 200 mm concrete pipe at mild slopes.



**Figure 11:** Velocity profile measured in the 200 and 380 mm concrete pipes. Note that the profiles superimpose noticeably in these figures.

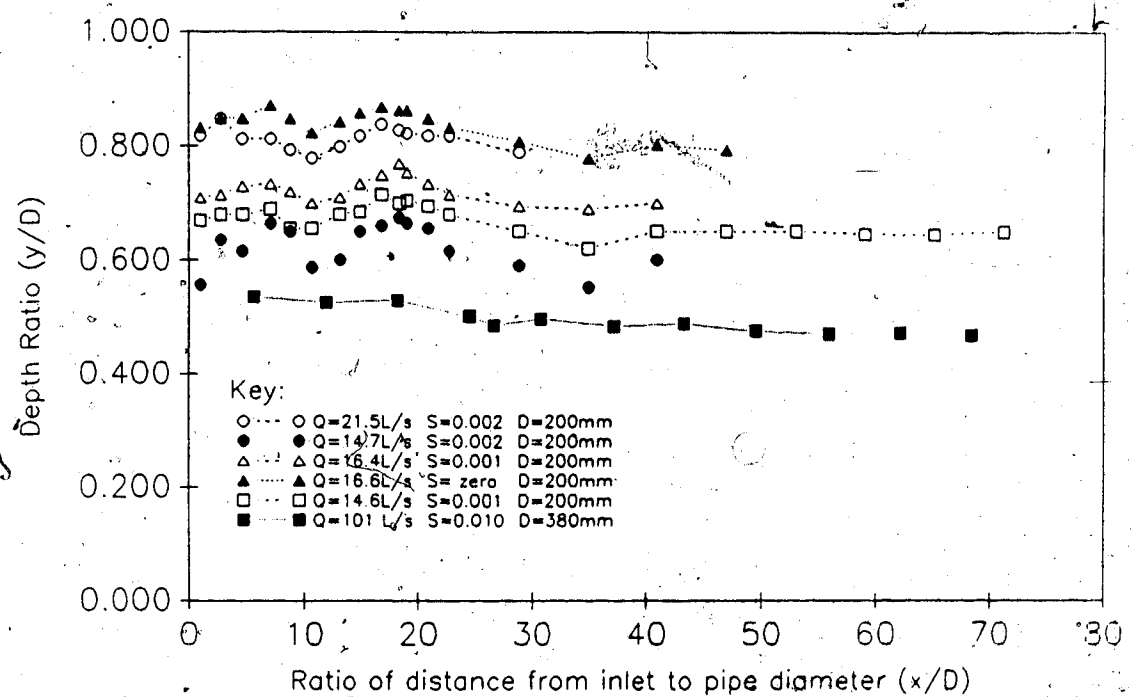


Figure 12: Non-dimensional depth and distance plotted to indicate the location where the surface curvature of flow indicates that the flow is fully developed.

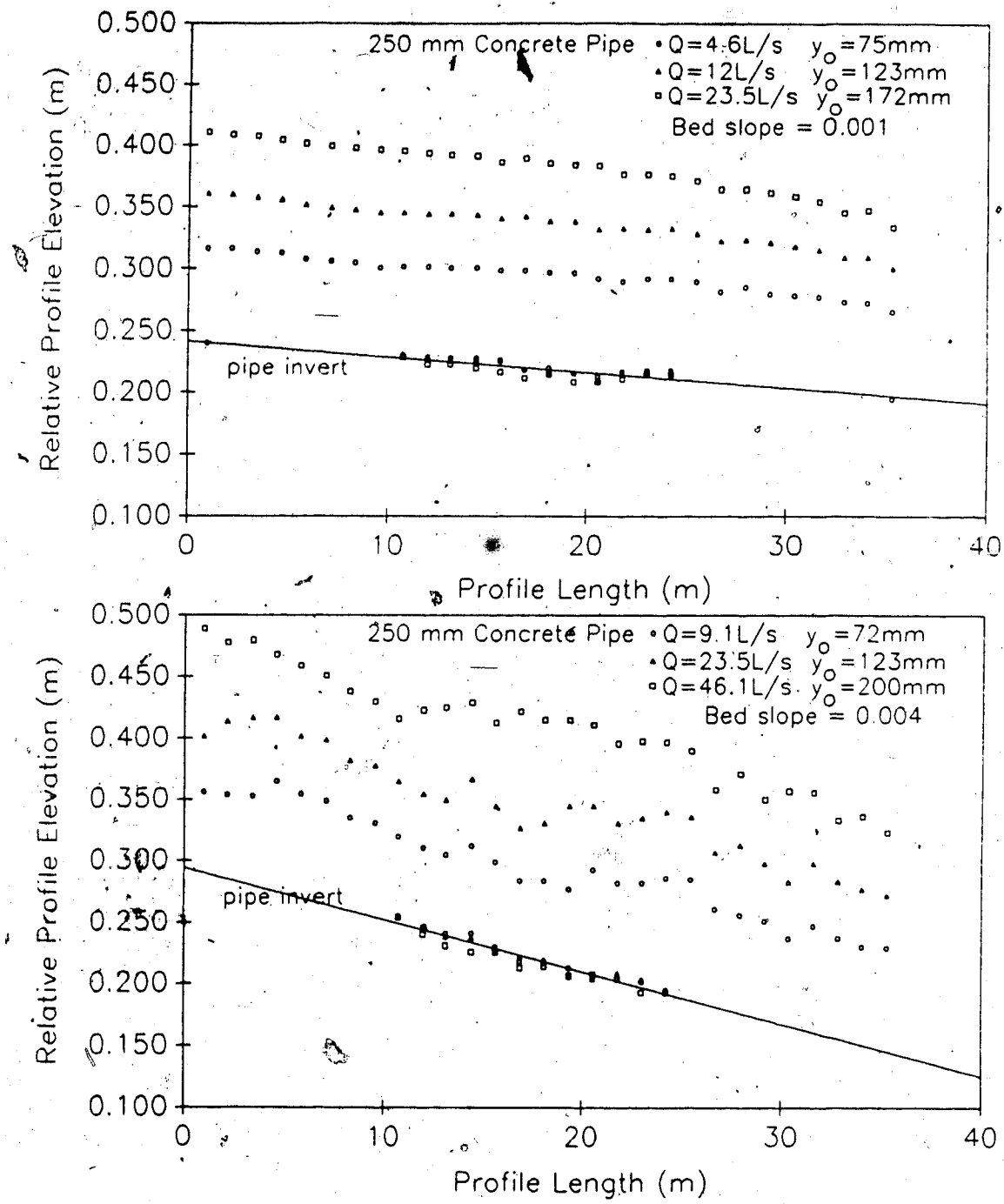
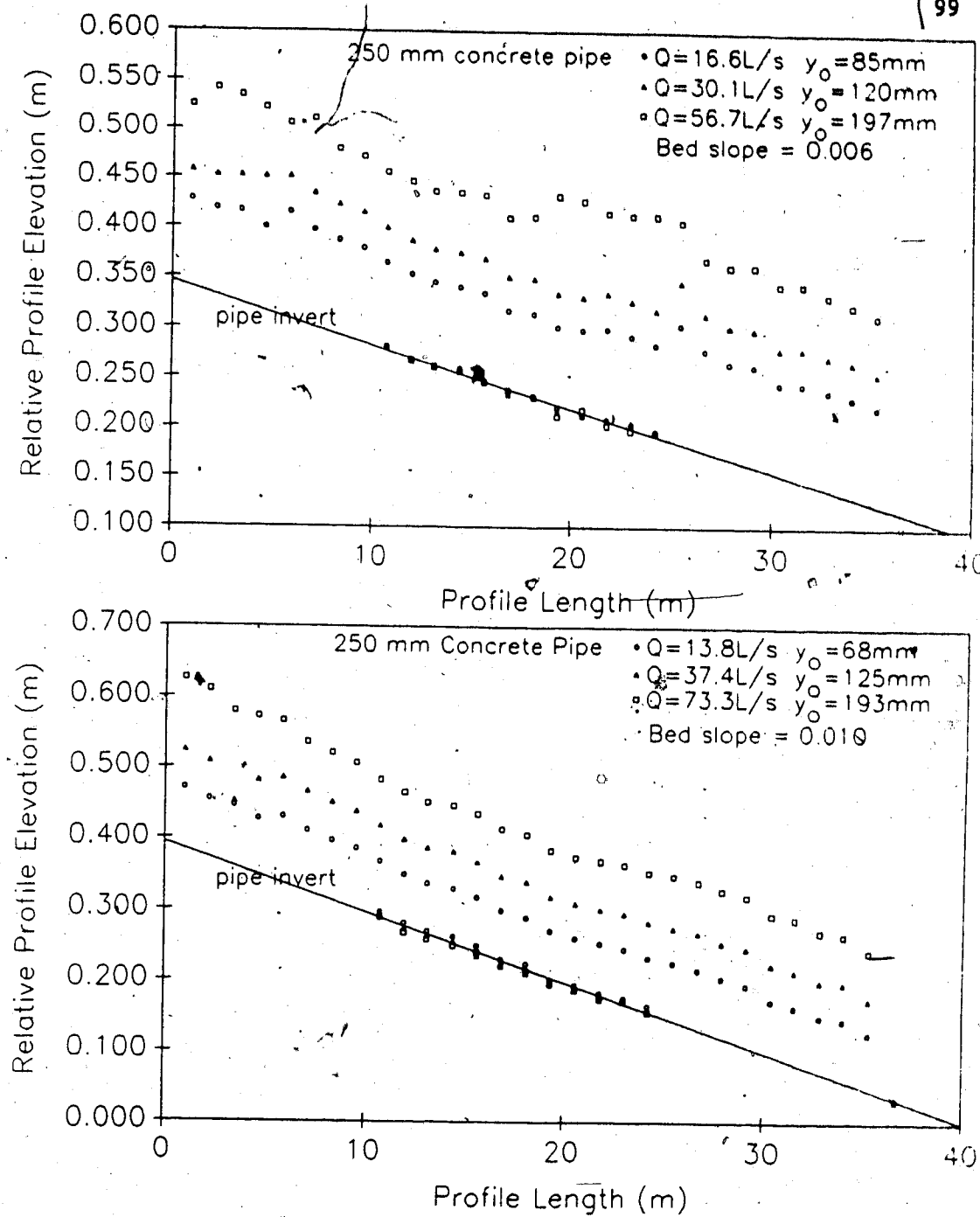
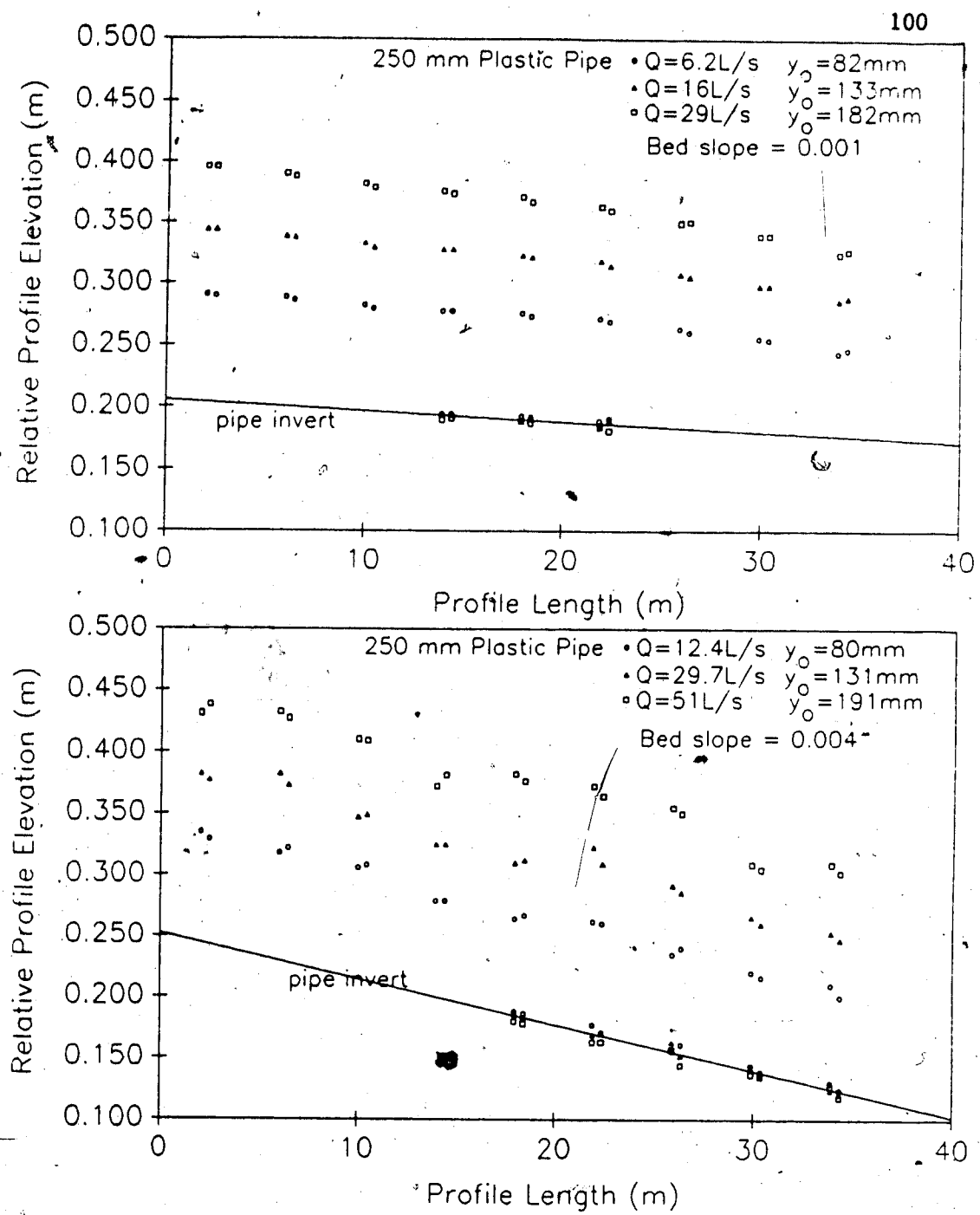


Figure 13: Water surface profiles in the 250 mm concrete pipe. Surface irregularities are well illustrated by the bottom figure.



**Figure 14: Surface profiles in the 250 mm concrete pipe. Surface disturbances are greatly reduced in the supercritical flow profile represented by the bottom figure.**



**Figure 15:** Water surface profiles for the 250 mm plastic pipe.

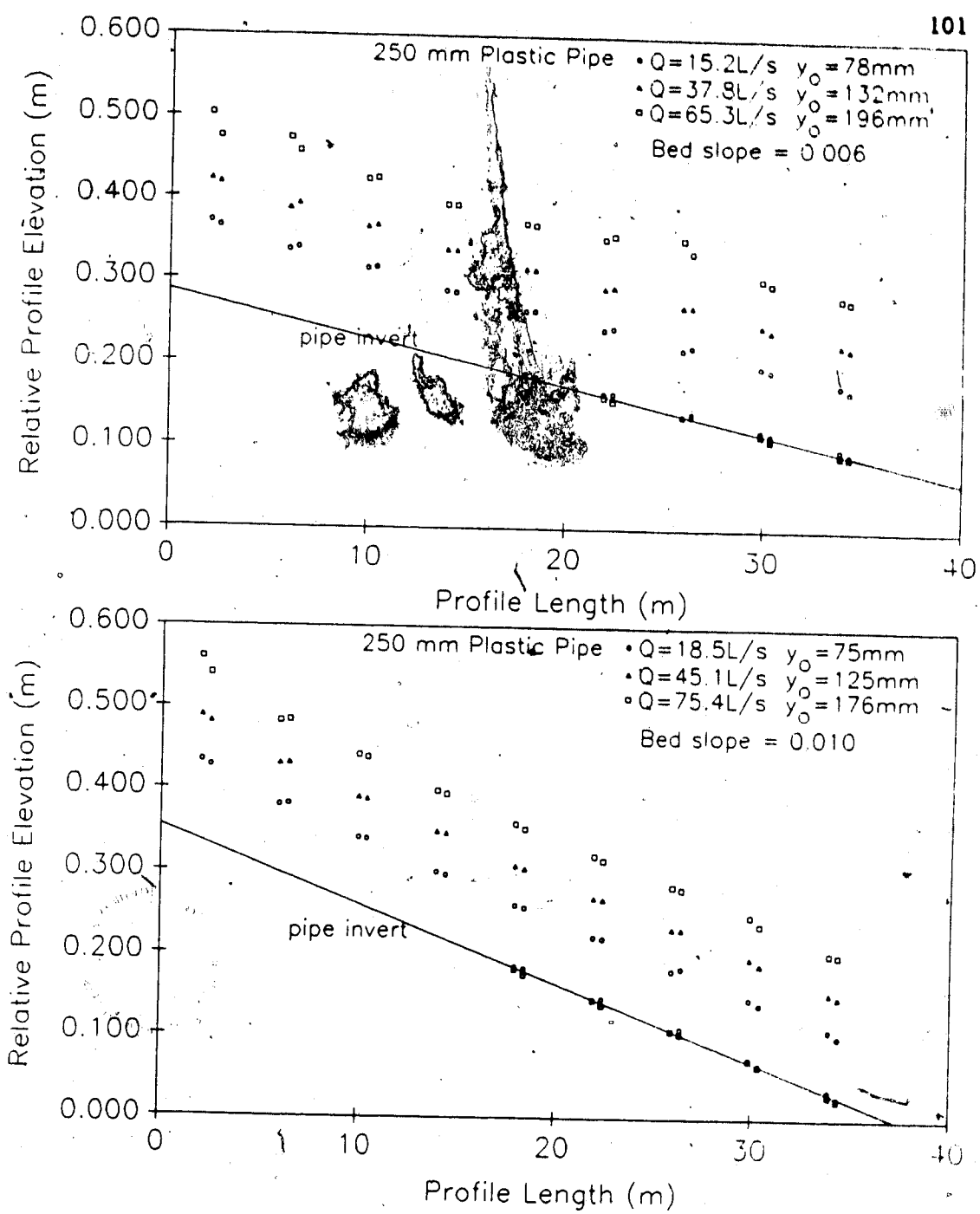


Figure 16: Water surface profiles in the 250 mm plastic pipe.

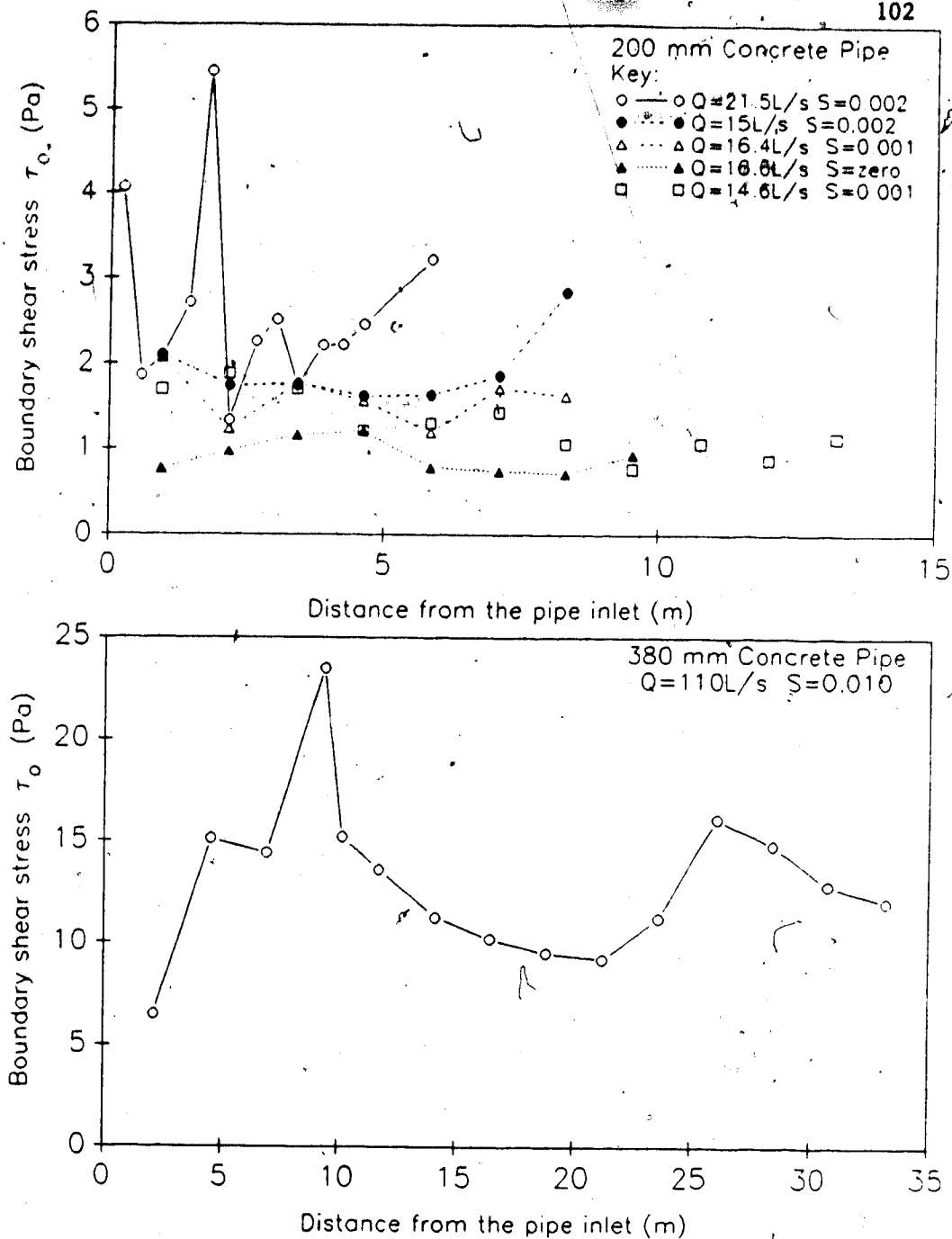


Figure 17: Shear stress downstream from the inlet of the 200 and 380 mm concrete pipes.

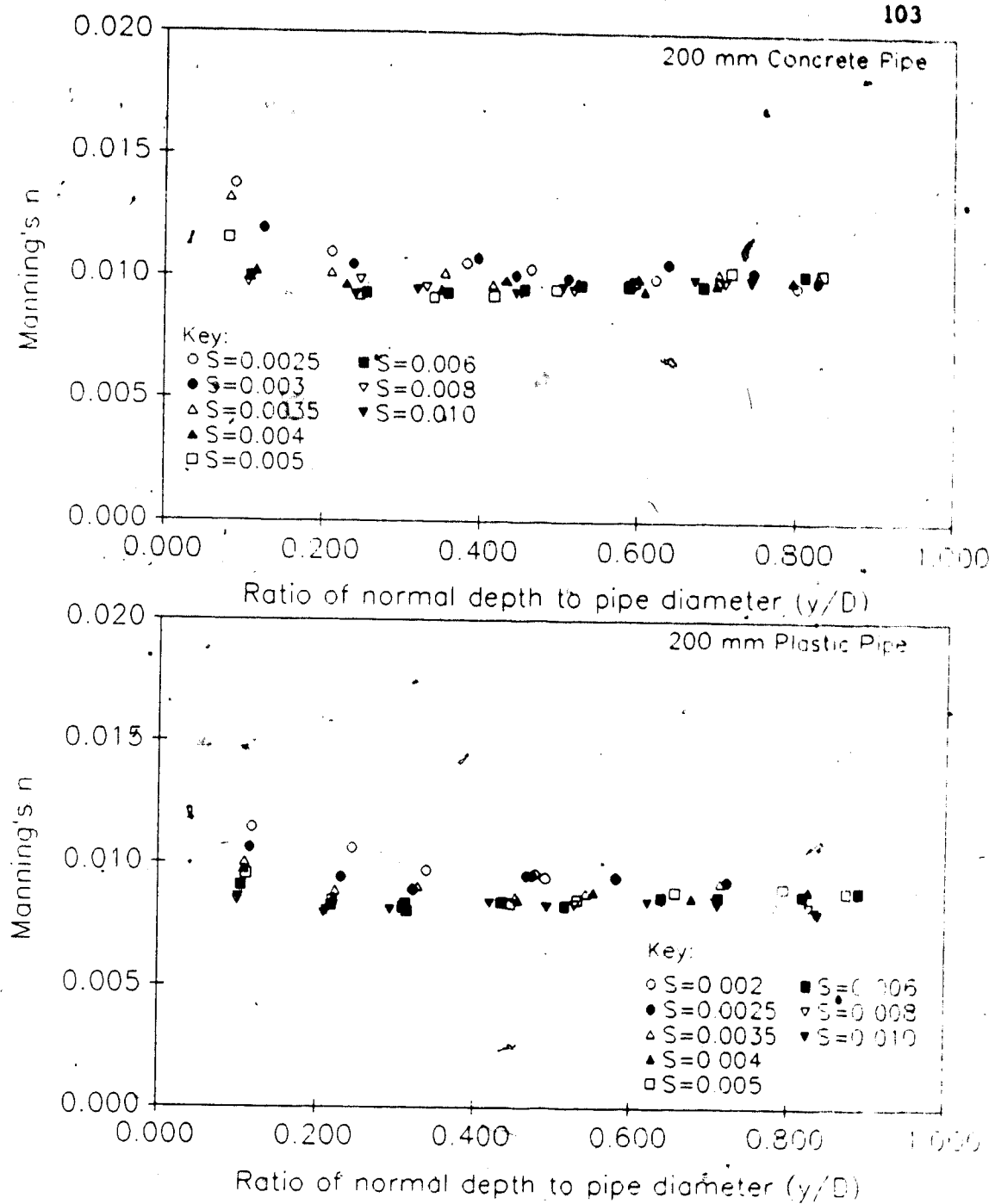


Figure 18: Manning's  $n$  versus depth ratio for the 200 mm concrete and plastic pipes.

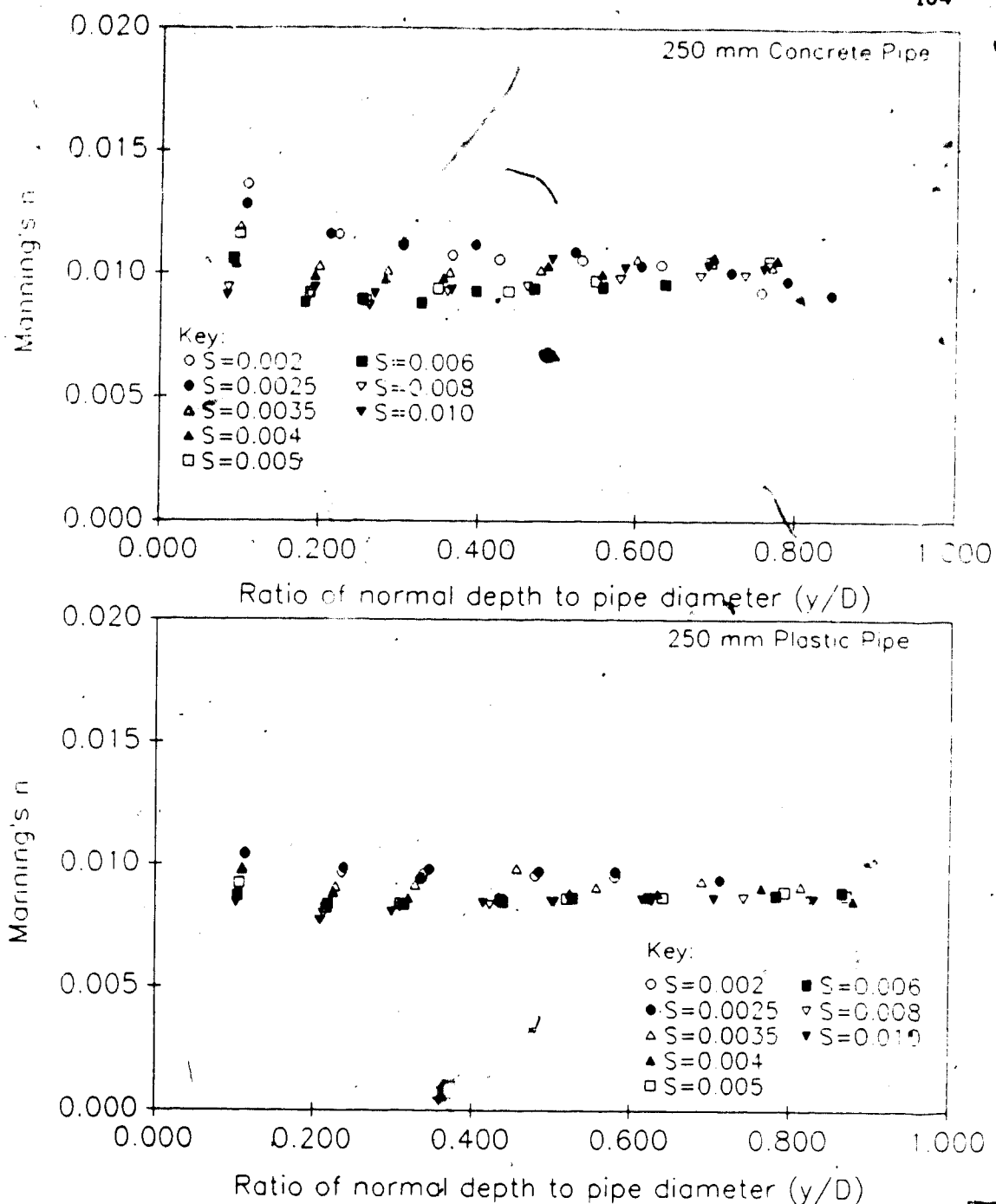


Figure 19: Manning's  $n$  versus the depth ratio for the 250 mm plastic and concrete pipes tested.

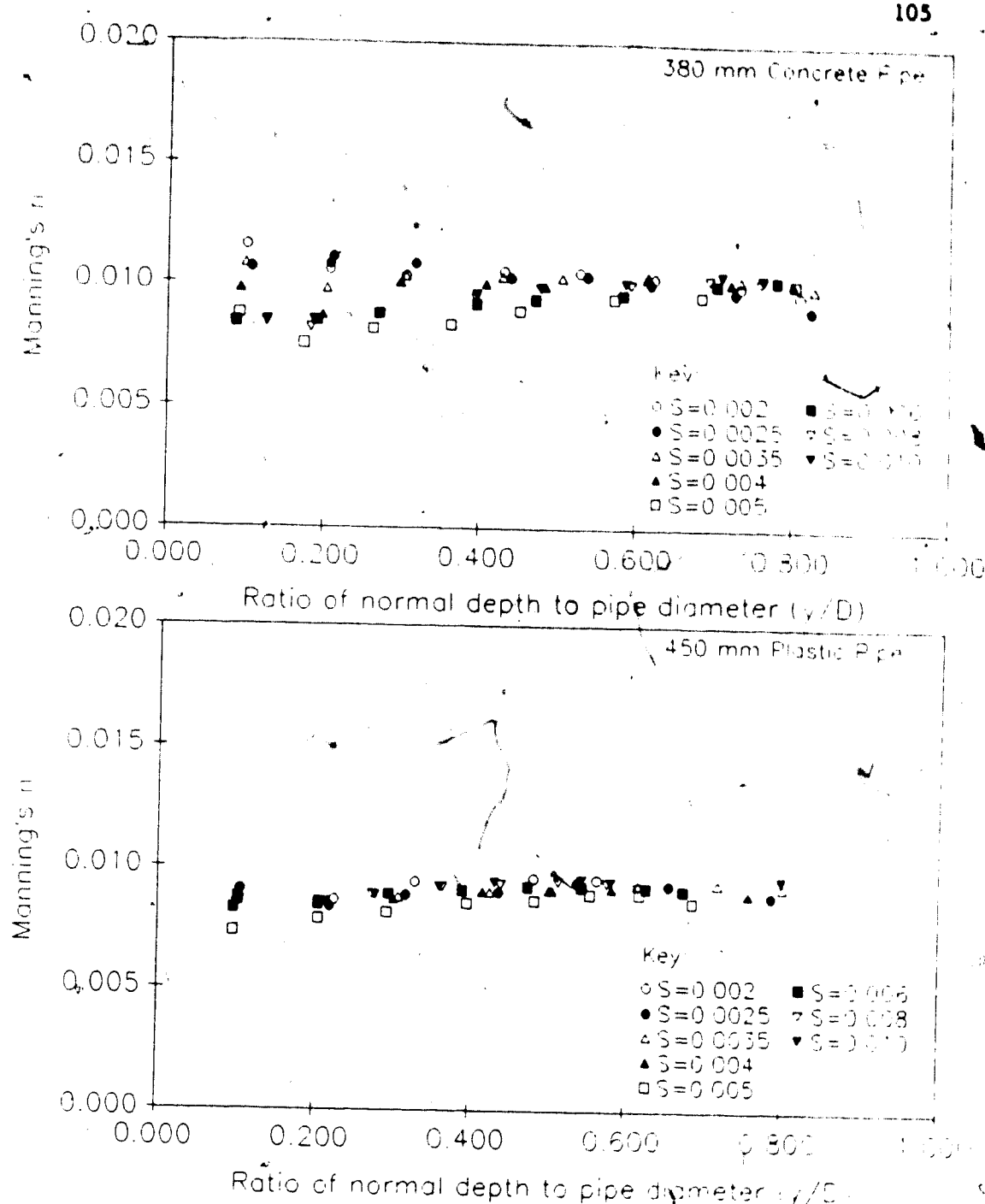
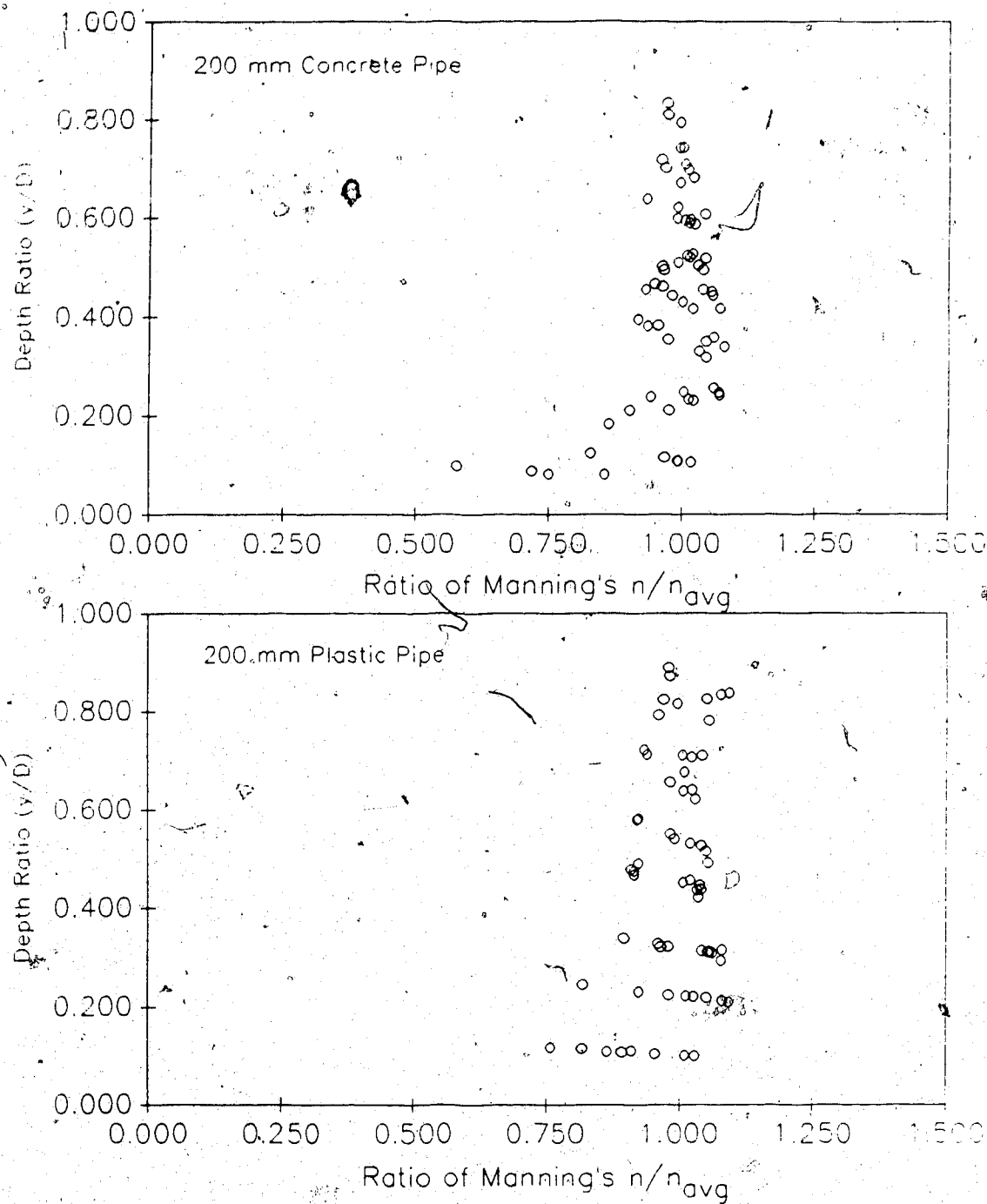
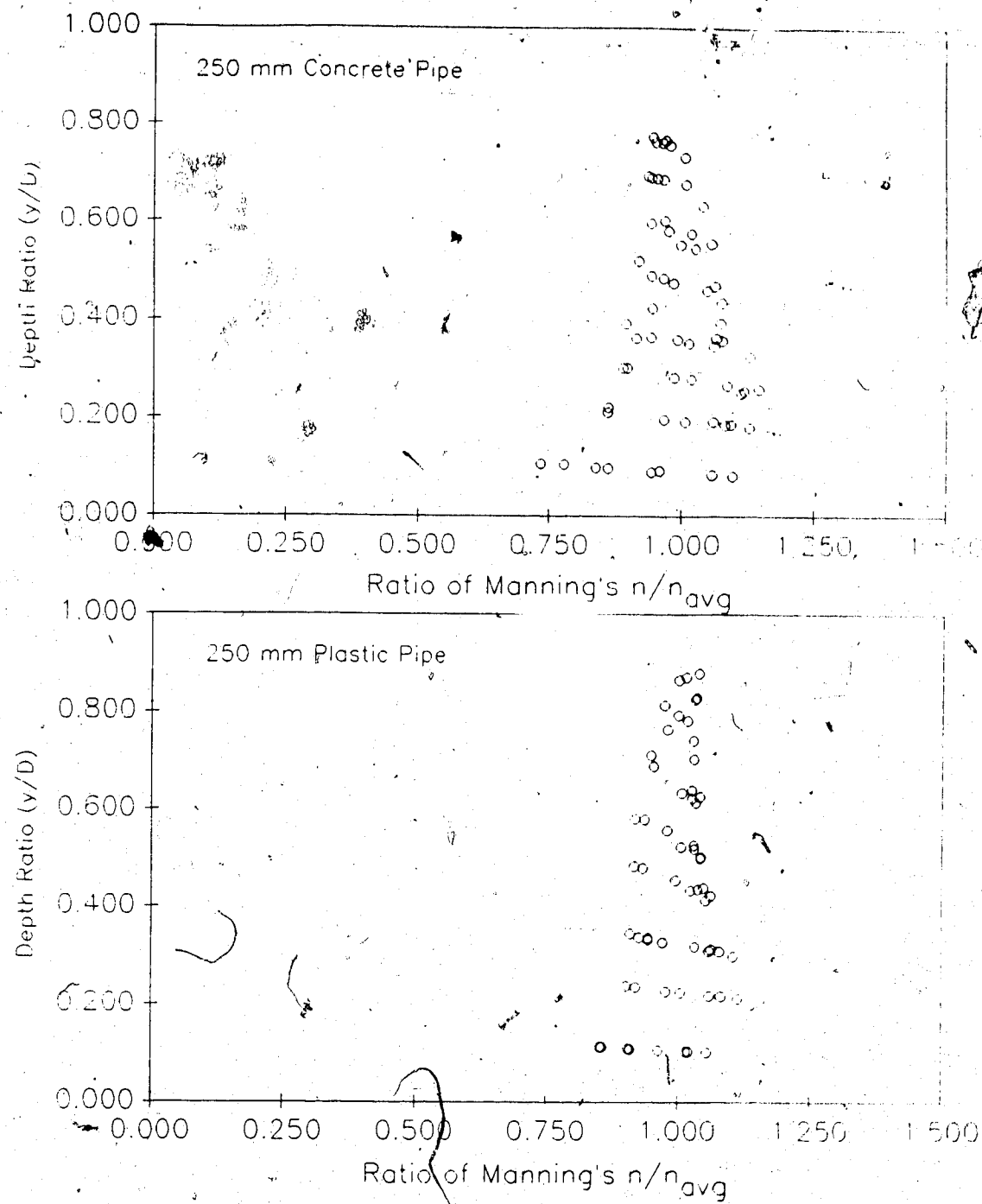


Figure 20: Manning's  $n$  versus depth ratio for the 380 mm concrete and the 450 mm plastic pipes.



**Figure 21:** Dispersion of Manning's  $n$  with depth ratio for the 200 mm concrete and plastic pipes. Manning's  $n$  is expressed as a ratio of measured values to the average Manning's  $n$  calculated for depth ratios greater than 0.25.



**Figure 22:** Dispersion of Manning's  $n$  with depth ratio for the 250 mm concrete and plastic pipes. Manning's  $n$  is expressed as a ratio of measured values to the average Manning's  $n$  calculated for depth ratios greater than 0.25.

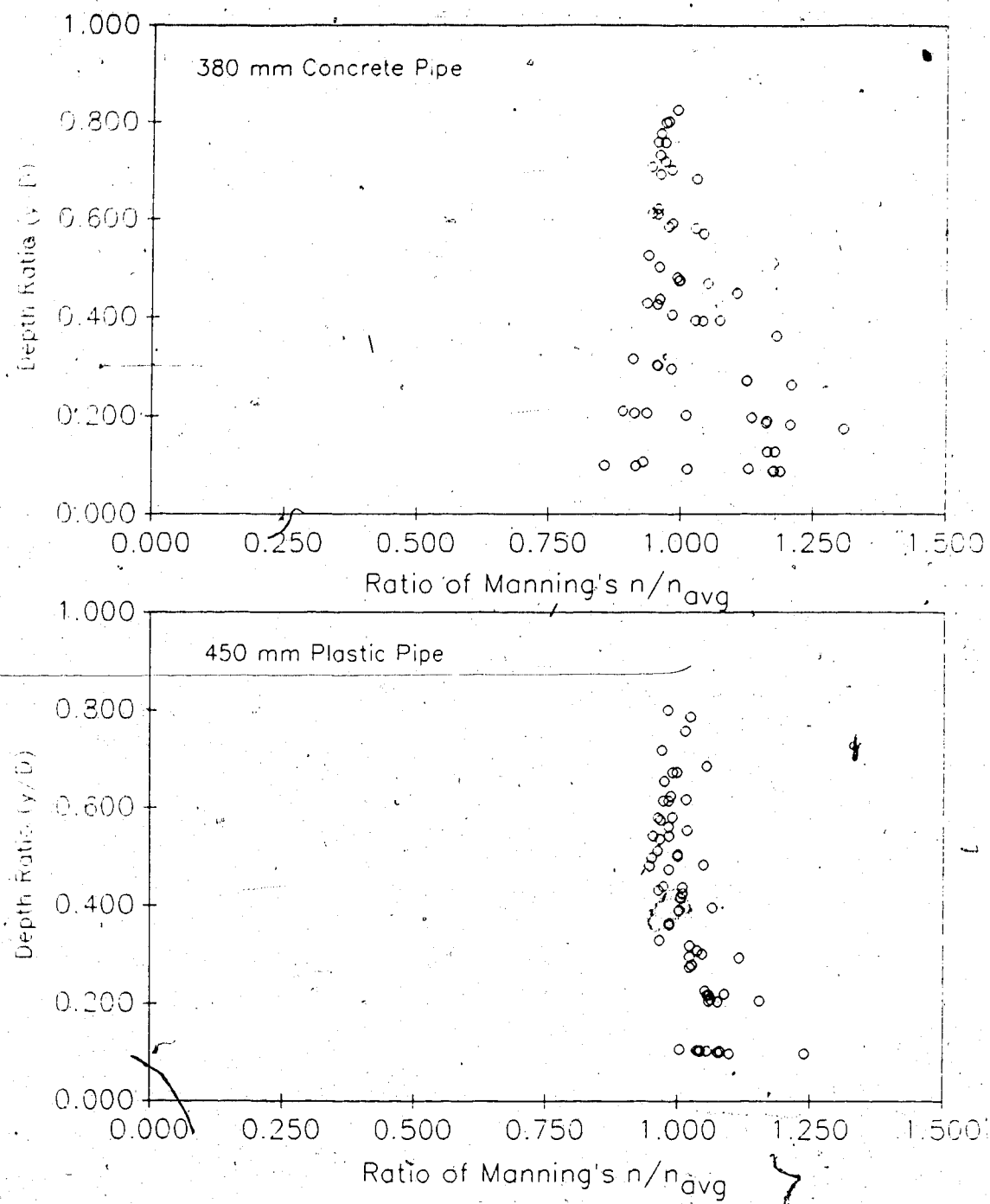


**Figure 23:** Dispersion of Manning's  $n$  with depth ratio for the 380 mm concrete and 450 mm plastic pipes. Manning's  $n$  is expressed as a ratio of measured values to the average Manning's  $n$  calculated for depth ratios greater than 0.25.

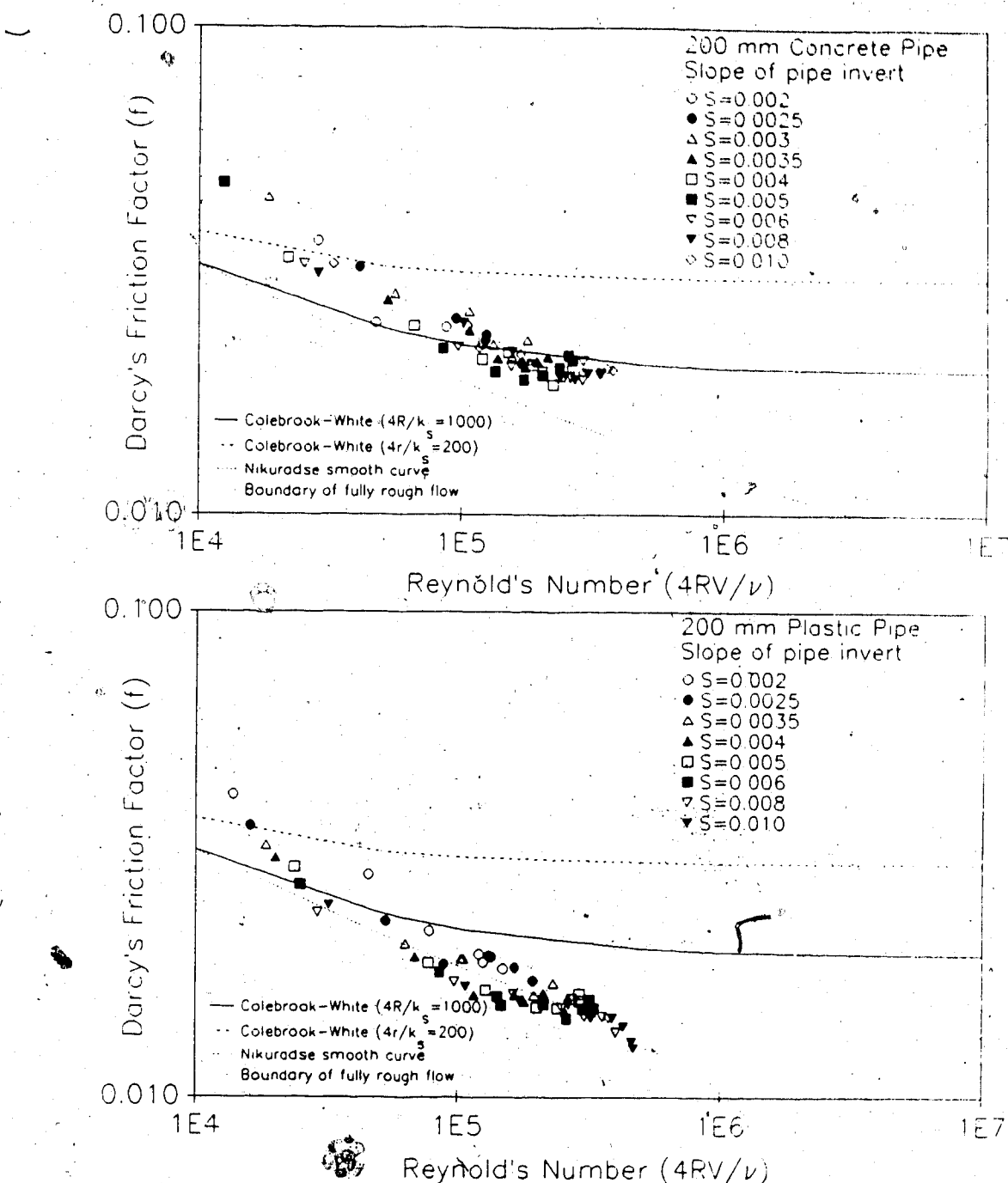
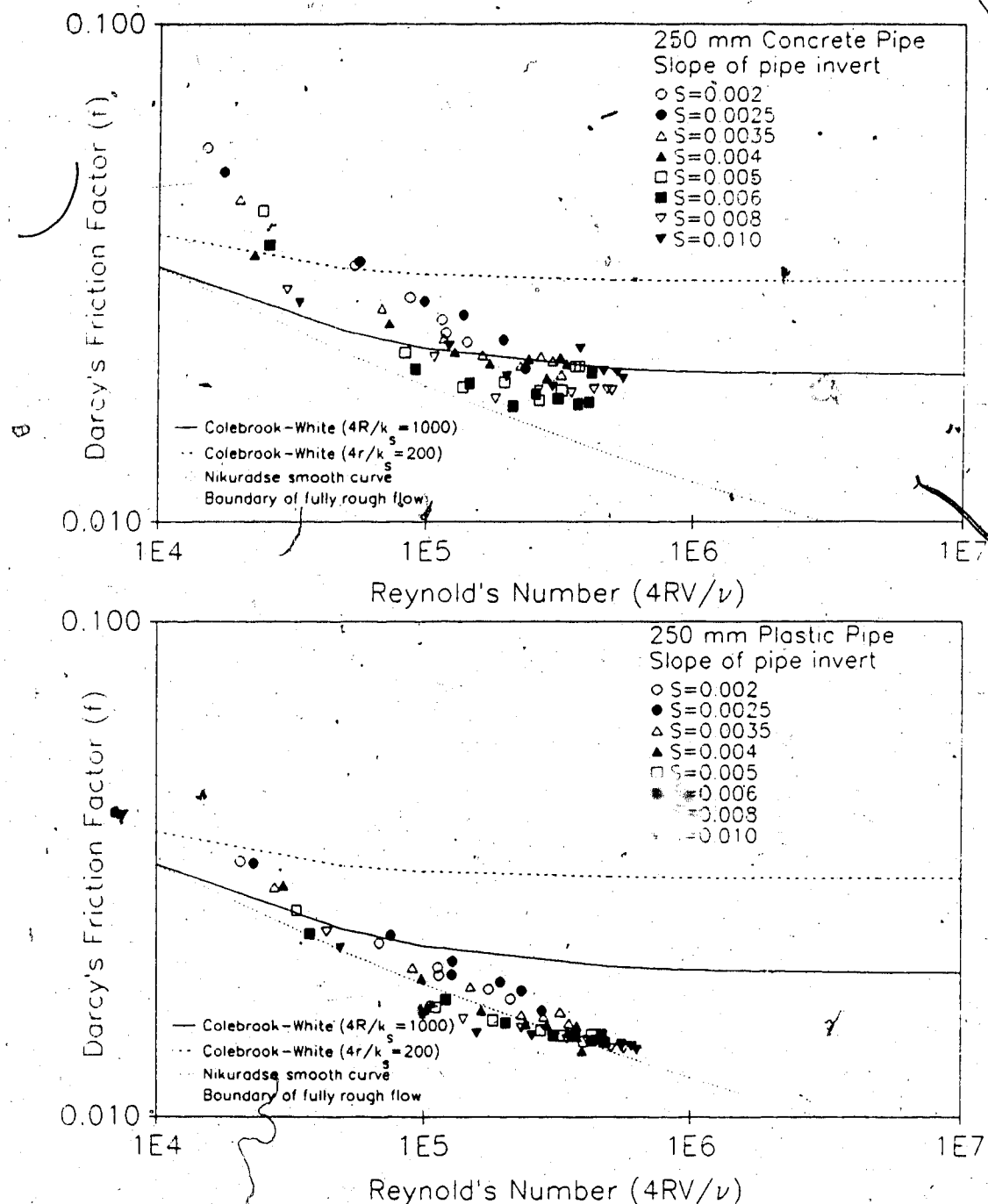


Figure 24: Moody diagram for the 200 mm plastic and concrete pipes.



**Figure 25: Moody diagrams for the 250 mm plastic and concrete pipes.**

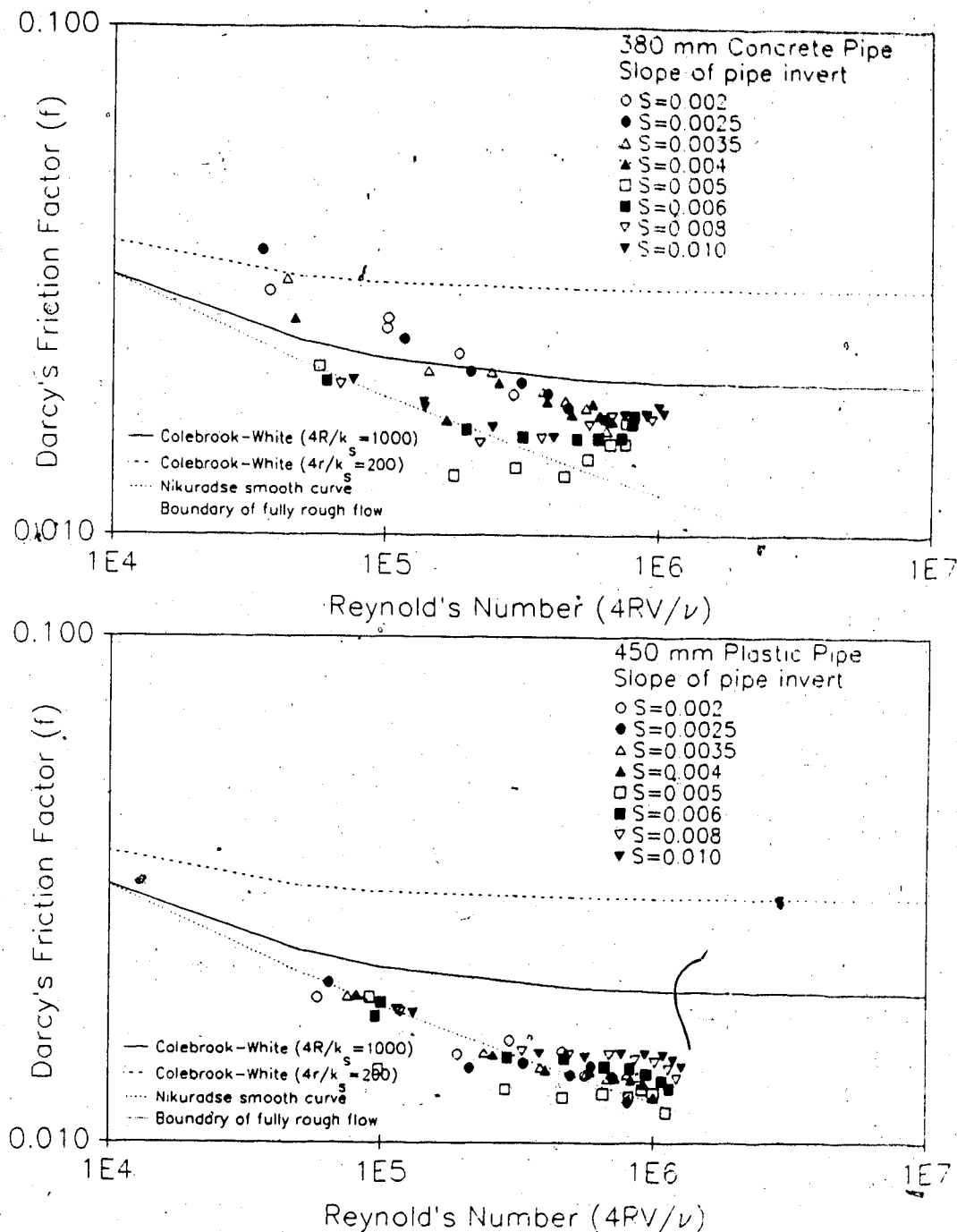


Figure 26: Moody diagrams for the 380mm concrete and the 450 mm Spiro-loc pipe.

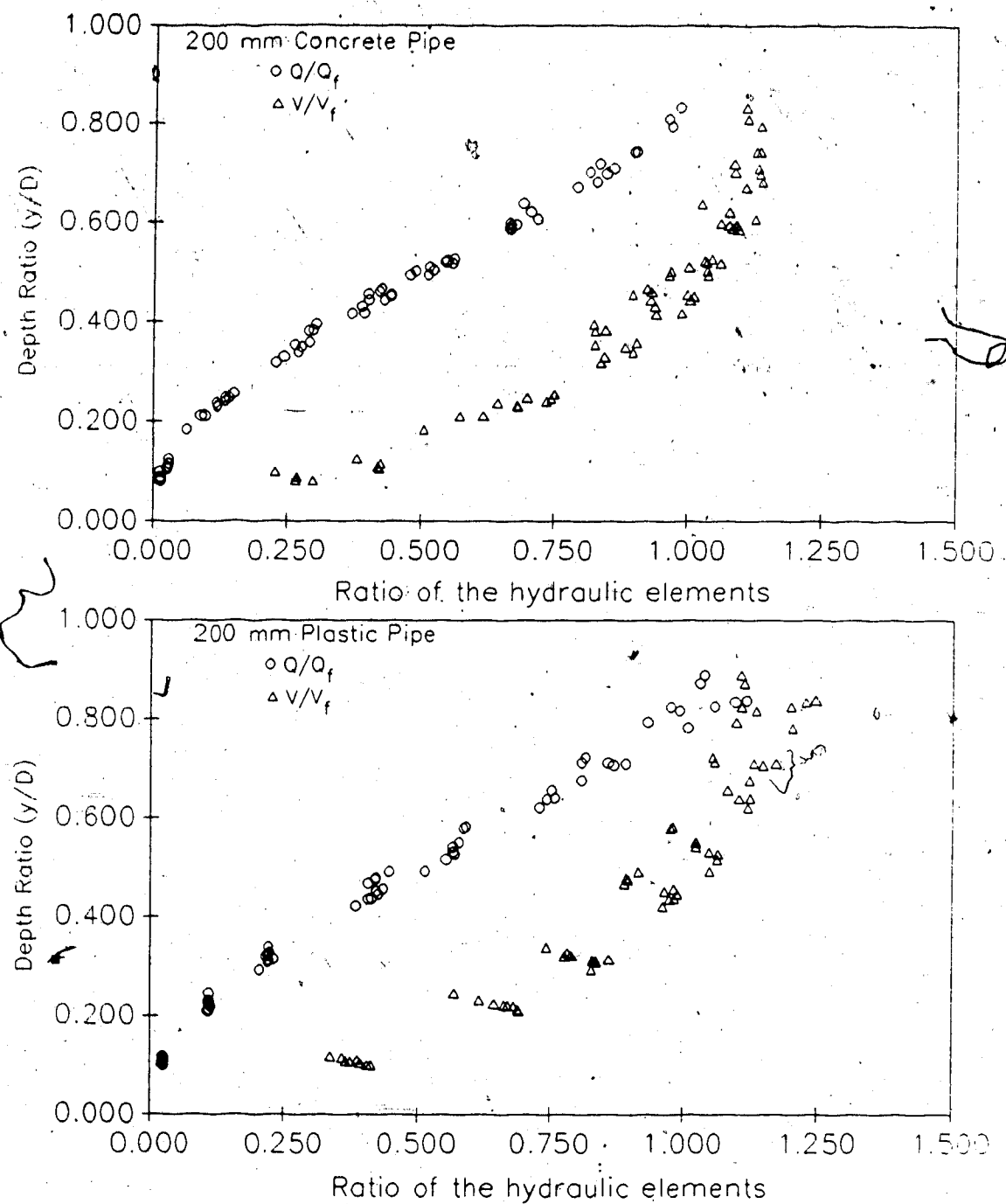


Figure 27: Plot of the part-full to pipe full velocity and discharge for the 200 mm concrete and plastic pipes.

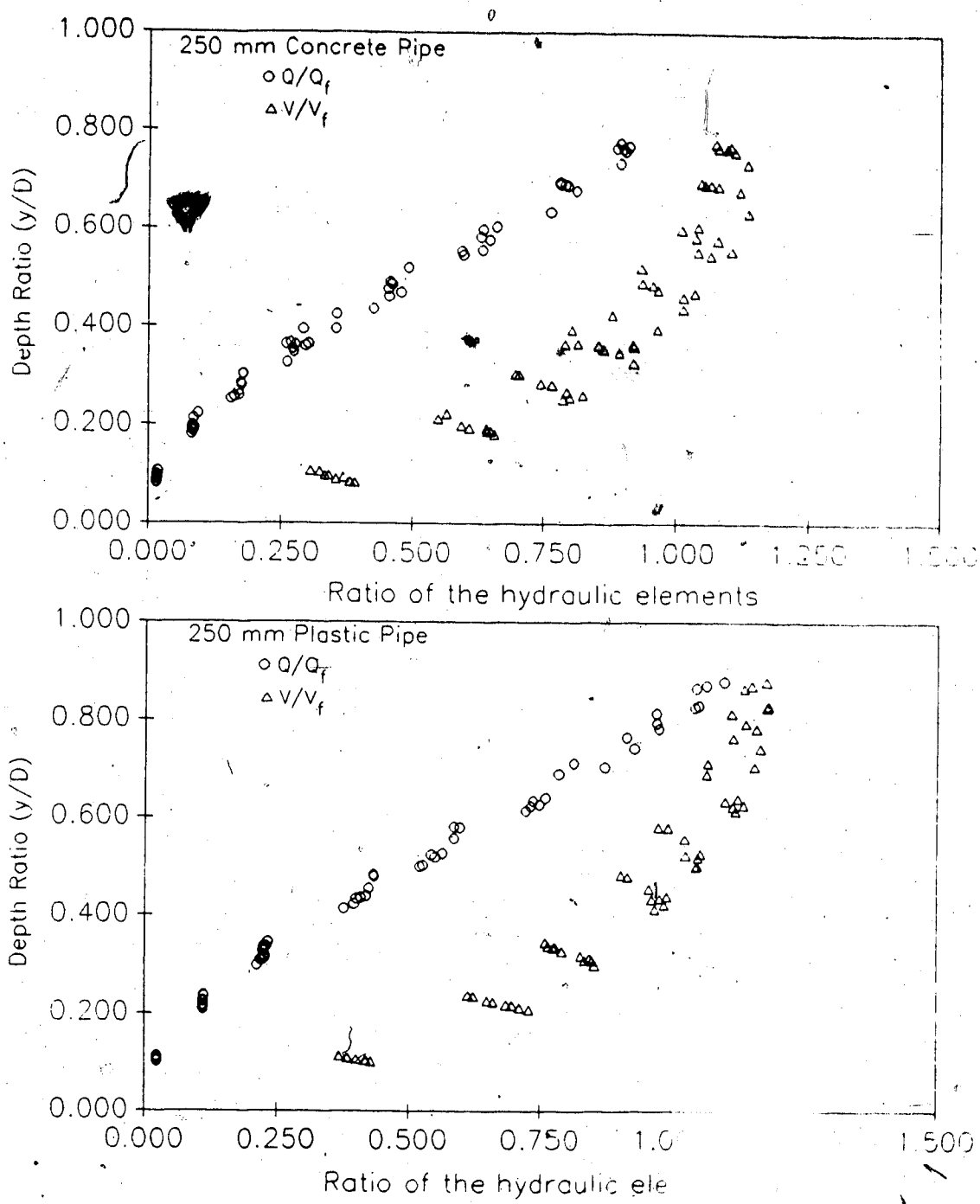
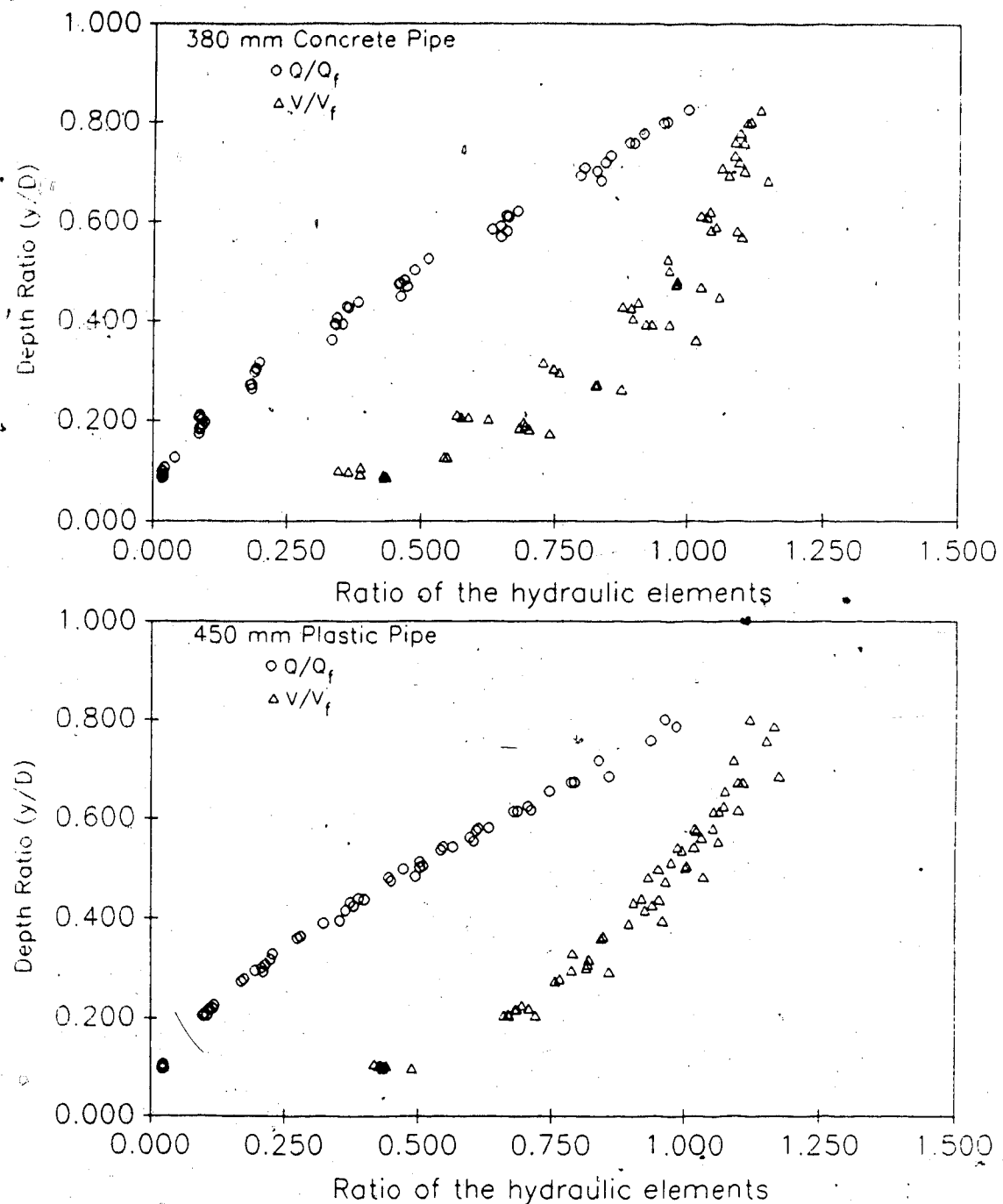
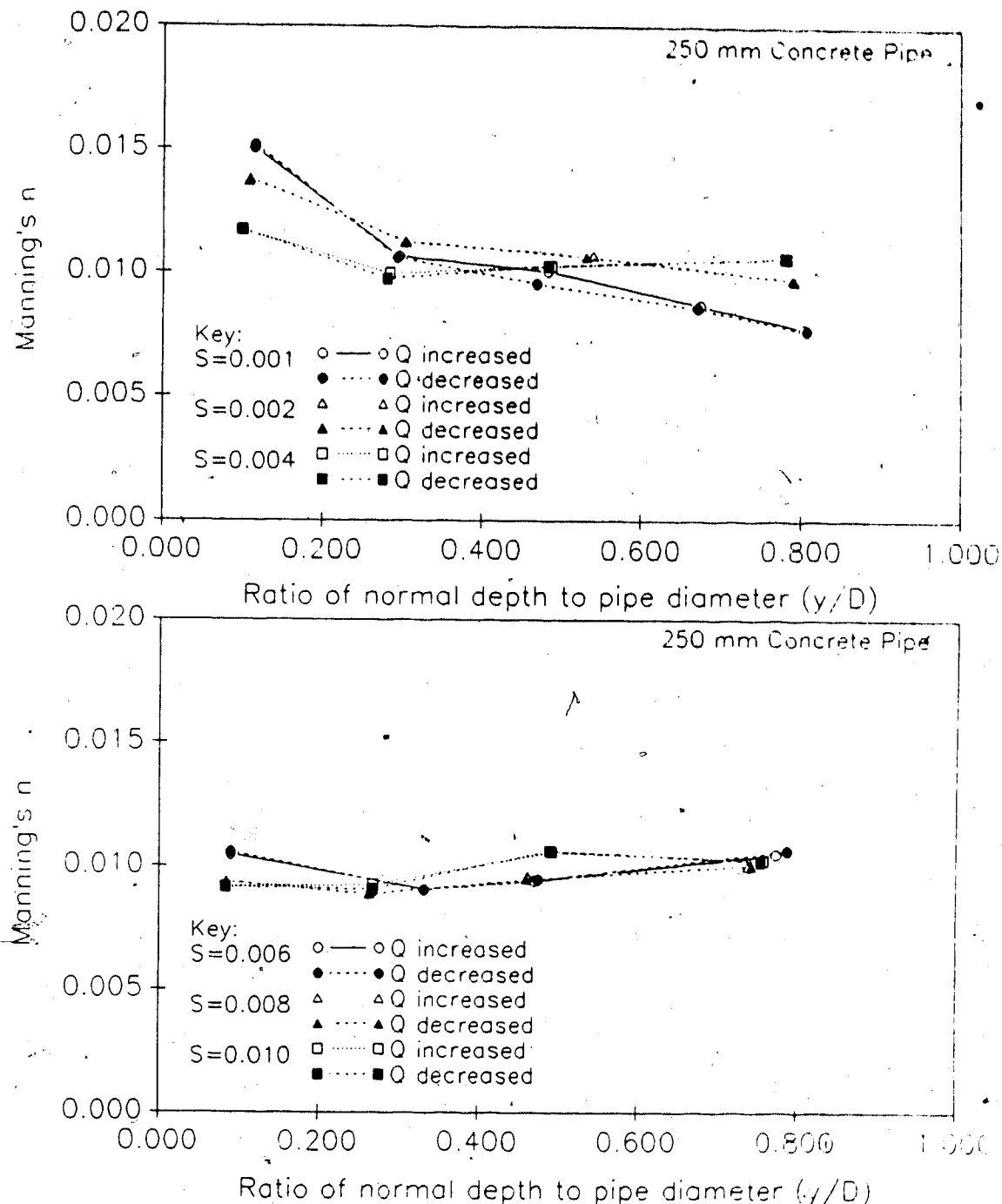


Figure 28: Plots of the part-full to pipe full velocity and discharge measurements in the 250 mm concrete and plastic pipes.



**Figure 29: Plots of the part-full to pipe full velocity and discharge measurements in the 380 mm concrete and 450 mm plastic pipes.**



**Figure 30:** This figure shows the repeatability of the results with discharge increased and decreased between tests in the 250 mm concrete pipe.

COLOUR PHOTOGRAPHS SHOULD NOT BE USED. THEY WILL APPEAR AS GREY OR BLACK. WE RECOMMEND THAT THE COPY OF THE THESIS SUBMITTED FOR MICRORFILMING INCLUDE BLACK AND WHITE PHOTOGRAPHS REPRINTED FROM THE COLOUR PHOTOGRAPHS BY A PHOTOGRAPHER IF NECESSARY.

LORSQUE MICROFILMEES, LES PHOTOGRAPHIES EN COULEURS PARAISSENT GRISES OU NOIRES. NOUS RECOMMANDONS QUE L'EXEMPLAIRE DE LA THESE A MICRORFILMER SOIT ACCOMPAGNE PLUTOT DE PHOTOGRAPHIES EN NOIR ET BLANC PRODUITES AU BESOIN PAR UN PHOTOGRAPHE A PARTIR DES PHOTOGRAPHIES EN COULEURS.

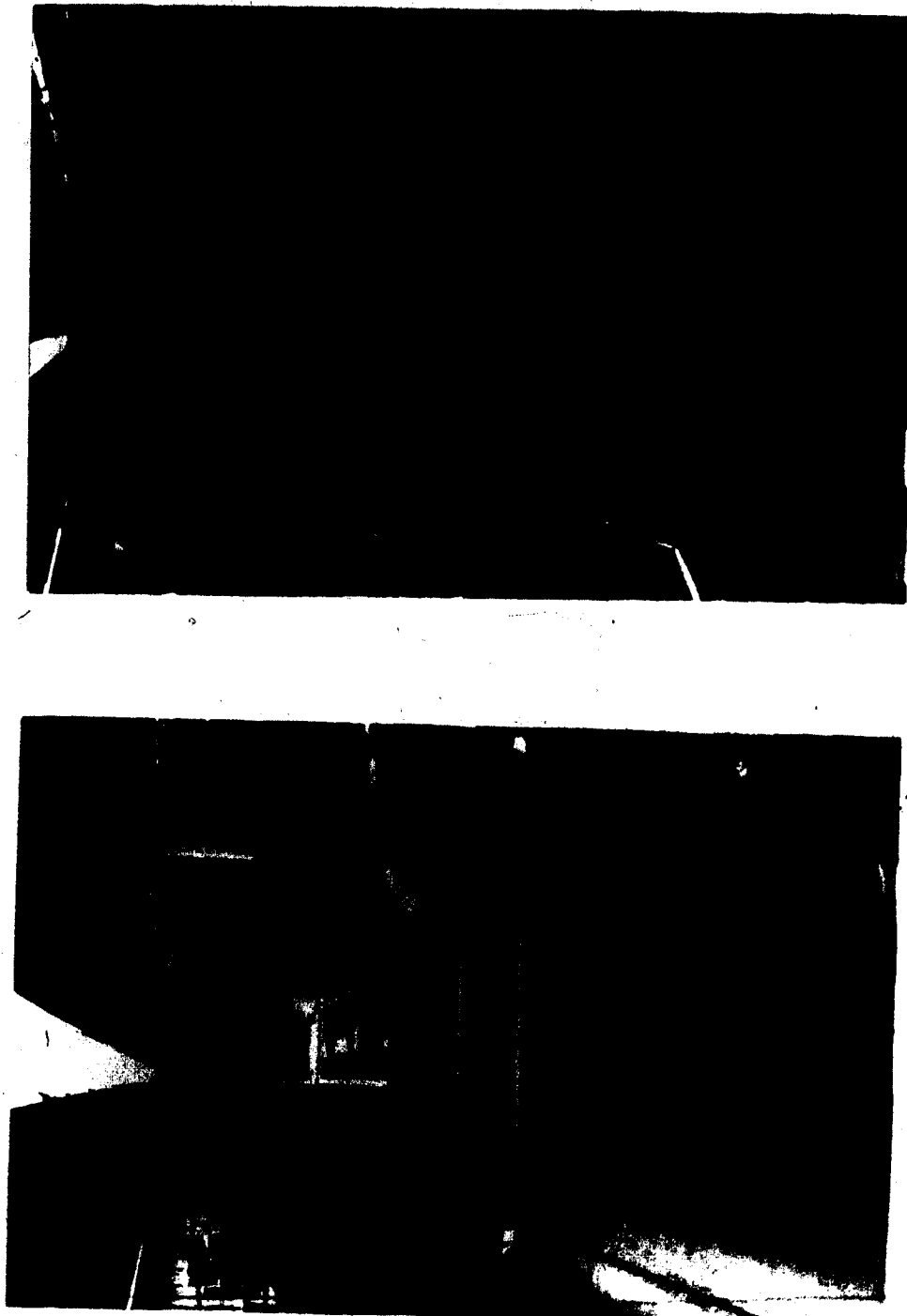


Plate 1: Experimental set-up showing the head tank, flume, and 380 mm concrete pipe installed in the flume. The sloping manometer board is visible to the right of the flume and the positions of the capacitance probes are indicated by the white cradles on top of the pipe.

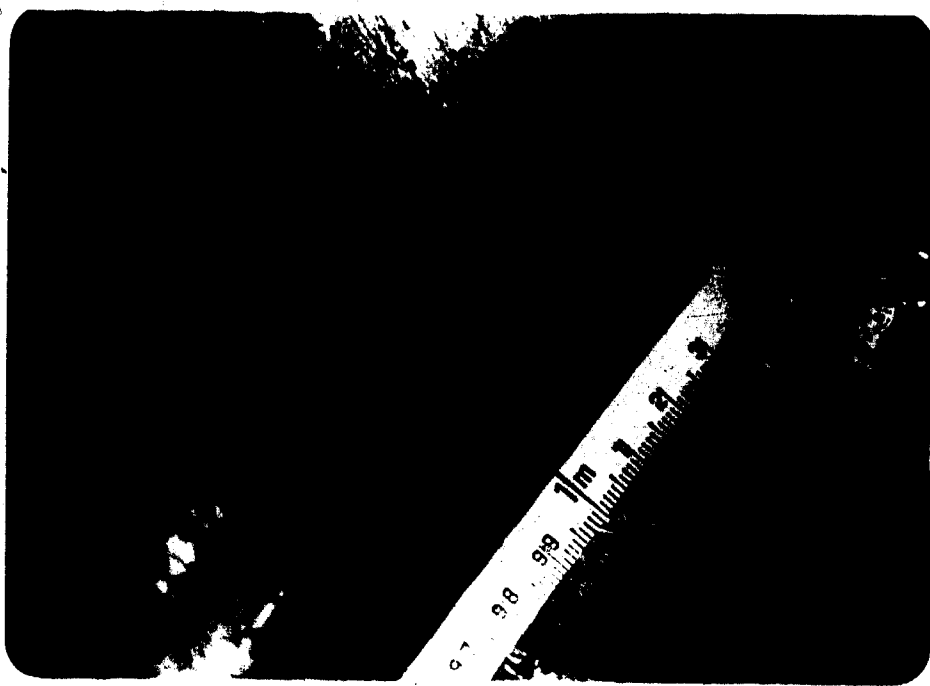


Plate 2: Typical joints in the 250 mm concrete pipe. The top photograph shows water surface disturbances created at the joint.

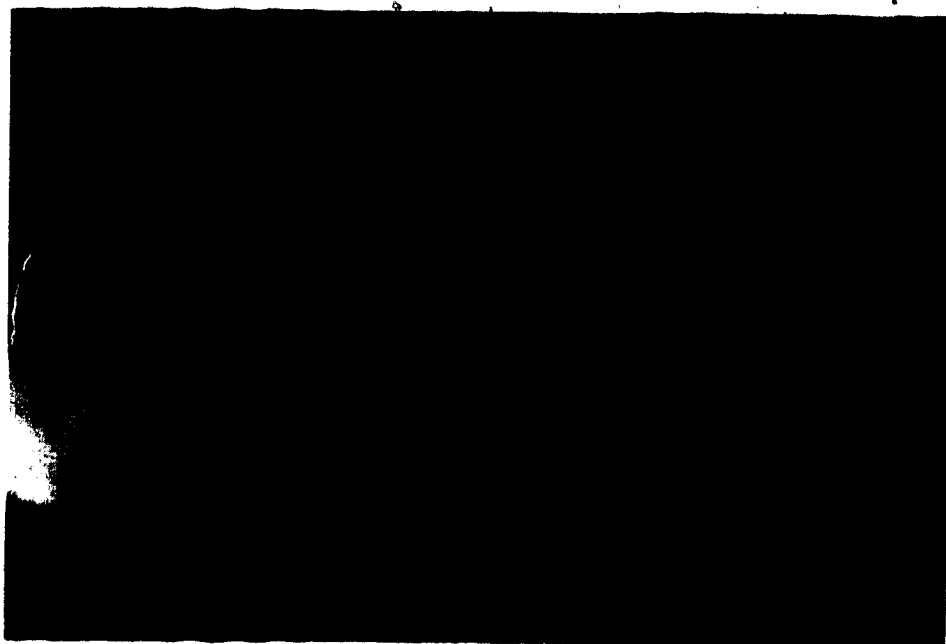


Plate 3: Roughness measuring device during test on a concrete pipe sample. The sample is mounted in a vice as shown by the bottom photograph. The top photograph shows the complete apparatus.

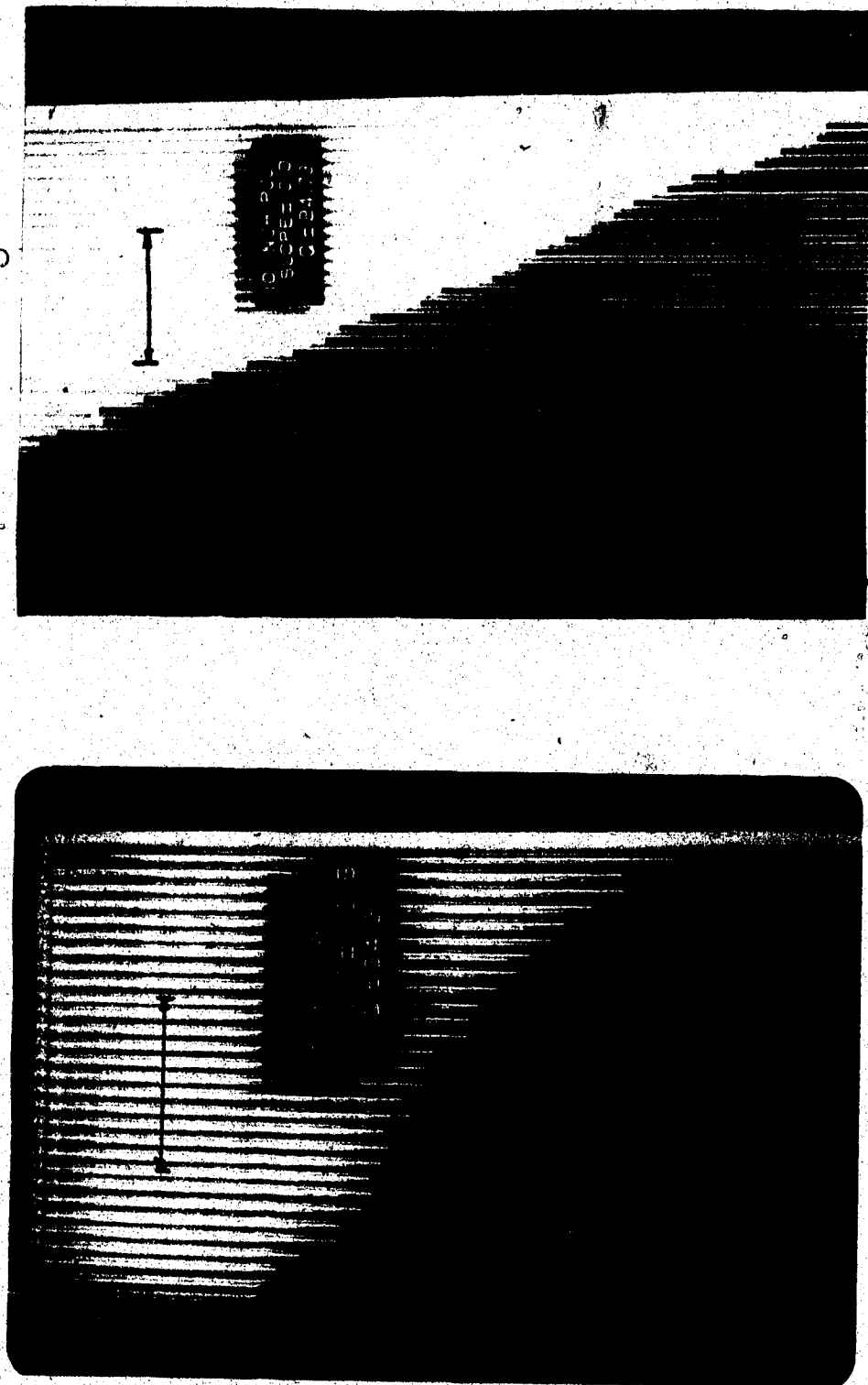


Plate 4: Manometers indicating the water surface profiles in the 250 mm concrete pipe for mild (slope of 0.0025) and steep (slope of 0.010) conditions. The left photograph is a typical subcritical water surface profile and the right photograph is a supercritical profile.

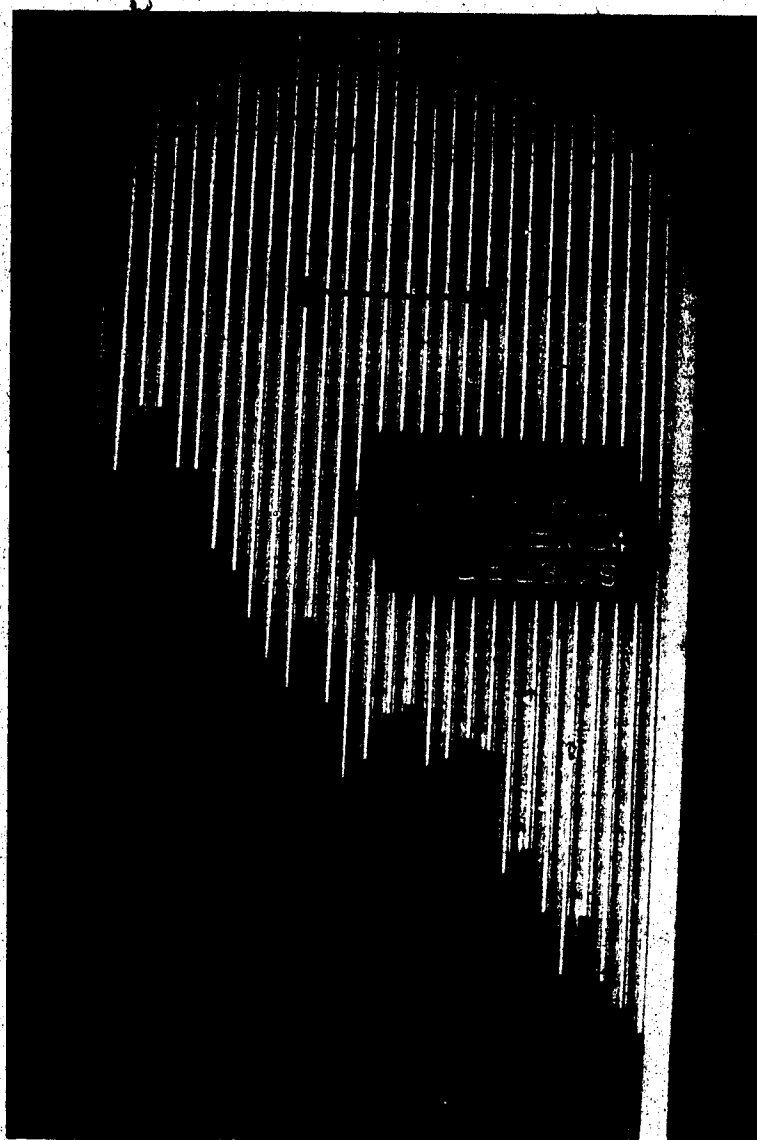


Plate 5: Manometers indicating the water surface profile in the 250 mm concrete pipe flowing at 23.75 L/s. The bed slope was 0.004. This is a typical transition profile. The standing surface waves resulting from the flow instability are very obvious. The line at the top of the photograph indicates the reach selected for uniform flow measurements.

## 9 References

Ackers, P., Resistance of fluids flowing in pipes and channels. Hydraulics Research Paper No. 1, London, H.M.S.O., 1958.

Ackers, P., An investigation of head losses at sewer manholes. Civil Engineering and Public Works Review. 54: part 1, no. 637, 882-885, part 2, no. 638, 1033-1036, 1959.

Ackers, P., The hydraulic resistance of drainage conduits. Proc. Inst of Civil Engineers. vol. 19: 307-336, July, 1961.

Ackers, P., M. Crickmore, and D. Holmes. Effects of use on the hydraulic resistance of drainage conduits. Proc. Inst. of Civil Engineers. vol. 28: 339-360, July, 1964.

ASCE Task Force. Friction factors in open channel. Journal of the Hydraulics Division, ASCE. Vol. 89 No. HY2: 97-132, 1963.

Besmehn, Y. Field measurements of resistance coefficients in sanitary sewers. A thesis submitted to the Faculty of Graduate Studies and Research in Partial fulfilment of the requirements for the degree of Master of Science, Dept. of Civil Engineering, Edmonton, Alberta. 1986

Bloodgood, D. and J. Bell. Manning's coefficient calculated from test data. J. Water Pollution Control Federation.

Vol. 33, No. 2: 176-183, 1961.

Camp, T., Design of sewers to facilitate flow. Sewage Works Journal, Vol. 18: 1-16, 1946.

Camp, T., Discussion on determination of Kutter's n for sewers partly filled, by C. F. Johnson, Transactions, ASCE, Vol. 109: 240-243, 1944.

Chow, V.T. Open Channel Hydraulics, McGraw-Hill Book Co., Inc., New York, N.Y., 1959.

Colebrook, C.F. Turbulent flow in pipes with particular reference to the transition region between the smooth and rough pipe laws. J. Inst of Civil Engineers, Vol. 11: 133-156, 1938-1939.

Coulter, G.C., Discussion on determination of Kutter's n for sewers partly filled, by C.F. Johnson, Transactions, ASCE, Vol. 109: 243-245, 1944.

Fair, G.M., Geyer, J.C., Okun, D.A., Water and Wastewater Engineering. Vol. 1 Water Supply and Wastewater Removal. John Wiley and Sons, N.Y., New York, 1966.

Henderson, F.M. Open Channel Flow. MacMillan Publishing Co., Inc., N.Y., New York, 1966.

Johnson, C.F., Determination of Kutter's n for sewers partly filled. Transactions, ASCE, Vol.71, no. 3, part 2: 223-247, 1944.

Keulegan, G.H. Laws of turbulent flow in open channels.

Journal, National Bureau of Standards, Washington, D.C.  
Research Paper 1151, Vol.21: 707-741, 1938

Manning, R. On flow of water in open channels and pipes.  
Transactions, Inst. of Civil Engineers, Ireland, Vol.20:  
161-207, 1891.

Mindess, S. and J.F. Young. Concrete. Prentice-Hall Inc.,  
Englewood Cliffs, New Jersey 07632, U.S.A., 1981.

Morris, H.M., A new concept of flow in rough conduits.  
Transactions, ASCE, Vol.120: 373-410, 1955.

Neale, L.C. and Price, R.E., Flow characteristics of PVC  
sewer pipe. Journal of the Sanitary Engineering  
Division, ASCE, Vol.90, No. SA3: 109-129, 1964.

Nikuradse, J., Stromungsgesetze in rauhen rohren, Verein  
Deutscher Ingenieure, Forschungsheft 361, 1933; or NACA  
TM 1292, November, 1950.

Peterson, A.W. and Howells, R.F., Users Manual for HYEPOL, A  
Hydraulic Engineering Problem Oriented Library, Dept. of  
Civil Engineering, The University of Alberta, Edmonton,  
Canada. 1981.

Pomeroy, R.D., Flow velocities in small sewers. Journal, Water Pollution Control Federation, Vol.39, No.9: 1525-1548, 1967.

Powell, R.W. Flow in a channel of definite roughness, Trans. ASCE, Vol. 3: 531-566, 1946.

Powell, R.W., Resistance to flow in rough channels, Trans. Amer. Geophysical Union, Vol.31:575-582, 1950 and Vol.32: 607-613, 1951.

Powell, R.W., and Posey, C.J., Resistance experiments in a triangular channel. J. Hydraulics Division, ASCE, Vol. 85, No.HY5: 31-66, 1959.

Ramser, C.E., Discussion on determination of Kutter's n for sewers partly filled, by C.F. Johnson, Transactions, ASCE, Vol. 109: 240-243, 1944.

Rephogle, J.A., and Chow, V.T., Tractive force distribution in open channels, J. Hydraulics Division, ASCE, vol.92 no.HY2: 169-191, 1966.

Rouse, H., and Ince, S., History of Hydraulics. Iowa Inst. of Hydraulic Research, 1957.

Schlichting, H., Boundary Layer Theory. McGraw-Hill Book Co., N.Y., New York, 1979.

Schmidt, O.J. Measurement of Manning's roughness coefficient, J. Sewage and Industrial Wastes, Vol.31, No.9: 995-1003, 1959.

Straub, L.G. and H.M. Morris. Hydraulic tests on concrete culvert pipes. St. Anthony Falls Hydraulic Laboratory, Minneapolis, Technical Paper 4, Series B, 1950.

Straub, L., Bowers, C.E., Pilch, M., Resistance to Flow in Two Types of Concrete Pipe. Technical Paper no.22, Series b, St. Anthony Falls Hydraulic Laboratory, Minneapolis, Minnesota, 1960.

Streeter, V.L. and Wylie, B.E., Fluid Mechanics. McGraw-Hill Ryerson Ltd, Toronto, Canada, 1981.

Taylor, J.R., An Introduction to Error Analysis, The Study of Uncertainty in Physical Measurements. University Science Books, Mill Valley, California, 1982.

Thijssse, J. Discussion on: Resistance to flow in rough channels, by R.W. Powell, Trans., Am. Geoph. Union, vol. 31, no. 4: 575-581, Aug. 1950. Discussion in: Trans., Am. Geoph. Union, vol. 32, no. 4: 609-610, 1951.

Wilcox, E.R. A comparative test of the flow of water in 8 inch concrete and vitrified clay sewer pipe, Engineering Experiment Station Series, Bulletin No. 27, University of Washington, Seattle, Washington, 1924.

**Appendix A : Pipe Specifications and Manufacturers**

Pipe	Nominal Diameter (mm)	ASTM Standards	Tradename	Supplier
<b><u>Concrete</u></b>				
NR	200	C-14-III	P	CC
NR	250	C-14-III	P	CC
R	380	C-76-IV	P	CC
<b><u>Plastic</u></b>				
PVC	200	3034	SDR-35 PSM	Scepter
PVC	250	D-3034	Cobra 1120 SDR-35 PSM	Grandview
PVC	450	F794	Perma-loc PS 320 sever	Manville
<b>KEY:</b>				
NR	Non-reinforced			
R	Reinforced			
PVC	polyvinyl chloride			
PSM	Plastic sewer main			
CC	Consolidated Concrete Ltd.			
P	Packerhead			

## Appendix B: Specifications for Pumps and Meters

### (1) Pumps

Range of  
Discharge

#### Goulds Centrifugal Pump

0 - 10 l/s

Index: 62434322  
Model: 3643  
Size: 2.5

Motor: Marathon 3 Phase  
Model: CC 182TTDR8619BAV  
Frame: 182T  
Type: YDRBCZ  
@60 HZ: S.F. = 1.15  
Volts = 208-220/440  
Amps = 12.8/6.4  
Full Load RPM = 3465

#### Fairbanks-Morse Figure 6310 Propeller Pump 10 - 250 l/s

Serial No.: P2B4466  
Pump Size: 14  
Stages: 1  
Propellers: B-1304-A  
RPM: 1160

Motor: Induction Type KZKV  
Frame: 365UP  
Number: F367105  
Specif.: T1032-1  
@60 HZ: S.F. = 1.15  
25 H.P.  
Full Load RPM = 1165

(2) Magnetic Flow MetersSmall SystemRange of  
Discharge

0 - 10 l/s

Type: Foxboro 1803 SANS-CA  
 Size: 3 Inch  
 Serial No.: 476542  
 Liner: Neoprene  
 Material: 304S.S.  
 Electrode: 316S.S.  
 Rating: @60 HZ: 2.08 Amps  
                   115 Volts  
                   25 Watts  
                   Series Connection  
 Output: 0.01519 mV per USGPM

Large System

0 - 250 l/s

Type: Foxboro 1808 SANS-BA  
 Size: 8 Inch  
 Serial No.: M-84925  
 Liner: Neoprene  
 Material: 304S.S.  
 Electrode: 316S.S.  
 Rating: @60 HZ: 12.4 Amps  
                   115 Volts  
                   225 Watts  
                   Parallel Connection  
 Output: 0.003924 mV per USGPM

Magnetic Flowmeter Transmitter

Model: Foxboro E96R-VA ST.C  
Serial No.: M-374650 C  
Frequency: 60 HZ  
Input: 0 - 5 mV  
Output: 0 - 10 VDC

Magnetic Flowmeter Calibrator

Model: Foxboro 8120-6  
Serial No.: 3051265  
Volts: 118/236  
Frequency: 60 Hz  
Volts\*Amps: 1.5  
Phase Band: E

Capacitance Depth Probe

Make: Delavan Electronics  
Model: CS 54  
Input: 115 VAC  
Output: 0-10 VDC

Linear Voltage Displacement Transducer (roughness measurements)

Make: Hewlett Packard  
Model: DC-DT  
7 DCDT-1000

**Appendix C: Inside Diameter Measurements of Test Pipes**

**(1) CONCRETE PIPE**

<u>NOMINAL PIPE DIAMETER</u>	200 MM		250 MM		380 MM	
	SPIGOT END	BELL END	SPIGOT END	BELL END	SPIGOT END	BELL END
	203.66	203.20	255.68	254.10	375.74	382.73
	203.89	203.07	256.01	254.76	377.67	382.17
	203.81	203.02	255.63	253.24	378.61	382.14
	204.04	201.09	254.71	253.59	378.74	382.07
	203.23	202.26	255.37	254.86	377.14	382.47
	203.73	202.67	256.06	254.38	378.43	380.52
	203.66	202.06	255.70	254.99	378.13	382.70
	203.71	202.03	255.47	254.56	379.65	383.54
	203.68	202.06	255.98	252.55	379.93	380.34
	203.48	202.41	256.08	252.17	379.27	383.64
	203.23	201.45	255.68	254.08		
	203.50	201.37	256.16	254.86		
	203.33	202.29	256.06	252.02		
	203.30	201.68	256.29	252.12		
	202.69	202.46	255.98	255.14		
	203.53	203.07	255.68	254.97		
	204.22	202.08	255.88	255.02		
	203.56	202.69	255.85	255.04		
	203.99	201.17	255.50	254.46		
	203.76	201.04	254.79	253.16		
<u>MEAN (MM)</u>	204.22	202.16	255.73	254.00	378.33	382.23
<u>STANDARD DEVIATION</u>	0.33	0.67	0.40	1.06	1.19	1.04
<u>MEAN: OVERALL (MM)</u>	202.88		254.87		380.28	
<u>STANDARD DEVIATION</u>	0.89		1.18		2.25	
<u>RANGE: MAXIMUM (MM)</u>	204.22	203.20	256.29	255.14	379.93	383.64
<u>MINIMUM</u>	202.69	201.04	254.71	252.02	375.74	380.34

## (2) PLASTIC PIPE

<u>NOMINAL PIPE DIAMETER</u>	200 MM		250 MM		450 MM	
	SPIGOT END	BELL END	SPIGOT END	BELL END	SPIGOT END	BELL END
200.99	198.58	249.91	248.59	447.65	448.61	
199.85	199.75	250.75	248.64	449.63	448.28	
196.93	198.98	251.87	249.53	449.15	450.80	
201.27	199.80	248.67	250.01	448.95	446.05	
198.12	200.38	249.28	249.02	446.41	448.82	
201.50	198.63	251.38	248.54	450.85	450.72	
200.84	198.63	249.35	249.35	451.18	448.44	
198.17	199.01	250.60	250.55	446.79	449.83	
199.59	199.06	248.92	248.56	447.65	447.83	
198.83	199.49	250.85	248.97	449.38	449.55	
200.28	200.20	250.32	249.56	447.68	446.28	
199.39	200.51	250.32	249.86	450.47	449.35	
198.27	200.99	249.86	250.60	448.21	448.44	
201.04	198.22	250.47	249.86	448.59	448.82	
197.31	198.48	249.96	249.02	447.29	450.75	
202.29	200.56	250.57	249.66	449.83	446.25	
198.40	199.54	249.22	249.40	449.66	447.85	
200.48	200.28	250.04	250.88	446.56	448.87	
199.90	198.45	250.01	251.08	449.07	447.19	
200.00	200.58	249.40	249.45	448.06	451.99	
198.37	199.72	248.49	249.43	451.84	449.86	
200.48	198.96	251.00	250.95	447.98	449.76	
200.53	200.58	250.65	249.00	448.64	449.53	
199.009	199.47	249.05	248.72	448.89	447.98	
<u>MEAN (MM)</u>	199.66	199.53	250.04	249.55	448.77	448.83
<u>STANDARD DEVIATION</u>	1.36	0.81	0.85	0.77	1.41	1.48
<u>OVERALL MEAN (MM)</u>	199.60		249.79		448.80	
<u>STANDARD DEV. (MM)</u>	1.12		0.85		1.44	
<u>RANGE: MAXIMUM (MM)</u>	202.29	200.99	251.87	251.08	451.84	451.99
<u>MINIMUM</u>	196.93	198.22	248.49	248.54	446.41	446.05

Appendix D: Sample data sheet. This example was used to record data from the 380 mm concrete pipe.

DATE	Sept 6/65	TIME	1200	PIPE	REC.	DIAM = 15 in
SLOPE OF FLUME = <u>0.6</u> %						
SLOPE OF MANOMETER BOARD = <u>31</u> °						
TEMP OF WATER = <u>20.0 °C</u>						
DEPTH GAUGE				MANOMETERS		
STN	SURFACE (ft)	INVERT (ft)	DEPTH (mm)	STN (m)	READINGS (m)	AVERAGE DIPPER (mm)
①	②	③	④	⑤	⑥	⑦
1	19.00	1.94	0.532	287.12	1 34.83	72.03
2	18.00	1.90	0.523	279.50	2 32.85	72.05
3	17.00	1.80	0.521	280.11	3 30.07	71.75
4	15.32	1.10	0.514	216.15	4 28.66	71.45
5	14.37	1.442	0.510	284.07	5 25.29	70.75
6	13.37	1.557	0.521	315.77	6 22.88	71.20
7	12.16	1.612	0.521	332.59	7 20.53	70.45
8	10.96	1.600	0.510	332.23	8 18.41	69.75
9	10.03	1.550	0.517	314.86	9 15.72	69.65
10	8.55	1.571	0.529	317.60	10 13.37	70.35
11	7.34	1.543	0.539	326.02	11 10.96	70.25
12	6.21	1.424	0.510	276.15	12 8.55	69.70
13	5.32	1.444	0.513	283.77	13 6.21	69.55
14	3.80	1.446	0.523	281.33	14 3.80	69.05
15	2.93	1.422	0.520	274.93	15 1.42	67.80
$\bar{y} = 296.14 \text{ mm}$						
DISCHARGE						
PUMP : <input checked="" type="checkbox"/> LARGE <input type="checkbox"/> SMALL						
DISCHARGE (l/sec)				COMMENTS		
READING ①	READING ②					
84.36	84.59				~ PERCENT FULL = <u>90</u> %	
31	60				Values fully open	
76	63				by-pass open	
32	53				large waves again	
60	82				S = 0.006	
42	60					
25.01	39					
21.28	51					
78	71					
44	42					
34	52					
72	62					
$\bar{Q}$	$\bar{Q} = 84.559 \times 2 = 169.118 \text{ l/s}$					

**Appendix E : Root mean squared roughness measurements from samples of the six pipes tested.**

Where: the root mean squared roughness in mm is indicated by RMS

**(1) Concrete Pipes**

**(a) 200 mm concrete pipe:**

sample	RMS (mm)
C-8-1	0.19
C-8-2	0.20
C-8-3	0.20
C-8-4	0.12
C-8-5	0.16
C-8-6	0.15
C-8-7	0.14
C-8-8	0.10

Mean RMS = 0.16 mm  
Standard dev. = 0.037 mm

**(b) 250 mm concrete pipe**

C-10-1	0.15
C-10-2	0.06
C-10-3	0.06
C-10-4	0.07
C-10-5	0.06
C-10-6	0.06
C-10-7	0.09
C-10-8	0.07
C-10-9	0.10
C-10-10	0.05
C-10-11	0.10
C-10-12	0.18

Mean RMS = 0.09 mm  
Standard dev. = 0.004 mm

**(3) 380 mm concrete pipe:**

C-15-1	0.11
C-15-2	0.14
C-15-3	0.13
C-15-4	0.26
C-15-5	0.19

C-15-6	0.11
C-15-7	0.20
C-15-8	0.09
C-15-9	0.12
C-15-10	0.08
C-15-11	0.08

Mean RMS = 0.14 mm  
 Standard dev. = 0.057 mm

### (2) Plastic Pipes

#### (a) 200 mm plastic pipe

P-8-1	0.05
P-8-2	0.06
P-8-3	-
P-8-4	0.03
P-8-5	-
P-8-6	-
P-8-7	0.05
P-8-8	0.05
P-8-9	0.06
P-8-10	0.06
P-8-11	0.03

Mean RMS = 0.049 mm  
 Std. dev. = 0.012 mm

#### (b) 250 mm plastic pipe:

P-10-1	0.066
P-10-2	0.076
P-10-3	0.107
P-10-4	0.031
P-10-5	0.073
P-10-6	0.036
P-10-7	0.088
P-10-8	0.026
P-10-9	0.072
P-10-10	0.05
P-10-11	0.034
P-10-12	0.027

Mean RMS = 0.057 mm  
 Std. dev. = 0.027 mm

**Appendix F:** Included are the Fortran programs used in the analysis of the boundary layer development and for calculating the various uniform flow parameters in part full circular sections. HYEPOL subroutines written by Peterson and Howells (1981), were accessed on the University of Alberta mainframe.

```

1 C
2 C PROGRAM TO EVALUATE THE DISPLACEMENT THICKNESS
3 C (DELTA STAR) AND THE MOMENTUM THICKNESS (THETA) BY
4 C NUMERICAL INTEGRATION USING THE TRAPEZOID RULE.
5 C
6 C READ IN THE DATA WHERE:
7 C
8 C NP= NUMBER OF VELOCITY PROFILES
9 C N= NUMBER OF DATA POINTS IN THE PROFILE
10 C DELTA= THE DEPTH OF THE BOUNDARY LAYER (M)
11 C UMAX= THE FREE STREAM VELOCITY (M/S)
12 C
13 C DIMENSION U(30),Y(30),FI(30),TITLE(20)
14 C READ(5,53) TITLE
15 C WRITE(6,62) TITLE
16 C READ(5,56) NP
17 C DO 600 I=1,NP
18 C READ(5,50) N
19 C READ(5,52) DELTA,UMAX,X,D
20 C DO 10 I=1,N
21 C READ(5,51) U(I),Y(I)
22 C Y(I)=Y(I)/1000.
23 C CONTINUE
24 C
25 C SEARCH FOR THE LARGEST VALUE OF U.
26 C
27 C USAVE=U(1)
28 C DO 100 I=1,N
29 C IF (U(I+1).GT.USAVE) GO TO 22
30 C U(I+1)=USAVE
31 C GO TO 100
32 C 22 USAVE=U(I+1)
33 C 100 CONTINUE
34 C IF (UMAX.GT.USAVE) UMAX=USAVE
35 C
36 C CALCULATE THE INTEGRALS
37 C
38 C N=N-1
39 C SUM=0.0
40 C SUMT=0.0
41 C DO 500 I=1,M
42 C
43 C TEST PARAMETERS: IF DEPTH IS GREATER THAN DELTA
44 C OR IF U(I) IS GREATER THAN OR EQUAL TO UMAX
45 C STOP.
46 C
47 C
48 C IF(Y(I).GT.DELTA.OR.U(I).GE.UMAX) GO TO 500
49 C F=((1.0-U(I)/UMAX)+(1.0-U(I+1)/UMAX))/2
50 C FIN=F*(Y(I+1)-Y(I))
51 C FINT=F*FIN
52 C SUM=SUM+FINT
53 C 500 SUMT=SUM*1000.
54 C DELST=SUM*1000.
55 C THETA=SUMT*1000.
56 C H=DELST/THETA
57 C WRITE(6,61) X,D
58 C DELTA=DELTA*1000.
59 C WRITE(6,60) DELTA,UMAX,DELST,THETA,H
60 C 500 CONTINUE
61 C
62 C FORMAT STATEMENTS
63 C
64 C 50 FORMAT(12)
65 C 51 FORMAT(2F10.4)
66 C 52 FORMAT(4F10.4)
67 C 53 FORMAT(20A4)
68 C 55 FORMAT(12)
69 C 60 FORMAT(//10X,'THE BOUNDARY LAYER THICKNESS (DELTA) = ',F10.4,
70 C //10X,'THE FREE STREAM VELOCITY = ',F10.4,
71 C //10X,'THE DISPLACEMENT THICKNESS (DELTA STAR) = ',F10.4,
72 C //10X,'THE MOMENTUM THICKNESS (THETA) = ',F10.4,
73 C //10X,'DELTA STAR / THETA = ',F10.4//)
74 C 61 FORMAT(//5X,'STATION ',F10.4,' M. D/S FROM INLET')
75 C 62 FORMAT(//20A4/30(' '))
76 C STOP
77 C
78 C END

```

```

1 C
2 C PROGRAM TO DETERMINE FLOW CONDITIONS FOR PIPE TESTS
3 C ASSUMING MANNINGS' N VALUES FOR CONCRETE AND PLASTIC
4 C PIPE OF 0.0108 AND 0.008 RESPECTIVELY.
5 C
6 C VARIABLE DEFINITION
7 C -----
8 C
9 C NP = NUMBER OF PIPES
10 C FPCC = MANNING N ASSUMED FOR CONCRETE PIPE (0.0108)
11 C FPVC = MANNING N ASSUMED FOR PVC PIPE (0.008)
12 C G = GRAVITATIONAL CONSTANT
13 C D() = PIPE DIAMETERS (INCHES)
14 C A = CROSS-SECTIONAL AREA OF PIPE
15 C PF = PERCENT OF CROSS-SECTIONAL AREA OCCUPIED BY
16 C FLOWING WATER
17 C AF = AREA OF CROSS-SECTION OCCUPIED BY FLOWING
18 C WATER
19 C Y = DEPTH OF FLOW
20 C P = WETTED PERIMETER
21 C Q = DISCHARGE
22 C S = SLOPE OF PIPE INVERT
23 C DUF = NORMAL DEPTH OF FLOW
24 C YCR = CRITICAL DEPTH OF FLOW
25 C SCR = CRITICAL DEPTH OF FLOW FOR GIVEN DISCHARGE
26 C
27 C INITIALIZE PARAMETERS AND READ DATA
28 C
29 C EXTERNAL CHANNEL
30 C DIMENSION D(6)
31 C NP=6
32 C FPCC=0.0108
33 C FPVC=0.008
34 C G=9.81
35 C -----
36 C READ(5,500) (D(I),I=1,NP)
37 C -----
38 C WRITE(6,600)
39 C
40 C DO 10 I=1,NP
41 C DMM=D(I)*25.4
42 C IF(I.LE.3) GO TO 21
43 C WRITE(6,607)
44 C GO TO 22
45 C 21 WRITE(6,606)
46 C 22 WRITE(6,601) D(I),DMM
47 C A=(3.14159265*(D(I)*0.0254)**2)/4.
48 C AFT=10.76426*A
49 C WRITE(6,602) A,AFT
50 C IF(I.LE.3) GO TO 12
51 C C=FPVC
52 C GO TO 13
53 C 12 C=FPCC
54 C 13 WRITE(6,608) C
55 C PF=0.08
56 C AF=A*PF
57 C AFES=AFT*PF
58 C PPP=PF*100.
59 C WRITE(6,603) PPP,AF,AFES
60 C DM=DMM/1000.
61 C Y=-1.5
62 C P=-1.5
63 C CALL POYAP(DM,Y,0,V,S,OMANN,C,G)
64 C YMM=1000.-Y
65 C WRITE(6,604) YMM
66 C S=0.000001
67 C 15 CONTINUE
68 C O=-1.5
69 C V=-0.5
70 C CALL POYQV(DM,Y,O,V,S,OMANN,C,G)
71 C CALL PPDUF(DM,O,S,OMANN,C,G,DUF)
72 C CALL PPYCR(DM,O,G,YCR,HCR)
73 C ACR=-1.5
74 C PCR=-1.5
75 C CALL POYAP(DM,YCR,ACR,PCR)
76 C SCR=(C*C*Q*Q*(PCR**1.33333))/(ACR**3.33333)
77 C SP=S*100.
78 C DUFM=DUF*1000.
79 C YCRM=YCR*1000.
80 C SCRP=SCR*100.
81 C QLS=0*1000.
82 C VMS=Q/AF
83 C WRITE(6,608) SP,QLS,VMS,YCRM,SCR
84 C S=S+0.0005
85 C IF(S.GT.0.011) GO TO 14
86 C GO TO 15
87 C 14 PF=PF+0.05
88 C IF(PF.GT.1.0) GO TO 10
89 C GO TO 11
90 C 10 CONTINUE
91 C STOP

```

```
82      C
83      C
84      C      FORMAT STATEMENTS
85      C
86  500  FORMAT(10F10.6)
87  500  FORMAT(//10X, 'TABLE OF FLOW PROPERTIES FOR '
88  *'CAST CONCRETE AND PVC PIPE'//10X,5B(''')//)
89  601  FORMAT(10X, 'PIPE DIAMETER = ',F10.2, ' INCHES'
90  *'24X, '='',F10.4, ' MM')
91  .602  FORMAT(10X, 'CROSS-SECTIONAL AREA = ',E10.4,
92  *' SQUARE METERS/3IX, '='',F10.6, ' SQUARE FEET')
93  603  FORMAT(//10X,110('''),//10X, 'PERCENT FULL = ',F10.2, ' %'/10X,
94  *'AREA OF FLOW = ',E10.4, ' SQUARE METERS'/23X,
95  *' = ',F10.6, ' SQUARE FEET')
96  604  FORMAT(10X, 'DEPTH OF FLOW = ',F10.4, ' MM///10X,
97  *'SLOPE',1BX,'DISCHARGE',11X,'FLOW VELOCITY',8X,
98  *'CRITICAL DEPTH',6X,'CRITICAL SLOPE'/8IX,
99  *'FOR GIVEN FLOW DEPTH'/1IX,'(%')',17X,'(L/S)',
100 *'1BX, '(M/S)',16X,'(MM)',16X,'(X)''')
101  605  FORMAT(2(10X,F10.6),2(10X,F10.4),10X,F10.6)
102  606  FORMAT(//10X,5B(''')//10X, 'TYPE OF PIPE = CONCRETE'//10X,5B(''')//)
103  *')///)
104  607  FORMAT(//10X,5B(''')//10X, 'TYPE OF PIPE = PVC'//10X,5B(''')//)
105  608  FORMAT(//10X, 'ASSUMED MANNING N = ',F10.4//10X,4B(''')//)
106  STOP
107  END
```

```

1 C
2 C PROGRAM TO CALCULATE FLOW PROPERTIES IN A PIPE
3 C GIVEN DEPTH OF FLOW, PIPE DIAMETER, PIPE SLOPE,
4 C AND DISCHARGE USING HYEPOL SUBROUTINE PPROP.
5 C
6 C
7 C D = PIPE DIAMETER (M)
8 C H(I) = DEPTH OF FLOW (MM)
9 C SD = BED SLOPE
10 C N = NUMBER OF DATA POINTS PER SLOPE
11 C NS = NUMBER OF SLOPES PER PIPE IN QUESTION
12 C PF = PERCENT FULL
13 C FMAN = MANNINGS N
14 C Q = DISCHARGE IN LITERS PER SECOND
15 C A = AREA OF FLOW IN SQUARE METERS
16 C P = WETTED PERIMETER IN METERS
17 C FR = FROUDE NUMBER OF FLOW
18 C
19 C DIMENSION VARIABLES
20      DIMENSION D(20),H(20),TITLE(20)
21      PI=3.14159
22      G=9.80665
23 C
24 C READ DATA
25      READ(5,52) TITLE
26      READ(5,50) D
27      READ(5,53) NS
28      WRITE(6,62) TITLE
29      WRITE(6,65) D
30      DO 20 I=1,NS
31      READ(5,56) N
32      READ(5,54) SD
33      READ(5,55) (D(I),I=1,N)
34      READ(5,51) (H(I),I=1,N)
35      WRITE(6,63) SD
36      WRITE(6,61)
37      AFULL=PI*D*D/4.0
38      DO 10 J=1,N
39      DEPTH=H(J)/1000.
40      Q=Q(J)/1000.
41      CALL PPROP(D,DEPTH,A,T,PAY)
42      PF=(A/AFULL)*100.
43      FMAN=((A**1.66667)*SORT(SD))/((P**.66667)*Q)
44      FR=SORT((Q*Q*T)/(G*A*A))
45      QW=Q*1000.
46      VEL=QW/A
47      YD=DEPTH/D
48      Y=DEPTH*1000.
49      WRITE(6,60)PF,QW,VEL,YD,FMAN,FR
50      10 CONTINUE
51      20 CONTINUE
52 C
53      50 FORMAT(F10.6)
54      51 FORMAT(20F10.6)
55      52 FORMAT(20A4)
56      53 FORMAT(13)
57      54 FORMAT(F10.6)
58      55 FORMAT(20F10.6)
59      56 FORMAT(13)
60      62 FORMAT(//10X,20A4)
61      60 FORMAT(10X,B(F10.4,5X),F10.6,5X,F10.4)
62      61 FORMAT(//14X,'PERCENT',5X,'DISCHARGE',5X,'AVERAGE',
63      *5X,'AVERAGE',5X,'DEPTH',5X,'MANNING N',5X,'FROUDE',
64      *7X,'FULL',10X,'L/SEC',11X,'VELOCITY',7X,'DEPTH',10X,
65      *P0(''),22X,'NUMBER'/45X,'M/SEC',10X,'MM',12X,'DIAMETER'//)
66      63 FORMAT(//13X,'PIPE BED SLOPE = ',F10.4)
67      65 FORMAT(//10X,'PIPE DIAMETER = ',F10.6,' M. '//)
68      STOP
69      END

```

```

1 C MAIN PROGRAM TO READ DATA, TO TEST RELIABILITY
2 C OF THE DATA, AND TO CALL SUBROUTINES FOR
3 C CALCULATION OF DESIRED HYDRAULIC PARAMETERS.
4 C
5 C *****
6 C DATA TO BE READ INTO THE PROGRAM
7 C *****
8 C
9 C
10 C NUMBER = NUMBER OF PIPES TESTED
11 C TITLE = TYPE OF PIPE (CONCRETE OR PLASTIC)
12 C D = PIPE DIAMETER (IN)
13 C DO = UNCERTAINTY IN THE VALUE OF THE PIPE DIAMETER
14 C DUE TO MEASUREMENT ERROR, OUT-OF-ROUNDNESS,
15 C AND DEVIATION OF THE DIAMETER WITHIN AND
16 C BETWEEN EACH PIPE SECTION.
17 C NS = NUMBER OF SLOPES PER PIPE IN QUESTION
18 C NP = PIPE NUMBER (COUNTER USED TO SET THE FULL
19 C SCALE DISCHARGE FOR CALCULATING THE EXPECTED
20 C ERROR IN DISCHARGE READINGS.
21 C FNAVGI = AVERAGE MANNING'S N FROM TEST RESULTS FOR 0.28<Y/D<1.0
22 C N = NUMBER OF DATA POINTS PER SLOPE
23 C ND = NUMBER OF DATA POINTS OBTAINED USING THE SMALL
24 C PUMP AND MAGNETIC FLOW METER
25 C SO = BED SLOPE
26 C Q(I) = DISCHARGE IN LITRES PER SECOND
27 C H(I) = DEPTH OF FLOW (MM)
28 C DY(I) = ERROR IN THE AVERAGE CENTRELINE DEPTH
29 C MEASUREMENT (INCLUDES UNCERTAINTIES DUE
30 C TO SURFACE WAVES)
31 C
32 C *****
33 C HYDRAULIC PARAMETERS CALCULATED BY PROGRAM WITH ADDITIONAL
34 C REFERENCE TO HYEPOL SUBROUTINES (PETERSON AND HOWELL)
35 C *****
36 C
37 C VEL = AVERAGE VELOCITY OF FLOW (M/SEC)
38 C A = AREA OF FLOW IN SQUARE METERS
39 C P = WETTED PERIMETER IN METERS
40 C R = HYDRAULIC RADIUS = A/P
41 C PF = PERCENT OF THE CROSS SECTIONAL AREA OF THE PIPE
42 C OCCUPIED BY FLUID
43 C FMAN = MANNINGS N
44 C FRA = FROUDE NUMBER (USING THE RATIO OF AREA FLOW
45 C DIVIDED BY DEPTH OF FLOW (A/y) AS A LENGTH SCALE
46 C FRY = FROUDE NUMBER USING THE AVERAGE DEPTH AS LENGTH SCALE
47 C FRP = FROUDE NUMBER USING THE WETTED-PERIMETER (P) AS
48 C THE LENGTH SCALE
49 C FRR = FROUDE NUMBER USING THE HYDRAULIC RADIUS (R) AS THE
50 C LENGTH SCALE
51 C XNU = KINEMATIC VISCOSITY AT 20 DEGREES CELSIUS
52 C RE = REYNOLDS NUMBER WITH 4R REPLACING DIAMETER
53 C FD = DARCY'S FRICTION FACTOR
54 C XKC = EQUIVALENT ROUGHNESS (N) BASED ON THE COLEBROOK-WHITE
55 C EQUATION WITH HYDRAULIC RADIUS REPLACING THE PIPE
56 C DIAMETER.
57 C XKM = EQUIVALENT ROUGHNESS (N) CALCULATED FROM MANNING'S N
58 C OFULL = DISCHARGE FLOWING FULL. CALCULATED USING THE MEAN VALUE
59 C OF MANNING'S N BETWEEN Y/D=0.28 AND Y/D=1.0
60 C AFULL = AREA FLOWING FULL
61 C PFULL = WETTED-PERIMETER FLOWING FULL = PI*D
62 C RFULL = HYDRAULIC RADIUS FLOWING FULL = AFULL/FFULL
63 C QOF = Q/OFULL
64 C AAF = A/AFULL
65 C XNAVQ = N/FNAVQ
66 C VVF = V/VFULL
67 C RRF = R/RFULL
68 C VS = SHEAR VELOCITY
69 C RV = WALL REYNOLD'S NUMBER
70 C
71 C
72 C
73 C
74 C
75 C
76 C
77 C DIMENSION VARIABLES
78 C DIMENSION Q(20),H(20),TITLE(20),DY(20)
79 C EXTERNAL QMANN
80 C PI=3.14159
81 C G=0.00665
82 C XNU=1.007E-6
83 C
84 C READ GENERAL DATA
85 C READ(5,65) NUMBER
86 C
87 C DO 20 K=1,NUMBER
88 C READ(5,82) TITLE
89 C READ(5,80) D,DO
90 C READ(5,83) NS,NP
91 C READ(5,84) FNAVQ
92 C WRITE(6,64)
93 C WRITE(6,62) TITLE
94 C WRITE(6,65) D
95 C
96 C DO 20 II=1,NS
97 C
98 C READ SPECIFIC DATA FOR EACH SLOPE
99 C

```

```

100      READ(S,83) N,ND
101      READ(S,84) SD
102      READ(S,81) (O(I),I=1,N)
103      READ(S,81) (H(I),I=1,N)
104      READ(S,81) (DV(I),I=1,N)
104.3    READ(S,84) VM
105      C
106      DO 10 J=1,N
107      DEPTH=H(J)/1000.
108      DV=DV(J)/2000.
109      QD=Q(J)/1000.
110
111      C
112      CALL ERROR(PI,G,D,OO,DEPTH,SD,OO,DV,A,T,P,R,FMAN,PDN,
113      *DN,VEL,FD,DF,PDF)
114      C
115      IF(PDN.GT.25.) GO TO 10
116      C
117      CALL SCRIT(D,G,OO,FMAN,SCR)
118      C
119      IF(SD.GT.SCR) GO TO 100
120      C
121      CALL DRCO(D,G,OO,SD,FMAN,DEPTH,DX,YCR,DUF)
122      C
123      DX=ABS(DX)
124      XFD=0.5*37.
125      IF(DX.GT.XFD) GO TO 10
126      C
127      CALL PARAM(D,G,PI,XNU,OO,DEPTH,SD,FNAVG,FMAN,A,T,
128      *P,VEL,R,RE,XKC,XNM,OOF,VVF,FRA,FRY,FRP,FRR)
129      C
130      APULL=PI*D*D/4.0
131      PF=(A/APULL)*100.
132      OW=OO*1000.
133      Y=DEPTH*1000.
134      YD=DEPTH/0
135      IF(J.EQ.1) GO TO 101
136      GO TO 102
137
138      101     WRITE(S,83) SD
139      102     C
140      102     WRITE(S,86) VM
141      102     C
142      102     WRITE(S,81)
143      102     C
144      10     CONTINUE
145      20     CONTINUE
146      C
147      C      FORMAT STATEMENTS
148      C
149      55     FORMAT(13)
150      50     FORMAT(2F10.6)
151      51     FORMAT(20F10.6)
152      52     FORMAT(20A4)
153      53     FORMAT(21S)
154      54     FORMAT(F10.6)
155      52     FORMAT(/10X,20A4)
156      60     FORMAT(10X,B(F10.4,5X),F10.6)
157      61     FORMAT(/14X,'PERCENT',6X,'DISCHARGE',8X,'AVERAGE',
158      *8X,'AVERAGE',8X,'DEPTH',8X,'MANNING N',
159      */14X,'FULL',10X,'L/SEC',11X,'VELOCITY',7X,'DEPTH',10X,
160      *81'--'/45X,'M/SEC',10X,'MM',12X,'DIAMETER'//)
161      63     FORMAT(///13X,'PIPE BED SLOPE = ',F10.4)
162      64     FORMAT('1')
163      65     FORMAT(/10X,' PIPE DIAMETER = ',F10.6,' M.   //')
164      66     FORMAT(/10X,' THE LIMITING DESIGN VELOCITY AT',
165      *' THIS SLOPE FOR V/D = 0.5 IS ',F10.4,' M/S   //')
166      STOP
167
168      C
169      C      SUBROUTINE ERROR ANALYSIS PROGRAM
170      C
171      C      CALCULATES THE MAXIMUM ERROR IN
172      C      VALUES OF MANNINGS N AND FRICTION FACTOR F.
173      C
174      C      NUMBER = NUMBER OF PIPES TESTED
175      C      DV1,DV2 = UNCERTAINTY IN THE VERTICAL COMPONENT OF SLOPE
176      C      MEASUREMENT
177      C      DX1,DX2 = UNCERTAINTY IN THE HORIZONTAL COMPONENT OF SLOPE
178      C      MEASUREMENT
179      C      DELX = LENGTH OF THE FLUME = 30.48 M
180      C      D = PIPE DIAMETER (M)
181      C      OO = UNCERTAINTY IN THE VALUE OF THE PIPE DIAMETER DUE TO

```

```

182      C      DEVIATION IN THE DIAMETER WITHIN A SINGLE SECTION AND
183      C      OUT-OF-ROUNDNESS
184      C      FMAN = MANNINGS N
185      C
186      C      SUBROUTINE ERROR(P1,G,D,DD,DEPTH,SQ,OO,OYV,A,T,P,R,FMAN,PDN,
187      C      *DN,VEL,FD,DF,PDF)
188      C
189      C
190      DY2=.001
191      DY1=.0005
192      DX2=.010
193      DX1=.001
194      DELX=.37.0
195      RAD=0/2.
196      DD=DD/1000.
197      DR=DD/2.
198      DELY=.50*DELX
199      OOV=(DY2+DY1)/DELY
200      DDX=(DX2+DX1)/DELX
201      DS=OOV+DDX
202      CALL PPROP(D,DEPTH,A,T,P,AY)
203      FMAN=((A**1.66667)*SQRT(SQ))/((P**.66667)**OO)
204      VEL=OOV/A
205      R=A/P
206      XINT=.0*G*R*SQ
207      FD=XINT/(VEL*VEL)
208      X1=1./RAD
209      IF(DEPTH.LT.RAD) GO TO 9
210      XC=(DEPTH-RAD)/RAD
211      THETA=PI+2.*ASIN(XC)
212      X2=SORT(1.-(XC*XC))
213      GO TO 11
214      9      XC=(RAD-DEPTH)/RAD
215      THETA=2.*ACOS(XC)
216      X2=SORT(1.-(XC*XC))
217      11     CONTINUE
218      DSO=D**0
219      XA=THETA-SIN(THETA)
220      XDEL=OYV+(DEPTH*DR/RAD)
221      DTHTA=2.*((X1/X2)*XDEL)
222      DAREA=((1.-COS(THETA))*DSQ*DTHTA+2.*D*XA*OO)/8.
223      IF(NP.LE.4) GO TO 15
224      GO TO 16
225      15     IF(J.LE.ND) GO TO 13
226      QFS=.10
227      QERR=.0018*QFS
228      GO TO 12
229      16     IF(J.LE.ND) GO TO 13
230      QFS=.25
231      QERR=.00067*QFS
232      GO TO 12
233      13     QFS=.0.10
234      QERR=.0021*QFS
235      12     CONTINUE
236      DQQ=QERR/100
237      DP=(OO/D)*(DTHTA/THETA)
238      DDA=(8.*DAREA)/(8.*A)
239      DDAF=DDA/A
240      DDS=.5*DS
241      DDP=.66667*DP
242      DDN=DDA+DDS+DDP+DQQ
243      DN=FMAN*DDN
244      DF=(2.5*DDAF)+(0.5*DP)+DDS+(2.*DQQ))*FD
245      PDF=100.*DF
246      PDN=DDN*100.
247      C
248      RETURN
249      END
250      C
251      C      SUBROUTINE TO CALCULATE THE CRITICAL
252      C      SLOPE FOR THE GIVEN FLOW CONDITIONS
253      C
254      C      SCR = CRITICAL SLOPE AT THE GIVEN DISCHARGE
255      C
256      C
257      C      SUBROUTINE SCRIT(D,G,OO,FMAN,SCR)
258      C
259      C
260      CALL PPYCR(D,OO,G,YCR,PCR)
261      ACR=-1.5
262      PCR=-1.5
263      CALL PDYAP(D,YCR,ACR,PCR)
264      SCR=(FMAN*FMAN*OO**OO*(PCR**1.3333))/(ACR**3.3333)
265      RETURN
266      END
267      C
268      C      SUBROUTINE TO CALCULATE THE LENGTH OF THE
269      C      DRAWDOWN CURVE AT THE OUTLET OF THE PIPE
270      C      FOR MILD SLOPES

```

```

271 C DX = DISTANCE UPSTREAM FROM THE PIPE OUTLET TO THE
272 C POINT WHERE THE FLOW DEPTH IS 95 PERCENT OF THE
273 C NORMAL DEPTH (USING MANNING N CALCULATED FROM
274 C THE DATA)
275 C YCR = CRITICAL DEPTH OF FLOW AT THE GIVEN DISCHARGE
276 C DUF = NORMAL DEPTH OF FLOW
277 C
278 C SUBROUTINE D90(D,Q,SO,FMAN,DEPTH,DX,YCR,DUF)
279 C
280 C EXTERNAL OMANN
281 C
282 C CALL PPYCR(D,Q,Q,YCR,MCR)
283 C CALL PPQUF(D,Q,SO,OMANN,FMAN,Q,DUF)
284 C
285 C Y=DEPTH*.95
286 C
287 C CALL PQVFF(D,Q,SO,Y,OMANN,FMAN,Q,GVFF)
288 C DY=Y-YCR
289 C DX=GQVFF*DY
290 C
291 C RETURN
292 C
293 C
294 C PROGRAM TO CALCULATE FLOW PROPERTIES IN A PIPE
295 C GIVEN DEPTH OF FLOW ,PIPE DIAMETER, PIPE SLOPE,
296 C AND DISCHARGE USING HYEPOL SUBROUTINE PPROP.
297 C
298 C
299 C D = PIPE DIAMETER (M)
300 C H(I) = DEPTH OF FLOW (MM)
301 C SO = BED SLOPE
302 C N = NUMBER OF DATA POINTS PER SLOPE
303 C NS = NUMBER OF SLOPES PER PIPE IN QUESTION
304 C PF = PERCENT FULL
305 C FMAN = MANNINGS N
306 C Q = DISCHARGE IN LITERS PER SECOND
307 C A = AREA OF FLOW IN SQUARE METERS
308 C P = WETTED PERIMETER IN METERS
309 C FR= FROUDE NUMBER OF FLOW
310 C XNU= KINEMATIC VISCOSITY AT 20 DEGREES CELSIUS
311 C RE= REYNOLDS NUMBER WITH 4R REPLACING DIAMETER
312 C R= HYDRAULIC RADIUS = A/P
313 C FD= DARCY'S FRICTION FACTOR
314 C XKc= EQUIVALENT ROUGHNESS (M) BASED ON THE COLEBROOK-WHITE
315 C EQUATION WITH HYDRAULIC RADIUS REPLACING THE PIPE
316 C DIAMETER.
317 C XKM= EQUIVALENT ROUGHNESS (M) CALCULATED FROM MANNING'S N
318 C QF= DISCHARGE FLOWING FULL. CALCULATED USING THE MEAN VALUE
319 C OF MANNING'S N BETWEEN Y/D=0.28 AND Y/D=1.0
320 C AF= AREA FLOWING FULL
321 C PFULL= WETTED PERIMETER FLOWING FULL = PI*D
322 C FNAVQ= AVERAGE MANNING'S N FROM TEST RESULTS FOR 0.25<Y/D<1.0
323 C QOF= Q/QFULL
324 C AAF= A/AFULL
325 C XNAVQ= N/NAVQ
326 C VVF= V/VFULL
327 C RRF= R/RFULL
328 C VS = SHEAR VELOCITY
329 C RW = WALL REYNOLD'S NUMBER
330 C PNR = FRICTION FACTOR : FULLY ROUGH
331 C PMU = FRICTION REYNOLD'S NUMBER
332 C FMN = MANNING'S N CALCULATED FROM F
333 C
334 C
335 C
336 C SUBROUTINE PARAM(D,Q,PI,XNU,QO,DEPTH,SO,FNAVQ,FMAN,A,
337 C *T,P,VEL,R,RE,XKC,XKM,QOF,VVF,FRA,FRY,FRP,RRF)
338 C
339 C AFULL=PI*D*0.4/4.0
340 C PF=(A/AFULL)*100.
341 C FRA=VEL/SQRT(Q*A/DEPTH)
342 C RRF=VEL/(SQRT(Q*R))
343 C FRY=VEL/(SQRT(Q*DEPTH))
344 C FRP=VEL/(SQRT(Q*P))
345 C
346 C RE=(4.*R*VEL)/XNU
347 C XINT=8*SO
348 C VS=SQRT(XINT)
349 C XINT1=SQRT(32.*XINT)
350 C PD=(8.*XINT)/(VEL*VEL)
351 C XKC=14.8*PD*(10.0**(-VEL/XINT1)-(1.295*XNU)/(R*XINT1))
352 C XKM=D_3048*(32.*FMAN)**6.
353 C RW=(VS*XKC)/XNU
354 C PNR=(VEL/VS)-0.75*ALOG10(R)
355 C PMU=VS/XNU
356 C FNP=(R*0.100007)*SQRT(FD/(R*G))
357 C QFULL=(AFULL*((D/4.)**0.00007)*(SO**.8))/FNAVQ
358 C VFULL=QFULL/AFULL
359 C RFULL=D/4.
360 C QOF=QO/QFULL
361 C AAF=A/AFULL
362 C XNAVQ=FMAN/FNAVQ
363 C VVF=VEL/VFULL
364 C RRF=R/RFULL
365 C
366 C RETURN
367 C

```

```

1   C
2   C SUBROUTINE TO CALCULATE THE FRICTION
3   C FACTOR (F) USING THE COLEBROOK-WHITE
4   C FORMULA. THE SOLUTION IS DONE ITERATIVELY
5   C USING NEWTON'S METHOD TO FIND THE ROOT.
6   C
7   C      SUBROUTINE CWF(R,XKS,FD,RE,FCW)
8   C
9   C      NCT=0
10  C      ELOG=10.7*ALOG10(2.71828183)
11  C      ED=XKS/(4.*R)
12  C      FS=SQRT(FD)
13  C      FZ=0.9/(FD*FS)
14  C      ARG=ED+0.38/(RE*FS)
15  C      FF=1./FS-1.14*2.^ALOG10(ARG)
16  C      DF=FZ*ELOG*FZ/(ARG*RE)
17  C      DIF=FF/DF
18  C      F=F+DIF
19  C      NCT=NCT+1
20  C      IF(ABS(DIF).GT.0.00001.AND.NCT.LT.10) GO TO 2
21  C      RETURN
22  C      END

```

```

1   C
2   C SUBROUTINE TO CALCULATE THE LENGTH OF THE
3   C DRAWDOWN CURVE AT THE OUTLET OF THE PIPE
4   C FOR MILD SLOPES
5   C
6   C      SUBROUTINE DRDO(D,G,OO,SO,FMAN,DEPTH,DY,YCR,DUF)
7   C
8   C      EXTERNAL OMANN
9   C
10  C      CALL PPYCR(D,OO,G,YCR,MCR)
11  C      CALL PPDUF(D,OO,SO,OMANN,FMAN,G,DUF)
12  C
13  C      Y=DEPTH
14  C
15  C      CALL PGVFF(D,OO,SO,Y,OMANN,FMAN,G,QVFF)
16  C      DY=Y-YCR
17  C      DX=QVFF*DY
18  C
19  C
20  C      RETURN
21  C      STOP
22  C      END

```

```

1   C
2   C SUBROUTINE TO CALCULATE THE CRITICAL
3   C SLOPE FOR THE GIVEN FLOW CONDITIONS
4   C
5   C
6   C      SUBROUTINE SCRIT(D,G,OO,FMAN,SCR)
7   C
8   C
9   C      CALL PPYCR(D,OO,G,YCR,MCR)
10  C      CALL POYAP(D,YCR,ACR,PCR)
11  C      SCR=(FMAN-FMAN*OO*OO*(PCR**1.3333))/(ACR**3.3333)
12  C
13  C      RETURN
14  C      STOP
15  C      END

```

```

1 C SUBROUTINE ERROR ANALYSIS PROGRAM
2 C CALCULATES THE MAXIMUM ERROR IN
3 C VALUES OF MANNINGS N AND FRICTION FACTOR F.
4 C
5 C NUMBER = NUMBER OF PIPES TESTED
6 C DV1,DY2 = UNCERTAINTY IN THE VERTICAL COMPONENT OF SLOPE
7 C MEASUREMENT
8 C DX1,DX2 = UNCERTAINTY IN THE HORIZONTAL COMPONENT OF SLOPE
9 C MEASUREMENT
10 C DELX = LENGTH OF TIME-PHASE = 30.48 M
11 C D = PIPE DIAMETER (M)
12 C DO = UNCERTAINTY IN THE VALUE OF THE PIPE DIAMETER DUE TO
13 C DEVIATION IN THE DIAMETER WITHIN A SINGLE SECTION AND
14 C OUT-OF-ROUNDNESS
15 C H(I) = DEPTH OF FLOW (MM)
16 C SD = BED SLOPE
17 C N = NUMBER OF DATA POINTS PER SLOPE
18 C NS = NUMBER OF SLOPES PER PIPE IN QUESTION
19 C NP = PIPE NUMBER (USED TO SET FULL SCALE DISCHARGE
20 C MEASUREMENT FOR CALCULATING THE ERROR IN Q)
21 C ND = NUMBER OF DATA POINTS OBTAINED USING THE SMALL
22 C PUMP AND MAGNETIC FLOW METER
23 C FMAN = MANNINGS N
24 C Q(I) = DISCHARGE IN LITERS PER SECOND
25 C DY(I) = ERROR IN DEPTH MEASUREMENT (INCLUDES UNCERTAINTIES
26 C DUE TO SURFACE WAVES)
27 C A = AREA OF FLOW IN SQUARE METERS
28 C P = WETTED PERIMETER IN METERS
29 C R= HYDRAULIC RADIUS = A/P
30 C FNAVG= AVERAGE MANNING'S N FROM TEST RESULTS FOR 0.25<Y/D<1.0
31 C
32 C
33 C
34 C
35 C SUBROUTINE ERROR(PI,G,D,DO,SD,DEPTH,QQ,DYV,A,T,P,R,FMAN,PDN,
36 C *DN,VEL,YD,FD,DF,PDF)
37 C
38 C
39 C
40 C
41 C
42 C
43 C
44 C
45 C
46 C
47 C
48 C
49 C
50 C
51 C
52 C
53 C
54 C
55 C
56 C
57 C
58 C
59 C
60 C
61 C
62 C
63 C
64 C
65 C
66 C
67 C
68 C
69 C
70 C
71 C
72 C
73 C
74 C
75 C
76 C
77 C
78 C
79 C
80 C
81 C
82 C
83 C
84 C

```

CONTINUE

```
85      QERR=0.01*QFS
86      DQQ=QERR/QO
87      DP=(DD/D)+(DTHETA/THETA)
88      DDA=(S.*DAREA)/(3.*A)
89      DDAF=DAREA/A
90      DDS=.5*DS
91      DDP=0.66667*DP
92      DDN=DDA*DDS*DOP*DDO
93      DN=FMAN*DDN
94      DF=((2.*DDAF)+(0.5*DP)+DDS*(2.*DDO))*FD
95      PDF=100.*DF
96      PDN=DDN*100.
97      QW=QO*1000.
98      YD=DEPTH/D
99      Y=DEPTH*1000.
100     R=A/P
101     C
102     RETURN
103     STOP
104     END
```

**Appendix G : Summary of the Error Analysis Used to Determine  
the Reliability of the Calculated Values of Manning's n and  
Darcy's f.**

**(1) Manning's Equation:**

$$n = \frac{A^{5/3} S^{1/2}}{P^{2/3} Q}$$

The fractional error in n is obtained from:

$$\frac{\delta n}{n} = \frac{5\delta A}{3A} + \frac{1\delta S}{2S} + \frac{2\delta P}{3P} + \frac{\delta Q}{Q}$$

By definition:

$$A = \frac{1}{8}(\theta - \sin \theta)D^2$$

(a) The error in the area of flow becomes:

$$|\delta A| = \frac{1}{8}\{(1 - \cos \theta)D^2\delta\theta + 2(\theta - \sin \theta)D\delta D\}$$

where: theta is in radian

The fractional error in theta can be determined from the following:

If  $y < D/2$  then:

$$\theta = 2 \cos^{-1} \left( \frac{r+y}{r} \right)$$

and:

$$|\delta\theta| = 2 \left\{ \frac{1}{r \sqrt{1 - \left(\frac{y-r}{r}\right)^2}} \left( \delta y + y \frac{\delta r}{r} \right) \right\}$$

If  $y > D/2$  then:

$$\theta = \pi + 2 \sin^{-1} \left( \frac{y-r}{r} \right)$$

and:

$$|\delta\theta| = 2 \left\{ \frac{1}{r \sqrt{1 - \left(\frac{r-y}{r}\right)^2}} \left( \delta y + y \frac{\delta r}{r} \right) \right\}$$

The fractional error in the other terms is as follows:

$$\frac{\delta r}{r} = \frac{\delta D}{D}$$

$$\delta r = r \frac{\delta D}{D}$$

where:

$D$  = the pipe diameter: error involved in this term

originates from diameter measurements done on the test pipes.

$y$  = the normal depth measured. The error involved in these measurements were caused by standing waves and other irregularities of the surface profile.

$r$  = the pipe radius

(b) The error in the slope term is:

$$S = \frac{\Delta y}{\Delta x} = \frac{y_2 - y_1}{x_2 - x_1}$$

where:  $\Delta y$  = change in the water surface or bed elevation over the distance  $\Delta x$ .

Therefore:

$$\frac{\delta S}{S} = \frac{\delta \Delta y}{\Delta y} + \frac{\delta \Delta x}{\Delta x}$$

Since:

$$\Delta y = y_2 - y_1$$

$$\delta \Delta y = \delta y_2 + \delta y_1$$

and:

$$\delta \Delta x = \delta x_2 + \delta x_1$$

so:

$$\frac{\delta S}{S} = \frac{(\delta y_2 + \delta y_1)}{\Delta y} + \frac{(\delta x_2 + \delta x_1)}{\Delta x}$$

(c) Error in the wetted perimeter ( $P$ )

$$P = \left(\frac{D}{2}\right)\theta$$

Therefore:

$$\frac{\delta P}{P} = \frac{\delta D}{D} + \frac{\delta \theta}{\theta}$$

or:

$$\delta P = \frac{1}{2}(\delta D + D\delta\theta)$$

(d) Error in discharge:

The error in discharge as a percentage of the full scale reading, was determined from calibrating the large and small discharge meters. The results are as follows:

**Large discharge system:**

$$\frac{\delta Q}{Q} = 0.19\%$$

**Small discharge system:**

$$\frac{\delta Q}{Q} = 0.21\%$$

## (2) Darcy's Friction Factor

Darcy's  $f$  is defined as follows:

$$f = \frac{\sqrt{8gRS}}{V^2}$$

or:

$$f = 8^{1/2} g^{1/2} R^{1/2} S^{1/2} V^{-2}$$

so:

$$\frac{\delta f}{f} = \frac{1\delta R}{2R} + \frac{1\delta S}{2S} + 2\frac{\delta V}{V}$$

where:  $V = Q/A$  and  $R = A/P$

The error in  $f$  becomes:

$$\frac{\delta f}{f} = 2.5 \frac{\delta A}{A} + 0.5 \frac{\delta P}{P} + 0.5 \frac{\delta S}{S} + 2 \frac{\delta Q}{Q}$$

The variables are as defined in the body of the report.

For ease of computation, a Fortran program was written to read in the various flow parameters and their associated measurement error to produce an estimate of the total error in Manning's  $n$  and Darcy's  $f$ . The program is listed in Appendix F.

## Appendix H: Test Results

The following tables are arranged from mild slopes to steep slopes for each pipe tested starting with the three precast concrete pipes followed by the three plastic pipes. The various hydraulic parameters analyzed in this study are listed with the SI units used. Dimensionless parameters were obtained from the following:

Manning n:

$$n = \frac{R^{2/3} S^{1/2}}{V}$$

Darcy's f:

$$f = \frac{8gRS}{V^2}$$

Froude number:

$$F = \frac{V}{\sqrt{gy}}$$

Reynold's number:

$$R_s = \frac{4VR}{v}$$

Equivalent sand grain roughness:

$$\frac{1}{\sqrt{f}} = 1.14 - 2 \log \left( \frac{k_s}{4R} + \frac{9.35}{R_s \sqrt{f}} \right)$$

## CONCRETE PIPE

PIPE DIAMETER = 0.202880 M.

PIPE BED SLOPE = 0.0020

DEPTH DIAMETER	DISCHARGE (L/s)	AVERAGE VELOCITY (m/s)	NORMAL DEPTH (mm)	MANNING n	DARCY f	FROUDE NUMBER	REYNOLDS NUMBER	EQUIVALENT ROUGHNESS (mm)
0.0888	0.2380	0.1422	20.0400	0.0171	0.0988	0.3208	0.720E+04	0.463E-02
0.1838	1.2780	0.3122	37.2800	0.0114	0.0263	0.5181	0.282E+05	0.637E-03
0.2327	2.4100	0.4218	47.2200	0.0098	0.0247	0.6200	0.469E+05	0.128E-03
0.3841	5.9800	0.5237	77.8200	0.0103	0.0241	0.5981	0.877E+05	0.262E-03
0.4570	7.9800	0.5550	92.7200	0.0106	0.0243	0.5820	0.105E+06	0.334E-03
0.5055	9.7600	0.5884	102.1600	0.0103	0.0223	0.5979	0.121E+06	0.235E-03
0.4964	8.9800	0.5964	100.7000	0.0102	0.0223	0.6001	0.120E+06	0.228E-03

PIPE BED SLOPE = 0.0025

DEPTH DIAMETER	DISCHARGE (L/s)	AVERAGE VELOCITY (m/s)	NORMAL DEPTH (mm)	MANNING n	DARCY f	FROUDE NUMBER	REYNOLDS NUMBER	EQUIVALENT ROUGHNESS (mm)
0.0885	0.2600	0.1849	17.9600	0.0138	0.0659	0.4405	0.843E+04	0.172E-02
0.2112	1.8700	0.3981	42.6400	0.0110	0.0321	0.6111	0.404E+05	0.483E-03
0.3521	6.8000	0.8723	77.9300	0.0106	0.0252	0.5663	0.955E+05	0.354E-03
0.4685	9.8100	0.6397	95.0400	0.0104	0.0233	0.6626	0.124E+06	0.285E-03
0.4622	9.4200	0.6448	93.7700	0.0103	0.0227	0.6724	0.123E+06	0.247E-03
0.6228	15.7500	0.7441	126.3500	0.0100	0.0203	0.6685	0.170E+06	0.175E-03

PIPE BED SLOPE = 0.0030

DEPTH DIAMETER	DISCHARGE (L/s)	AVERAGE VELOCITY (m/s)	NORMAL DEPTH (mm)	MANNING n	DARCY f	FROUDE NUMBER	REYNOLDS NUMBER	EQUIVALENT ROUGHNESS (mm)
0.1244	0.6700	0.2893	25.2400	0.0118	0.0445	0.5814	0.182E+05	0.349E-03
0.2383	2.8800	0.4876	48.3500	0.0108	0.0283	0.7081	0.853E+05	0.334E-03
0.3982	7.4500	0.6248	80.3900	0.0106	0.0260	0.7037	0.107E+06	0.415E-03
0.4449	9.8100	0.7057	80.2700	0.0101	0.0222	0.7500	0.132E+06	0.216E-03
0.5119	12.8400	0.7880	103.2400	0.0100	0.0210	0.7822	0.185E+06	0.187E-03
0.6388	16.8200	0.7761	129.0000	0.0106	0.0227	0.6884	0.170E+06	0.331E-03

PIPE BED SLOPE = 0.0035

DEPTH DIAMETER	DISCHARGE (L/s)	AVERAGE VELOCITY (m/s)	NORMAL DEPTH (mm)	MANNING n	DARCY f	FROUDE NUMBER	REYNOLDS NUMBER	EQUIVALENT ROUGHNESS (mm)
0.0820	0.2730	0.2172	16.6400	0.0132	0.0621	0.5377	0.820E+04	0.138E-02
0.2111	2.5200	0.3070	42.8200	0.0102	0.0274	0.7824	0.817E+05	0.252E-03
0.3550	6.9600	0.6768	72.0200	0.0102	0.0238	0.8084	0.107E+06	0.247E-03
0.4186	9.8040	0.7893	84.8100	0.0087	0.0208	0.8450	0.137E+06	0.141E-03
0.5217	14.4400	0.8465	106.8500	0.0087	0.0200	0.8306	0.178E+06	0.144E-03
0.6000	17.5800	0.6996	121.7200	0.0100	0.0205	0.7850	0.184E+06	0.183E-03
0.7027	21.5800	0.6883	142.8500	0.0102	0.0209	0.7819	0.212E+06	0.239E-03

PIPE BED SLOPE = 0.0040

DEPTH DIAMETER	DISCHARGE (L/s)	AVERAGE VELOCITY (m/s)	NORMAL DEPTH (mm)	MANNING n	DARCY f	FROUDE NUMBER	REYNOLDS NUMBER	EQUIVALENT ROUGHNESS (mm)
0.1184	0.7730	0.3723	23.4200	0.0102	0.0374	0.7768	0.200E+04	0.265E-03
0.2306	3.3700	0.5002	46.7600	0.0087	0.0243	0.8834	0.518E+05	0.184E-03
0.3607	7.8000	0.7716	71.3400	0.0085	0.0207	0.8236	0.840E+05	0.141E-03
0.4321	10.8000	0.8207	87.6700	0.0088	0.0214	0.8851	0.104E+06	0.112E-03
0.5248	15.4800	0.8014	106.4200	0.0088	0.0202	0.8832	0.144E+06	0.111E-03
0.6066	19.2800	0.8000	123.4600	0.0088	0.0184	0.8835	0.184E+06	0.111E-03
0.6987	23.9600	0.8018	141.9300	0.0088	0.0182	0.8406	0.212E+06	0.111E-03
0.7904	27.3900	0.8008	161.3700	0.0089	0.0196	0.7897	0.232E+06	0.111E-03

PIPE BED SLOPE = 0.0050

DEPTH DIAMETER	DISCHARGE (L/s)	AVERAGE VELOCITY (m/s)	NORMAL DEPTH (mm)	MANNING <i>n</i>	DARCY <i>f</i>	FROUDE NUMBER	REYNOLDS NUMBER	EQUIVALENT ROUGHNESS (mm)
0.0610	0.3630	0.2943	16.4300	0.0115	0.0477	0.7331	0.183E+06	0.887E-03
0.2473	4.5350	0.7287	50.1700	0.0093	0.0218	1.0368	0.883E+06	0.812E-04
0.3407	6.5370	0.8762	69.1300	0.0082	0.0185	1.0666	0.134E+06	0.748E-04
0.4185	12.4060	0.9873	84.8100	0.0092	0.0188	1.0601	0.173E+06	0.807E-04
0.4863	16.2490	1.0148	100.6899	0.0095	0.0182	1.0213	0.208E+06	0.118E-03
0.5557	21.1260	1.0522	120.8500	0.0098	0.0190	0.9498	0.238E+06	0.175E-03
0.7189	26.3750	1.0602	145.8500	0.0103	0.0211	0.8868	0.268E+06	0.266E-03
0.8337	31.1840	1.0622	168.1400	0.0102	0.0207	0.8409	0.268E+06	0.243E-03

PIPE BED SLOPE = 0.0060

DEPTH DIAMETER	DISCHARGE (L/s)	AVERAGE VELOCITY (m/s)	NORMAL DEPTH (mm)	MANNING <i>n</i>	DARCY <i>f</i>	FROUDE NUMBER	REYNOLDS NUMBER	EQUIVALENT ROUGHNESS (mm)
0.1087	0.8550	0.4498	22.0500	0.0100	0.0324	0.9672	0.348E+06	0.231E-03
0.2555	5.2500	0.8085	51.8400	0.0093	0.0220	1.1298	0.870E+06	0.112E-03
0.3592	10.1330	0.8700	72.8800	0.0093	0.0200	1.1473	0.184E+06	0.108E-03
0.4562	15.3820	1.0708	92.5800	0.0088	0.0196	1.1240	0.203E+06	0.127E-03
0.5281	19.3860	1.1183	107.1399	0.0087	0.0197	1.0820	0.233E+06	0.154E-03
0.5884	23.1480	1.1701	119.3700	0.0087	0.0192	1.0818	0.268E+06	0.144E-03
0.6322	28.7160	1.2203	138.6099	0.0087	0.0188	1.0467	0.268E+06	0.148E-03
0.8108	33.3480	1.1881	164.4400	0.0102	0.0206	0.9386	0.291E+06	0.244E-03

PIPE BED SLOPE = 0.0080

DEPTH DIAMETER	DISCHARGE (L/s)	AVERAGE VELOCITY (m/s)	NORMAL DEPTH (mm)	MANNING <i>n</i>	DARCY <i>f</i>	FROUDE NUMBER	REYNOLDS NUMBER	EQUIVALENT ROUGHNESS (mm)
0.1055	0.8630	0.5234	21.4100	0.0087	0.0311	1.1423	0.282E+06	0.181E-03
0.2481	5.4180	0.8664	50.3400	0.0089	0.0247	1.2331	0.102E+06	0.220E-03
0.3205	9.7510	1.0457	67.0600	0.0086	0.0215	1.2886	0.156E+06	0.186E-03
0.4525	17.7700	1.2505	81.8000	0.0084	0.0181	1.3178	0.230E+06	0.113E-03
0.5192	22.2660	1.3134	108.3200	0.0085	0.0188	1.2823	0.271E+06	0.138E-03
0.5872	27.1230	1.3468	121.1600	0.0087	0.0184	1.2388	0.301E+06	0.166E-03
0.7108	34.3610	1.3886	144.1700	0.0088	0.0184	1.1762	0.338E+06	0.181E-03
0.7434	38.1780	1.4037	150.8300	0.0089	0.0185	1.1842	0.341E+06	0.188E-03

PIPE BED SLOPE = 0.0100

DEPTH DIAMETER	DISCHARGE (L/s)	AVERAGE VELOCITY (m/s)	NORMAL DEPTH (mm)	MANNING <i>n</i>	DARCY <i>f</i>	FROUDE NUMBER	REYNOLDS NUMBER	EQUIVALENT ROUGHNESS (mm)
0.1080	1.1100	0.5812	22.1200	0.0100	0.0325	1.2479	0.323E+06	0.288E-03
0.2416	6.1290	1.0176	49.0200	0.0083	0.0219	1.4677	0.117E+06	0.116E-03
0.3188	10.2820	1.1603	64.6700	0.0086	0.0212	1.4569	0.168E+06	0.149E-03
0.4448	19.3020	1.3888	90.2500	0.0084	0.0181	1.4763	0.269E+06	0.116E-03
0.5047	23.4220	1.4318	102.3899	0.0086	0.0185	1.4268	0.290E+06	0.163E-03
0.5902	29.7180	1.4967	119.7399	0.0088	0.0186	1.3812	0.332E+06	0.178E-03
0.6722	35.3340	1.5281	136.3499	0.0089	0.0189	1.3223	0.360E+06	0.206E-03
0.7439	40.1970	1.5586	150.9300	0.0100	0.0187	1.2811	0.378E+06	0.207E-03

## CONCRETE PIPE

PIPE DIAMETER = 0.284670 m.

PIPE BED SLOPE = 0.0020

DEPTH DIAMETER	DISCHARGE (L/s)	AVERAGE VELOCITY (m/s)	NORMAL DEPTH (mm)	MANNING n	DARCY f	FROUDE NUMBER	REYNOLDS NUMBER	EQUIVALENT ROUGHNESS (mm)
0.1072	0.6480	0.2195	27.3100	0.0126	0.0683	0.4242	0.191E+05	0.182E-02
0.2229	3.4180	0.4930	56.8000	0.0116	0.0327	0.5400	0.541E+05	0.729E-03
0.3386	6.4810	0.4988	77.3500	0.0112	0.0281	0.5688	0.588E+05	0.988E-03
0.3654	9.4860	0.5622	93.1300	0.0108	0.0283	0.5883	0.514E+05	0.439E-03
0.3665	9.8310	0.5803	93.4000	0.0106	0.0238	0.6083	0.118E+05	0.331E-03
0.4260	12.8780	0.6264	106.5700	0.0106	0.0228	0.6071	0.142E+05	0.318E-03

PIPE BED SLOPE = 0.0025

DEPTH DIAMETER	DISCHARGE (L/s)	AVERAGE VELOCITY (m/s)	NORMAL DEPTH (mm)	MANNING n	DARCY f	FROUDE NUMBER	REYNOLDS NUMBER	EQUIVALENT ROUGHNESS (mm)
0.1088	0.7480	0.2882	26.9700	0.0128	0.0502	0.5021	0.175E+05	0.132E-02
0.2121	3.4550	0.4373	54.0600	0.0116	0.0332	0.6006	0.563E+05	0.747E-03
0.3032	7.2980	0.5587	77.2800	0.0111	0.0276	0.6419	0.975E+05	0.537E-03
0.3846	11.9620	0.6392	100.5700	0.0112	0.0288	0.6437	0.137E+05	0.538E-03
0.5214	20.0340	0.7449	132.8800	0.0109	0.0231	0.6528	0.194E+05	0.416E-03
0.6064	26.8280	0.8304	154.3100	0.0103	0.0202	0.6780	0.234E+05	0.241E-03

PIPE BED SLOPE = 0.0035

DEPTH DIAMETER	DISCHARGE (L/s)	AVERAGE VELOCITY (m/s)	NORMAL DEPTH (mm)	MANNING n	DARCY f	FROUDE NUMBER	REYNOLDS NUMBER	EQUIVALENT ROUGHNESS (mm)
0.0888	0.8230	0.3182	25.2000	0.0119	0.0443	0.6340	0.200E+05	0.886E-03
0.1987	4.0310	0.5600	50.6500	0.0103	0.0268	0.7946	0.680E+05	0.298E-03
0.2847	8.4040	0.7021	73.5700	0.0101	0.0232	0.8322	0.116E+06	0.237E-03
0.3626	13.4360	0.8047	92.4100	0.0101	0.0215	0.8483	0.162E+06	0.212E-03
0.4778	21.9060	0.9108	121.7000	0.0102	0.0208	0.8538	0.224E+06	0.221E-03
0.5996	30.4320	0.9529	152.8200	0.0106	0.0214	0.7784	0.288E+06	0.322E-03
0.6826	37.4660	0.9837	176.5298	0.0106	0.0208	0.7582	0.287E+06	0.324E-03
0.7886	43.8100	1.0395	196.2100	0.0103	0.0196	0.7494	0.319E+06	0.244E-03

PIPE BED SLOPE = 0.0040

DEPTH DIAMETER	DISCHARGE (L/s)	AVERAGE VELOCITY (m/s)	NORMAL DEPTH (mm)	MANNING n	DARCY f	FROUDE NUMBER	REYNOLDS NUMBER	EQUIVALENT ROUGHNESS (mm)
0.0940	0.9070	0.3798	23.9700	0.0104	0.0343	0.7710	0.227E+05	0.316E-03
0.1936	4.2530	0.6133	48.3500	0.0098	0.0248	0.8816	0.727E+05	0.204E-03
0.2818	9.1080	0.7715	71.8600	0.0098	0.0218	0.9190	0.127E+06	0.170E-03
0.3648	14.0680	0.8687	90.3600	0.0098	0.0207	0.9228	0.172E+06	0.173E-03
0.4985	23.7380	0.9630	123.8900	0.0103	0.0211	0.8740	0.240E+06	0.271E-03
0.5852	30.5820	1.0504	141.5000	0.0100	0.0193	0.8817	0.283E+06	0.188E-03
0.6960	40.0130	1.0886	177.3800	0.0107	0.0212	0.8003	0.316E+06	0.382E-03
0.7786	46.0140	1.0836	197.6700	0.0106	0.0207	0.7784	0.333E+06	0.320E-03

PIPE BED SLOPE = 0.0050

DEPTH DIAMETER	DISCHARGE (L/s)	AVERAGE VELOCITY (m/s)	NORMAL DEPTH (mm)	MANNING n	DARCY f	FROUDE NUMBER	REYNOLDS NUMBER	EQUIVALENT ROUGHNESS (mm)
0.0962	0.9060	0.3884	25.0200	0.0116	0.0420	0.7781	0.244E+05	0.737E-03
0.1874	4.7810	0.7234	47.7700	0.0082	0.0218	1.0584	0.832E+05	0.886E-04
0.2871	9.3280	0.8891	58.5299	0.0088	0.0186	1.1216	0.137E+06	0.452E-04
0.3478	15.8760	1.0063	70.5400	0.0084	0.0190	1.0793	0.196E+06	0.104E-03
0.4376	24.8380	1.1431	117.2998	0.0083	0.0175	1.0830	0.268E+06	0.810E-04
0.5473	34.3380	1.2016	139.4899	0.0087	0.0183	1.0274	0.321E+06	0.143E-03
0.6521	45.2680	1.2018	176.3899	0.0106	0.0204	0.8138	0.388E+06	0.300E-03
0.7686	51.0100	1.2171	195.1300	0.0106	0.0204	0.8788	0.373E+06	0.310E-03

PIPE BED SLOPE = 0.0080

DEPTH DIAMETER	DISCHARGE (L/s)	AVERAGE VELOCITY (m/s)	NORMAL DEPTH (mm)	MANNING n	DA
0.0807	1.0120	0.4388	23.1200	0.0106	0.
0.1813	5.1080	0.8097	46.2000	0.0088	0.
0.2827	9.8130	0.9690	64.4100	0.0080	0.
0.3841	16.5180	1.1974	83.4388	0.0068	0.
0.3864	22.4230	1.1611	101.0200	0.0063	0.
0.4700	30.1230	1.2785	119.7888	0.0064	0.
0.5865	38.7860	1.3638	141.8300	0.0065	0.
0.6348	47.9860	1.4048	161.7888	0.0066	0.
0.7684	56.7140	1.3538	188.0700	0.0104	0.

PIPE BED SLOPE = 0.0080

DEPTH DIAMETER	DISCHARGE (L/s)	AVERAGE VELOCITY (m/s)	NORMAL DEPTH (mm)	MANNING n	DA
0.0846	1.1330	0.5454	21.5700	0.0084	0.
0.1882	6.1840	0.9245	47.9800	0.0082	0.
0.2610	12.4880	1.1753	66.8200	0.0087	0.
0.3588	21.7170	1.3136	81.7388	0.0093	0.
0.4617	33.2360	1.4458	107.8300	0.0098	0.
0.5781	47.0260	1.5386	147.3488	0.0098	0.
0.6781	58.8380	1.5877	173.0800	0.0098	0.
0.7347	65.0740	1.6198	187.2500	0.0100	0.

PIPE BED SLOPE = 0.0100

DEPTH DIAMETER	DISCHARGE (L/s)	AVERAGE VELOCITY (m/s)	NORMAL DEPTH (mm)	MANNING n	DA
0.0830	1.2880	0.6228	21.1600	0.0081	0.
0.1834	7.0600	1.0201	48.2800	0.0084	0.
0.2678	13.8700	1.2625	68.2488	0.0082	0.
0.3684	24.7300	1.4680	93.1200	0.0084	0.
0.4817	37.2720	1.4827	128.3188	0.0106	0.
0.5836	51.1420	1.6537	148.7888	0.0102	0.
0.6888	64.4839	1.7208	178.5600	0.0103	0.
0.7588	73.5210	1.7700	193.4000	0.0102	0.

## CONCRETE PIPE

PIPE DIAMETER = 0.380280 M.

PIPE BED SLOPE = 0.0020

DEPTH DIAMETER	DISCHARGE (L/s)	AVERAGE VELOCITY (m/s)	NORMAL DEPTH (mm)	MANNING n	DARCY f	FROUDE NUMBER	REYNOLDS NUMBER	EQUIVALENT ROUGHNESS (mm)
0.1067	2.3750	0.3655	40.5600	0.0106	0.0302	0.5795	0.373E+06	0.354E-03
0.2118	9.3270	0.5326	80.4200	0.0111	0.0267	0.5897	0.102E+06	0.510E-03
0.2071	9.1740	0.5397	78.7600	0.0106	0.0265	0.6141	0.101E+06	0.408E-03
0.3168	21.1890	0.6844	120.5200	0.0106	0.0228	0.6295	0.185E+06	0.398E-03
0.4394	40.8060	0.8513	167.1100	0.0103	0.0189	0.6650	0.295E+06	0.216E-03

PIPE BED SLOPE = 0.0028

DEPTH DIAMETER	DISCHARGE (L/s)	AVERAGE VELOCITY (m/s)	NORMAL DEPTH (mm)	MANNING n	DARCY f	FROUDE NUMBER	REYNOLDS NUMBER	EQUIVALENT ROUGHNESS (mm)
0.1008	2.1730	0.3631	38.3800	0.0116	0.0302	0.5821	0.381E+06	0.715E-03
0.2058	10.4770	0.6177	78.6400	0.0106	0.0243	0.7034	0.116E+06	0.336E-03
0.3045	22.9580	0.7849	115.7800	0.0104	0.0208	0.7366	0.208E+06	0.260E-03
0.4302	42.9560	0.8182	163.6000	0.0106	0.0198	0.7257	0.374E+06	0.293E-03
0.5270	61.1620	1.0077	200.4098	0.0106	0.0190	0.7188	0.383E+06	0.273E-03
0.6228	81.0600	1.0800	236.8300	0.0104	0.0177	0.7153	0.466E+06	0.216E-03

PIPE BED SLOPE = 0.0035

DEPTH DIAMETER	DISCHARGE (L/s)	AVERAGE VELOCITY (m/s)	NORMAL DEPTH (mm)	MANNING n	DARCY f	FROUDE NUMBER	REYNOLDS NUMBER	EQUIVALENT ROUGHNESS (mm)
0.0882	2.6600	0.4551	37.7400	0.0106	0.0318	0.7480	0.433E+06	0.442E-03
0.2028	12.8600	0.7783	77.1400	0.0098	0.0210	0.8960	0.144E+06	0.161E-03
0.3040	27.1420	0.8287	115.6199	0.0104	0.0208	0.8731	0.242E+06	0.267E-03
0.4283	51.4880	1.1062	162.8800	0.0104	0.0191	0.8768	0.377E+06	0.247E-03
0.5043	68.6710	1.1862	181.7699	0.0103	0.0183	0.8723	0.484E+06	0.230E-03
0.6120	93.4200	1.2824	232.7200	0.0104	0.0178	0.8489	0.543E+06	0.228E-03
0.7354	120.4030	1.3486	278.8087	0.0103	0.0172	0.8155	0.612E+06	0.210E-03
0.8261	141.1480	1.4028	314.1987	0.0100	0.0161	0.8013	0.646E+06	0.141E-03

PIPE BED SLOPE = 0.0040

DEPTH DIAMETER	DISCHARGE (L/s)	AVERAGE VELOCITY (m/s)	NORMAL DEPTH (mm)	MANNING n	DARCY f	FROUDE NUMBER	REYNOLDS NUMBER	EQUIVALENT ROUGHNESS (mm)
0.0831	2.7480	0.5162	38.4100	0.0088	0.0266	0.8761	0.463E+06	0.175E-03
0.1974	14.6100	0.9207	75.0588	0.0087	0.0168	1.0731	0.166E+06	0.142E-04
0.2970	28.4810	1.0081	112.9500	0.0101	0.0198	0.9578	0.258E+06	0.207E-03
0.4068	51.8790	1.1884	154.6298	0.0101	0.0183	0.9658	0.390E+06	0.187E-03
0.4831	70.6730	1.3004	183.7200	0.0100	0.0173	0.9688	0.480E+06	0.160E-03
0.6137	96.2780	1.3584	233.3800	0.0105	0.0182	0.8980	0.576E+06	0.256E-03
0.7204	127.2460	1.4826	273.9887	0.0102	0.0169	0.8862	0.656E+06	0.190E-03
0.7866	143.3230	1.4718	304.1887	0.0102	0.0168	0.8820	0.676E+06	0.186E-03

PIPE BED SLOPE = 0.0050

DEPTH DIAMETER	DISCHARGE (L/s)	AVERAGE VELOCITY (m/s)	NORMAL DEPTH (mm)	MANNING n	DARCY f	FROUDE NUMBER	REYNOLDS NUMBER	EQUIVALENT ROUGHNESS (mm)
0.0820	3.3460	0.6384	38.0000	0.0088	0.0214	1.0815	0.567E+06	0.264E-04
0.1743	14.6210	1.1014	68.2888	0.0076	0.0131	1.3660	0.177E+06	0.498E-04
0.2633	31.0080	1.2861	100.1400	0.0082	0.0136	1.3088	0.301E+06	0.178E-04
0.3639	56.1070	1.5078	137.9800	0.0084	0.0131	1.2982	0.453E+06	0.719E-05
0.4806	78.0070	1.5701	171.4200	0.0080	0.0141	1.2110	0.552E+06	0.313E-04
0.5711	106.4580	1.6328	217.1789	0.0085	0.0151	1.1188	0.687E+06	0.849E-04
0.6836	140.8790	1.7028	259.9637	0.0086	0.0151	1.0664	0.756E+06	0.973E-04
0.8025	161.5000	1.6831	308.1887	0.0102	0.0166	0.9556	0.760E+06	0.182E-03

PIPE BED SLOPE = 0.0080

DEPTH DIAMETER	DISCHARGE (L/s)	AVERAGE VELOCITY (m/s)	NORMAL DEPTH (mm)	MANNING n	DARCY $f$	FROUDE NUMBER	REYNOLDS NUMBER	EQUIVALENT ROUGHNESS (mm)
0.0882	3.4800	0.7098	33.8800	0.0084	0.0200	1.2378	0.804E+06	0.127E-06
0.1908	17.0760	1.1323	72.4400	0.0085	0.0161	1.3434	0.197E+06	0.866E-06
0.2710	39.4140	1.3438	103.0898	0.0086	0.0156	1.3363	0.318E+06	0.914E-06
0.3848	68.3230	1.5671	150.1198	0.0082	0.0155	1.2816	0.502E+06	0.688E-06
0.4707	87.4860	1.6646	178.0000	0.0084	0.0155	1.2944	0.604E+06	0.662E-06
0.5823	121.7845	1.7744	221.4800	0.0087	0.0155	1.2040	0.733E+06	0.108E-03
0.7029	182.9030	1.7838	267.9898	0.0101	0.0165	1.1072	0.903E+06	0.178E-03
0.7787	169.1180	1.7821	296.1298	0.0103	0.0171	1.0487	0.817E+06	0.217E-03

PIPE BED SLOPE = 0.0080

DEPTH DIAMETER	DISCHARGE (L/s)	AVERAGE VELOCITY (m/s)	NORMAL DEPTH (mm)	MANNING n	DARCY $f$	FROUDE NUMBER	REYNOLDS NUMBER	EQUIVALENT ROUGHNESS (mm)
0.0865	3.8070	0.8182	32.8800	0.0083	0.0197	1.4407	0.884E+06	0.421E-06
0.1824	18.7300	1.3217	69.3700	0.0082	0.0182	1.6024	0.222E+06	0.283E-06
0.2732	38.2310	1.5597	103.8898	0.0088	0.0155	1.5453	0.373E+06	0.379E-06
0.3933	72.6210	1.7508	148.5600	0.0085	0.0165	1.4458	0.560E+06	0.110E-03
0.4773	98.3820	1.8388	181.5000	0.0089	0.0171	1.3782	0.674E+06	0.167E-03
0.5821	138.1730	1.8728	228.1700	0.0101	0.0168	1.3277	0.822E+06	0.188E-03
0.6840	168.8810	2.0184	263.9187	0.0103	0.0173	1.2552	0.901E+06	0.227E-03
0.7590	181.4030	2.0684	288.6298	0.0102	0.0169	1.2300	0.848E+06	0.208E-03

PIPE BED SLOPE = 0.0100

DEPTH DIAMETER	DISCHARGE (L/s)	AVERAGE VELOCITY (m/s)	NORMAL DEPTH (mm)	MANNING n	DARCY $f$	FROUDE NUMBER	REYNOLDS NUMBER	EQUIVALENT ROUGHNESS (mm)
0.0866	4.3330	0.9054	32.9400	0.0084	0.0202	1.8830	0.758E+06	0.211E-06
0.1274	8.6290	1.1432	48.4400	0.0085	0.0182	1.6587	0.138E+06	0.281E-06
0.1270	8.6870	1.1883	48.2900	0.0084	0.0178	1.6788	0.138E+06	0.191E-06
0.1858	20.8110	1.4376	70.6400	0.0085	0.0163	1.7272	0.245E+06	0.258E-06
0.2715	49.3000	1.7362	103.2600	0.0088	0.0156	1.7254	0.413E+06	0.438E-06
0.3848	80.6460	1.8347	150.1198	0.0087	0.0168	1.5845	0.620E+06	0.133E-03
0.4762	108.3078	2.0489	181.0898	0.0100	0.0172	1.5375	0.780E+06	0.178E-03
0.5856	150.9110	2.1835	222.7099	0.0101	0.0172	1.4775	0.804E+06	0.202E-03
0.7089	181.8030	2.2278	268.5698	0.0108	0.0178	1.3702	0.100E+07	0.273E-03
0.7606	211.5800	2.2817	288.3598	0.0104	0.0173	1.3845	0.104E+07	0.240E-03

## PLASTIC PIPE

PIPE DIAMETER = 0.199600 M.

PIPE BED SLOPE = 0.0020

DEPTH DIAMETER	DISCHARGE (L/s)	AVERAGE VELOCITY (m/s)	NORMAL DEPTH (mm)	MANNING n	DARCY f	FROUDE NUMBER	REYNOLDS NUMBER	EQUIVALENT ROUGHNESS (mm)
0.1177	0.4860	0.2350	23.5000	0.0115	0.0420	0.4894	0.138E+06	0.604E-03
0.2482	2.3860	0.3650	48.5000	0.0105	0.0288	0.5714	0.452E+06	0.344E-03
0.3786	4.8290	0.5170	67.5000	0.0087	0.0220	0.6358	0.774E+06	0.117E-03
0.4786	9.1880	0.6212	86.5000	0.0086	0.0187	0.6418	0.120E+06	0.903E-04
0.4811	8.7620	0.6384	96.0000	0.0084	0.0190	0.6512	0.125E+06	0.655E-04
0.5820	12.8830	0.6822	116.1700	0.0084	0.0184	0.6392	0.148E+06	0.649E-04

PIPE BED SLOPE = 0.0025

DEPTH DIAMETER	DISCHARGE (L/s)	AVERAGE VELOCITY (m/s)	NORMAL DEPTH (mm)	MANNING n	DARCY f	FROUDE NUMBER	REYNOLDS NUMBER	EQUIVALENT ROUGHNESS (mm)
0.1181	0.5600	0.2787	22.5000	0.0106	0.0363	0.5893	0.161E+06	0.334E-03
0.2312	2.6410	0.4822	46.1500	0.0084	0.0231	0.7167	0.524E+06	0.793E-04
0.3223	5.3620	0.6150	64.2400	0.0089	0.0188	0.7742	0.884E+06	0.873E-05
0.4673	9.9190	0.6916	83.2700	0.0088	0.0196	0.7231	0.131E+06	0.819E-04
0.4786	10.2360	0.6976	84.9200	0.0085	0.0195	0.7230	0.134E+06	0.804E-04
0.5801	14.2930	0.7593	115.7500	0.0085	0.0185	0.7126	0.164E+06	0.804E-04
0.7219	19.8370	0.8202	144.0800	0.0083	0.0174	0.6900	0.194E+06	0.566E-04

PIPE BED SLOPE = 0.0035

DEPTH DIAMETER	DISCHARGE (L/s)	AVERAGE VELOCITY (m/s)	NORMAL DEPTH (mm)	MANNING n	DARCY f	FROUDE NUMBER	REYNOLDS NUMBER	EQUIVALENT ROUGHNESS (mm)
0.1086	0.6200	0.3375	21.6700	0.0100	0.0330	0.7321	0.184E+06	0.208E-03
0.2243	3.1180	0.5841	44.7500	0.0088	0.0207	0.8865	0.628E+06	0.233E-04
0.3278	6.4380	0.7217	68.4200	0.0080	0.0193	0.9010	0.108E+06	0.443E-04
0.3206	6.3080	0.7166	64.0300	0.0080	0.0193	0.9042	0.103E+06	0.384E-04
0.4818	12.1870	0.8876	90.1900	0.0086	0.0163	0.8438	0.164E+06	0.181E-04
0.5418	16.3120	0.8425	108.1400	0.0088	0.0162	0.8182	0.186E+06	0.136E-04
0.7126	23.2400	0.8743	142.2400	0.0082	0.0172	0.8249	0.230E+06	0.623E-04

PIPE BED SLOPE = 0.0040

DEPTH DIAMETER	DISCHARGE (L/s)	AVERAGE VELOCITY (m/s)	NORMAL DEPTH (mm)	MANNING n	DARCY f	FROUDE NUMBER	REYNOLDS NUMBER	EQUIVALENT ROUGHNESS (mm)
0.1078	0.6730	0.3701	21.8200	0.0087	0.0312	0.8056	0.200E+06	0.154E-03
0.2222	3.3800	0.5828	44.3500	0.0086	0.0194	0.9001	0.685E+06	0.117E-05
0.3118	6.8890	0.8247	62.2400	0.0082	0.0162	1.0556	0.115E+06	0.266E-04
0.4860	13.4290	0.9666	91.0100	0.0085	0.0158	1.0232	0.180E+06	0.458E-05
0.5510	17.7980	1.0072	108.8700	0.0088	0.0164	0.9698	0.212E+06	0.243E-04
0.5766	24.8730	1.1040	138.0400	0.0086	0.0150	0.8983	0.256E+06	0.348E-05
0.8238	30.0380	1.0882	164.4400	0.0080	0.0161	0.8577	0.263E+06	0.342E-04

PIPE BED SLOPE = 0.0050

DEPTH DIAMETER	DISCHARGE (L/s)	AVERAGE VELOCITY (m/s)	NORMAL DEPTH (mm)	MANNING n	DARCY f	FROUDE NUMBER	REYNOLDS NUMBER	EQUIVALENT ROUGHNESS (mm)
0.1104	0.8080	0.4280	22.0400	0.0096	0.0298	0.9206	0.237E+06	0.136E-03
0.2208	3.7880	0.7378	44.0700	0.0085	0.0189	1.1223	0.770E+06	0.177E-05
0.3132	7.6800	0.8130	62.5000	0.0083	0.0166	1.1661	0.128E+06	0.100E-04
0.4488	14.6890	1.0686	88.0000	0.0084	0.0153	1.1652	0.200E+06	0.732E-06
0.5318	19.8130	1.1537	108.1600	0.0085	0.0153	1.1307	0.238E+06	0.358E-05
0.5888	28.9200	1.1817	130.9000	0.0088	0.0159	1.0618	0.273E+06	0.316E-04
0.7832	32.1480	1.2077	158.3300	0.0080	0.0163	0.9582	0.281E+06	0.488E-04
0.8725	38.4430	1.2338	174.1600	0.0088	0.0158	0.8362	0.282E+06	0.321E-04

PIPE BED SLOPE = 0.0060

DEPTH DIAMETER	DISCHARGE (L/s)	AVERAGE VELOCITY (m/s)	NORMAL DEPTH (mm)	MANNING n	DARCY f	FROUDE NUMBER	REYNOLDS NUMBER	EQUIVALENT ROUGHNESS (mm)
0.1042	0.8220	0.4788	20.7900	0.0081	0.0274	1.0630	0.249E+06	0.882E-04
0.2190	4.1740	0.8232	43.7100	0.0083	0.0181	1.2873	0.883E+06	0.660E-04
0.3067	8.3430	1.0113	61.8100	0.0082	0.0161	1.2990	0.141E+06	0.131E-04
0.3146	8.7580	1.0368	62.7800	0.0080	0.0188	1.3230	0.146E+06	0.229E-04
0.4388	18.3680	1.1726	86.8800	0.0084	0.0188	1.2707	0.212E+06	0.181E-04
0.5187	20.8810	1.2834	102.8288	0.0083	0.0146	1.3774	0.289E+06	0.872E-04
0.6387	28.0800	1.3284	127.4800	0.0086	0.0182	1.1689	0.301E+06	0.174E-04
0.7108	32.3830	1.3620	141.8088	0.0087	0.0181	1.1550	0.321E+06	0.184E-04
0.8167	37.4410	1.3688	163.0198	0.0087	0.0183	1.0633	0.350E+06	0.264E-04
0.8890	39.1630	1.3324	177.4498	0.0088	0.0188	1.0100	0.317E+06	0.390E-04

PIPE BED SLOPE = 0.0080

DEPTH DIAMETER	DISCHARGE (L/s)	AVERAGE VELOCITY (m/s)	NORMAL DEPTH (mm)	MANNING n	DARCY f	FROUDE NUMBER	REYNOLDS NUMBER	EQUIVALENT ROUGHNESS (mm)
0.0898	0.8380	0.5750	19.9400	0.0085	0.0240	1.3003	0.289E+06	0.881E-04
0.2133	4.6890	0.9619	42.3800	0.0081	0.0173	1.4886	0.874E+06	0.148E-04
0.3111	8.6420	1.1615	62.0000	0.0083	0.0164	1.4885	0.162E+06	0.101E-04
0.4375	18.0100	1.3483	87.3300	0.0083	0.0183	1.4788	0.248E+06	0.888E-04
0.5269	24.7880	1.4837	108.1600	0.0083	0.0147	1.4610	0.304E+06	0.820E-04
0.6301	33.0650	1.5631	127.7698	0.0085	0.0147	1.3964	0.388E+06	0.137E-04
0.7062	37.7790	1.5984	140.9600	0.0085	0.0145	1.3803	0.377E+06	0.143E-04
0.7818	43.9130	1.6730	156.0600	0.0082	0.0136	1.3824	0.403E+06	0.184E-04
0.8285	46.1190	1.6684	164.7600	0.0083	0.0137	1.3133	0.403E+06	0.286E-04

PIPE BED SLOPE = 0.0100

DEPTH DIAMETER	DISCHARGE (L/s)	AVERAGE VELOCITY (m/s)	NORMAL DEPTH (mm)	MANNING n	DARCY f	FROUDE NUMBER	REYNOLDS NUMBER	EQUIVALENT ROUGHNESS (mm)
0.1004	1.0360	0.6329	20.0300	0.0086	0.0249	1.4281	0.320E+06	0.343E-04
0.2097	5.1380	1.0781	41.8500	0.0080	0.0169	1.6828	0.107E+06	0.131E-04
0.2940	9.8890	1.2896	58.6800	0.0081	0.0188	1.7000	0.172E+06	0.493E-04
0.4213	18.7200	1.4849	84.0800	0.0084	0.0156	1.6462	0.264E+06	0.148E-04
0.4826	25.0610	1.6328	98.3300	0.0083	0.0145	1.6624	0.321E+06	0.480E-04
0.6206	35.5340	1.7410	123.9088	0.0084	0.0146	1.5794	0.380E+06	0.158E-04
0.7086	43.3280	1.8247	141.6388	0.0083	0.0140	1.5483	0.430E+06	0.877E-04
0.8238	53.2930	1.9137	166.4800	0.0081	0.0130	1.4976	0.461E+06	0.881E-04
0.8378	64.3370	1.9410	187.2200	0.0080	0.0126	1.5156	0.468E+06	0.110E-04

## PLASTIC PIPE

PIPE DIAMETER = 0.248780 M.

PIPE BED SLOPE = 0.0020

DEPTH DIAMETER	DISCHARGE (L/s)	AVERAGE VELOCITY (m/s)	NORMAL DEPTH (mm)	MANNING n	DARCY f	FROUDE NUMBER	REYNOLDS NUMBER	EQUIVALENT ROUGHNESS (mm)
0.1128	0.8870	0.2916	28.1700	0.0104	0.0328	0.5548	0.206E+05	0.280E-03
0.2354	4.3270	0.4919	56.7800	0.0097	0.0225	0.6478	0.679E+05	0.114E-03
0.3372	8.7810	0.6061	83.2988	0.0096	0.0201	0.6558	0.113E+06	0.980E-04
0.3360	8.8910	0.6161	83.7798	0.0095	0.0194	0.6781	0.114E+06	0.692E-04
0.4785	16.8180	0.7240	119.7788	0.0095	0.0182	0.6580	0.175E+06	0.808E-04
0.5801	23.1230	0.7844	144.9000	0.0095	0.0174	0.6580	0.212E+06	0.721E-04

PIPE BED SLOPE = 0.0025

DEPTH DIAMETER	DISCHARGE (L/s)	AVERAGE VELOCITY (m/s)	NORMAL DEPTH (mm)	MANNING n	DARCY f	FROUDE NUMBER	REYNOLDS NUMBER	EQUIVALENT ROUGHNESS (mm)
0.1127	0.8850	0.3273	28.1600	0.0104	0.0325	0.6228	0.231E+05	0.287E-03
0.2372	4.8170	0.5416	59.2500	0.0096	0.0234	0.7105	0.763E+05	0.167E-03
0.3334	9.7850	0.6448	83.2800	0.0094	0.0195	0.7578	0.127E+06	0.811E-04
0.4652	10.0880	0.6726	86.2200	0.0098	0.0207	0.7315	0.128E+06	0.142E-03
0.4834	18.7290	0.7882	120.7400	0.0087	0.0188	0.7335	0.184E+06	0.119E-03
0.5805	25.3770	0.8601	145.0100	0.0097	0.0181	0.7212	0.233E+06	0.112E-03
0.7123	35.1740	0.8420	177.8298	0.0094	0.0164	0.7134	0.278E+06	0.615E-04

PIPE BED SLOPE = 0.0035

DEPTH DIAMETER	DISCHARGE (L/s)	AVERAGE VELOCITY (m/s)	NORMAL DEPTH (mm)	MANNING n	DARCY f	FROUDE NUMBER	REYNOLDS NUMBER	EQUIVALENT ROUGHNESS (mm)
0.1082	1.1710	0.4036	27.2800	0.0098	0.0291	0.7801	0.276E+05	0.163E-03
0.2267	5.8820	0.8775	56.6300	0.0091	0.0201	0.8081	0.908E+05	0.517E-04
0.3270	11.5100	0.8263	81.6898	0.0082	0.0184	0.8232	0.150E+06	0.569E-04
0.4586	21.7230	0.9093	113.8098	0.0088	0.0161	0.8458	0.233E+06	0.273E-04
0.5902	29.9960	1.0666	139.0898	0.0081	0.0160	0.8158	0.283E+06	0.408E-04
0.6898	40.1310	1.1128	172.3300	0.0083	0.0163	0.8841	0.326E+06	0.673E-04
0.8140	49.5660	1.1608	203.3300	0.0081	0.0168	0.8217	0.380E+06	0.438E-04

PIPE BED SLOPE = 0.0040

DEPTH DIAMETER	DISCHARGE (L/s)	AVERAGE VELOCITY (m/s)	NORMAL DEPTH (mm)	MANNING n	DARCY f	FROUDE NUMBER	REYNOLDS NUMBER	EQUIVALENT ROUGHNESS (mm)
0.1057	1.2870	0.4303	27.4000	0.0088	0.0293	0.8302	0.286E+05	0.182E-03
0.2239	6.0520	0.7384	56.8300	0.0088	0.0192	0.8970	0.876E+05	0.288E-04
0.3188	12.4280	0.8251	78.5700	0.0086	0.0164	1.0472	0.188E+06	0.488E-05
0.4338	21.5880	1.0734	108.3800	0.0087	0.0158	1.0411	0.242E+06	0.891E-05
0.5236	26.7410	1.1453	130.7588	0.0088	0.0154	1.0114	0.282E+06	0.223E-04
0.6343	40.2580	1.2280	158.4498	0.0088	0.0148	0.9851	0.347E+06	0.188E-04
0.7643	50.0180	1.2446	190.8100	0.0081	0.0183	0.8986	0.374E+06	0.414E-04
0.8798	60.0280	1.3148	219.6800	0.0086	0.0136	0.8868	0.382E+06	0.272E-05

PIPE BED SLOPE = 0.0050

DEPTH DIAMETER	DISCHARGE (L/s)	AVERAGE VELOCITY (m/s)	NORMAL DEPTH (mm)	MANNING n	DARCY f	FROUDE NUMBER	REYNOLDS NUMBER	EQUIVALENT ROUGHNESS (mm)
0.1088	1.3900	0.5000	26.4000	0.0082	0.0262	0.9632	0.333E+06	0.868E-04
0.2158	6.7700	0.8688	53.9300	0.0082	0.0167	1.1962	0.111E+06	0.105E-04
0.3091	13.4600	1.0446	77.2000	0.0084	0.0157	1.2006	0.182E+06	0.466E-05
0.4388	26.0100	1.2197	108.8500	0.0086	0.0150	1.1808	0.276E+06	0.736E-05
0.5198	33.6800	1.3088	128.7600	0.0086	0.0146	1.1610	0.333E+06	0.108E-04
0.6497	46.5400	1.4033	160.0988	0.0087	0.0142	1.1202	0.398E+06	0.127E-04
0.7838	59.3500	1.4227	188.2198	0.0089	0.0147	1.0204	0.429E+06	0.308E-04
0.8718	68.1800	1.4367	217.6868	0.0088	0.0143	0.9633	0.430E+06	0.198E-04

PIPE BED SLOPE = 0.0060

DEPTH DIAMETER	DISCHARGE (L/s)	AVERAGE VELOCITY (m/s)	NORMAL DEPTH (mm)	MANNING n	DARCY f	FROUDE NUMBER	REYNOLDS NUMBER	EQUIVALENT ROUGHNESS (mm)
0.1040	1.5500	0.5740	25.9700	0.0087	0.0235	1.1375	0.378E+06	0.278E-04
0.2175	7.3800	0.9386	54.3200	0.0084	0.0173	1.2860	0.181E+06	0.827E-04
0.3133	15.2000	1.1874	78.2700	0.0084	0.0188	1.3211	0.203E+06	0.814E-04
0.4391	28.0600	1.3586	106.6800	0.0085	0.0147	1.3071	0.308E+06	0.882E-04
0.5270	37.7500	1.4414	131.6500	0.0086	0.0166	1.2685	0.388E+06	0.162E-04
0.6236	49.0000	1.5248	156.7700	0.0087	0.0143	1.2337	0.428E+06	0.178E-04
0.7829	65.2698	1.5887	185.5600	0.0088	0.0142	1.1481	0.478E+06	0.230E-04
0.8656	70.0310	1.5536	216.2200	0.0089	0.0147	1.0689	0.466E+06	0.348E-04

PIPE BED SLOPE = 0.0080

DEPTH DIAMETER	DISCHARGE (L/s)	AVERAGE VELOCITY (m/s)	NORMAL DEPTH (mm)	MANNING n	DARCY f	FROUDE NUMBER	REYNOLDS NUMBER	EQUIVALENT ROUGHNESS (mm)
0.1038	1.7770	0.6892	28.9400	0.0088	0.0238	1.3070	0.491E+06	0.469E-04
0.2122	8.9170	1.1218	59.0100	0.0080	0.0186	1.5585	0.141E+06	0.183E-04
0.3081	17.2300	1.3430	76.9600	0.0083	0.0182	1.5455	0.239E+06	0.864E-04
0.4228	30.7000	1.5578	105.6200	0.0084	0.0144	1.5085	0.348E+06	0.638E-04
0.5027	40.8280	1.6581	125.5600	0.0085	0.0144	1.4675	0.412E+06	0.181E-04
0.6268	57.8720	1.7932	156.8600	0.0085	0.0138	1.4771	0.498E+06	0.143E-04
0.7425	71.8780	1.8420	185.4700	0.0087	0.0105	1.3645	0.590E+06	0.211E-04
0.8263	80.5730	1.8608	206.4100	0.0086	0.0147	1.3005	0.496E+06	0.180E-04

PIPE BED SLOPE = 0.0100

DEPTH DIAMETER	DISCHARGE (L/s)	AVERAGE VELOCITY (m/s)	NORMAL DEPTH (mm)	MANNING n	DARCY f	FROUDE NUMBER	REYNOLDS NUMBER	EQUIVALENT ROUGHNESS (mm)
0.1018	1.9830	0.7578	25.4200	0.0084	0.0220	1.5178	0.486E+06	0.182E-04
0.2081	9.5000	1.2665	51.8800	0.0077	0.0148	1.8019	0.159E+06	0.240E-04
0.2983	18.8070	1.5000	74.5000	0.0081	0.0146	1.7654	0.258E+06	0.483E-04
0.4136	32.7010	1.7063	103.3100	0.0084	0.0147	1.6976	0.372E+06	0.168E-04
0.4995	45.1330	1.8441	124.7700	0.0085	0.0144	1.6671	0.457E+06	0.208E-04
0.6148	62.4650	1.8768	153.5600	0.0086	0.0141	1.6106	0.551E+06	0.238E-04
0.7048	75.3900	2.0423	176.0400	0.0086	0.0139	1.5544	0.602E+06	0.253E-04
0.8303	80.7159	2.0688	207.3800	0.0086	0.0137	1.4626	0.628E+06	0.218E-04

## PLASTIC PIPE

PIPE DIAMETER = 0.448800 M.

PIPE BED SLOPE = 0.0020

DEPTH DIAMETER	DISCHARGE (L/s)	AVERAGE VELOCITY (m/s)	NORMAL DEPTH (mm)	MANNING n	DARCY f	FROUDE NUMBER	REYNOLDS NUMBER	EQUIVALENT ROUGHNESS (mm)
0.1044	4.3060	0.4908	46.8500	0.0087	0.0183	0.7243	0.578E+05	0.287E-04
0.2261	21.3100	0.7844	101.4700	0.0087	0.0150	0.7983	0.180E+06	0.224E-04
0.3302	41.1120	0.9024	148.1788	0.0086	0.0160	0.7486	0.287E+06	0.540E-04
0.4814	80.2420	1.0648	216.0600	0.0086	0.0152	0.7315	0.463E+06	0.691E-04
0.6621	107.7700	1.1768	252.2700	0.0083	0.0136	0.7482	0.565E+06	0.250E-04

PIPE BED SLOPE = 0.0025

DEPTH DIAMETER	DISCHARGE (L/s)	AVERAGE VELOCITY (m/s)	NORMAL DEPTH (mm)	MANNING n	DARCY f	FROUDE NUMBER	REYNOLDS NUMBER	EQUIVALENT ROUGHNESS (mm)
0.1061	4.7880	0.5342	47.8000	0.0081	0.0207	0.7819	0.640E+05	0.281E-04
0.2201	23.3840	0.9055	98.7900	0.0084	0.0141	0.8189	0.212E+06	0.335E-04
0.3180	45.3060	1.0468	142.7398	0.0085	0.0144	0.8849	0.335E+06	0.664E-05
0.4372	80.7430	1.2148	196.2200	0.0080	0.0136	0.8755	0.455E+06	0.133E-04
0.6358	108.7000	1.2708	240.8100	0.0084	0.0142	0.8275	0.881E+06	0.484E-04
0.8851	150.7180	1.3724	293.8897	0.0083	0.0135	0.8063	0.707E+06	0.372E-04
0.7887	188.4920	1.4882	352.6286	0.0088	0.0121	0.8003	0.806E+06	0.331E-06

PIPE BED SLOPE = 0.0035

DEPTH DIAMETER	DISCHARGE (L/s)	AVERAGE VELOCITY (m/s)	NORMAL DEPTH (mm)	MANNING n	DARCY f	FROUDE NUMBER	REYNOLDS NUMBER	EQUIVALENT ROUGHNESS (mm)
0.1036	6.5590	0.6448	46.4500	0.0088	0.0185	0.9553	0.754E+05	0.842E-05
0.2174	26.1840	1.0310	97.5600	0.0086	0.0151	1.0540	0.238E+06	0.142E-05
0.3062	51.1880	1.2354	138.3200	0.0088	0.0141	1.0607	0.385E+06	0.800E-05
0.4288	90.8840	1.4186	180.8500	0.0080	0.0137	1.0577	0.567E+06	0.238E-04
0.5060	121.9688	1.5177	226.6300	0.0081	0.0135	1.0180	0.681E+06	0.288E-04
0.6144	163.0880	1.5884	278.7498	0.0084	0.0137	0.9668	0.798E+06	0.497E-04
0.7178	200.3280	1.6480	322.0086	0.0084	0.0135	0.8290	0.877E+06	0.508E-04
0.8004	228.9180	1.6808	358.2387	0.0083	0.0131	0.8008	0.817E+06	0.386E-04

PIPE BED SLOPE = 0.0040

DEPTH DIAMETER	DISCHARGE (L/s)	AVERAGE VELOCITY (m/s)	NORMAL DEPTH (mm)	MANNING n	DARCY f	FROUDE NUMBER	REYNOLDS NUMBER	EQUIVALENT ROUGHNESS (mm)
0.1041	6.0210	0.6882	46.7300	0.0088	0.0186	1.0181	0.811E+05	0.188E-04
0.2178	26.1980	1.1077	97.7988	0.0086	0.0148	1.1310	0.287E+06	0.871E-05
0.3018	53.0140	1.3172	138.4498	0.0087	0.0138	1.1428	0.403E+06	0.648E-05
0.4188	93.0880	1.4960	186.6188	0.0080	0.0138	1.1058	0.588E+06	0.301E-04
0.5014	128.4380	1.6181	229.0100	0.0081	0.0138	1.0883	0.722E+06	0.321E-04
0.6008	161.7840	1.6874	260.8887	0.0082	0.0133	1.0616	0.826E+06	0.378E-04
0.6730	200.3680	1.7748	303.0188	0.0082	0.0131	1.0313	0.924E+06	0.358E-04
0.7872	238.9880	1.8388	338.8288	0.0080	0.0129	1.0183	0.100E+07	0.174E-04

PIPE BED SLOPE = 0.0050

DEPTH DIAMETER	DISCHARGE (L/s)	AVERAGE VELOCITY (m/s)	NORMAL DEPTH (mm)	MANNING n	DARCY f	FROUDE NUMBER	REYNOLDS NUMBER	EQUIVALENT ROUGHNESS (mm)
0.1038	6.5540	0.7718	46.4500	0.0087	0.0184	1.1437	0.803E+05	0.249E-04
0.2078	7.0080	0.8840	43.7400	0.0073	0.0140	1.3497	0.977E+05	0.653E-04
0.3048	30.3600	1.3028	91.8300	0.0078	0.0128	1.3722	0.298E+06	0.327E-04
0.3938	60.1680	1.5811	131.8888	0.0081	0.0123	1.3638	0.488E+06	0.198E-04
0.3960	100.7780	1.7286	177.7188	0.0088	0.0125	1.3064	0.855E+06	0.172E-06
0.4838	141.1740	1.8664	216.8888	0.0087	0.0124	1.2604	0.813E+06	0.639E-04
0.5838	178.3980	1.9172	246.5500	0.0088	0.0127	1.2287	0.906E+06	0.224E-04
0.6187	203.3800	1.9863	276.7788	0.0080	0.0126	1.2054	0.886E+06	0.225E-04
0.6890	244.9580	2.1210	307.4387	0.0088	0.0118	1.2215	0.111E+07	0.156E-06

PIPE BED SLOPE = 0.0080

DEPTH DIAMETER	DISCHARGE (L/s)	AVERAGE VELOCITY (m/s)	NORMAL DEPTH (mm)	MANNING n	DARCY $f$	FROUDE NUMBER	REYNOLDS NUMBER	EQUIVALENT ROUGHNESS (mm)
0.1032	7.3760	0.8881	46.3300	0.0086	0.0188	1.2685	0.888E+06	0.812E-04
0.0975	6.8140	0.8866	43.7700	0.0083	0.0178	1.3106	0.848E+06	0.881E-04
0.2048	30.8840	1.3269	91.7788	0.0088	0.0148	1.3067	0.291E+06	0.488E-04
0.2960	61.1140	1.5600	132.8400	0.0088	0.0147	1.3068	0.470E+06	0.943E-04
0.3800	101.0460	1.7693	178.0100	0.0081	0.0142	1.3505	0.653E+06	0.441E-04
0.4741	140.6500	1.9036	212.7800	0.0082	0.0141	1.3178	0.820E+06	0.566E-04
0.5626	176.8460	2.0196	243.9800	0.0083	0.0137	1.3029	0.949E+06	0.528E-04
0.6249	220.8600	2.1220	280.4387	0.0082	0.0133	1.2795	0.107E+07	0.483E-04
0.6726	248.0840	2.1673	301.9897	0.0081	0.0128	1.2734	0.114E+07	0.378E-04

PIPE BED SLOPE = 0.0080

DEPTH DIAMETER	DISCHARGE (L/s)	AVERAGE VELOCITY (m/s)	NORMAL DEPTH (mm)	MANNING n	DARCY $f$	FROUDE NUMBER	REYNOLDS NUMBER	EQUIVALENT ROUGHNESS (mm)
0.1026	8.6120	1.0069	46.0600	0.0084	0.0181	1.4982	0.117E+06	0.198E-04
0.1013	8.3560	0.9953	45.4900	0.0088	0.0183	1.4904	0.114E+06	0.163E-04
0.2061	35.3000	1.5113	92.0700	0.0086	0.0182	1.5806	0.332E+06	0.222E-04
0.2750	61.1520	1.7285	123.4188	0.0088	0.0150	1.5721	0.480E+06	0.244E-04
0.3646	101.0800	1.9377	163.8500	0.0082	0.0180	1.5296	0.680E+06	0.586E-04
0.4396	140.6960	2.1013	197.2800	0.0083	0.0146	1.5107	0.888E+06	0.751E-04
0.5127	181.8860	2.2236	230.1188	0.0088	0.0145	1.4802	0.101E+07	0.937E-04
0.5747	219.6580	2.3382	257.9067	0.0084	0.0140	1.4653	0.113E+07	0.742E-04
0.6148	247.8180	2.4260	278.5388	0.0083	0.0134	1.4786	0.122E+07	0.367E-04

PIPE BED SLOPE = 0.0100

DEPTH DIAMETER	DISCHARGE (L/s)	AVERAGE VELOCITY (m/s)	NORMAL DEPTH (mm)	MANNING n	DARCY $f$	FROUDE NUMBER	REYNOLDS NUMBER	EQUIVALENT ROUGHNESS (mm)
0.1024	8.5860	1.1291	48.8700	0.0084	0.0181	1.6787	0.130E+06	0.206E-04
0.2081	40.7600	1.7064	93.4088	0.0086	0.0181	1.7861	0.381E+06	0.282E-04
0.2786	70.4800	1.8556	125.1200	0.0089	0.0148	1.7654	0.561E+06	0.439E-04
0.3608	110.6750	2.1544	161.0000	0.0092	0.0180	1.7103	0.760E+06	0.741E-04
0.4319	150.8310	2.3071	183.8288	0.0084	0.0180	1.6734	0.951E+06	0.508E-04
0.4983	181.0010	2.4255	223.6188	0.0086	0.0148	1.6378	0.108E+07	0.102E-03
0.5426	220.7560	2.5182	243.5088	0.0086	0.0146	1.6286	0.118E+07	0.560E-04
0.5785	247.8150	2.6044	260.0488	0.0085	0.0142	1.6308	0.127E+07	0.334E-04